PB93-227718

Use of Tire Chips as Lightweight and Conventional Embankment Fill. Phase 1. Laboratory

Maine Dept. of Transportation, Augusta

Prepared for:

Federal Highway Administration, Augusta, ME

May 92

U.S. DEPARTMENT OF COMMERCE
National Technical Information Service
NTIS

PB93-227718

USE OF TIRE CHIPS AS LIGHTWEIGHT AND CONVENTIONAL EMBANKMENT FILL
Phase I - Laboratory

Technical Services Division
Technical Paper 91-1
May, 1992

Prepared by:
William P. Manion
Dana N. Humphrey

DEPARTMENT OF CIVIL ENGINEERING
UNIVERSITY OF MAINE
ORONO, MAINE

The contents of this report reflect the views of the authors who are responsible for the facts and the accuracy of the data presented herein. The contents do not necessarily reflect the official views or policies of the State of Maine Department of Transportation or the Federal Highway Administration. This report does not constitute a standard, a specification, or a regulation.

PROTECTED UNDER INTERNATIONAL COPYRIGHT
ALL RIGHTS RESERVED.
NATIONAL TECHNICAL INFORMATION SERVICE
U.S. DEPARTMENT OF COMMERCE

TECHNICAL REPORT STANDARD TITLE PAGE

1. Report No.
FHWA-ME-91-1

2.
PB93-227718

3. Recipient's Catalog No.

4. Title and Subtitle
Use of Tire Chips As Lightweight and
Conventional Embankment Fill
Phase I - Laboratory

5. Report Date
March 1992

6. Performing Organization Code

7. Author(s)
W. P. Manion, D. N. Humphrey

8. Performing Organization Report No.
ME91-1

9. Performing Organization Name and Address
Maine Department of Transportation
Technical Services Division in Cooperation with the
University of Maine
State House Station 16, Augusta, Maine 04333

10. Work Unit No.

11. Contract or Grant No.

12. Sponsoring Agency Name and Address
U.S. Department of Transportation
Federal Highway Administration
Washington, D.C. 20590

13. Type of Report and Period Covered
FY-91-92 Phase I

14. Sponsoring Agency Code

15. Supplementary Notes

16. Abstract

Waste tires that have been chipped into 2-in. to 3-in. pieces have the potential to be used as lightweight and conventional fill beneath paved roads. A laboratory study was conducted to determine the properties that would affect the performance of tire chips as fill. The properties that were determined included: gradation, specific gravity, absorption, compacted unit weight, and compressibility. Compressibility was measured in a 12-in. diameter container designed to accommodate the large size and high compressibility of tire chips. These properties were used to determine the reduction in settlement that would be possible by using tire chips as lightweight fill and the effect of a tire chip layer on pavement deflection. The thickness of conventional soil needed between the top of the tire chip layer and the bottom of the pavement to keep pavement deflections below acceptable levels was determined. The cost of using tire chips as lightweight fill was estimated.

17. Key Words
gradation, compacted unit weight,
lightweight fill, tire chips, pavement
deflection

18. Distribution Statement
No restrictions, this document is
available to the public through the
National Technical Information Service
Springfield, Virginia 22161

19. Security Classif. (of this report)	20. Security Classif. (of this page)	21. No. of Pages	22. Price
Unclassified	Unclassified	192	

Form DOT F 1700.7 (8-69)

TABLE OF CONTENTS

PAGE

TABLE OF CONTENTS ... iii
LIST OF TABLES ... v
LIST OF FIGURES ... vii
EXECUTIVE SUMMARY ... xi
CHAPTER 1. INTRODUCTION ... 1
    1.1 PROBLEM STATEMENT ... 1
    1.2 OBJECTIVES OF THE STUDY ... 6
    1.3 ORGANIZATION OF REPORT ... 6
CHAPTER 2. LITERATURE REVIEW ... 9
    2.1 INTRODUCTION ... 9
    2.2 PARTICLE SIZES ... 9
    2.3 UNIT WEIGHT ... 11
    2.4 COMPACTION ... 12
    2.5 COMPRESSIBILITY ... 13
    2.6 CASE HISTORIES ... 16
        2.6.1 Hedbom Forest Road - Floodwood, Minnesota ... 16
        2.6.2 Eden Prairie, Minnesota - Roadway ... 21
        2.6.3 Highway 10 in Rice, Minnesota ... 23
        2.6.4 Test Embankment - Dane County Landfill #2, Wisconsin ... 24
        2.6.5 Camas Valley Landslide- Oregon Highway 35 ... 29
        2.6.6 Putnamville, Vermont slope flattening ... 29
        2.6.7 Georgia, Vermont town highway base ... 32
        2.6.8 New Route I 76, Denver, Colorado ... 34
    2.7 ENVIRONMENTAL EFFECTS ... 36
    2.8 SUMMARY ... 37
CHAPTER 3. BASIC ENGINEERING PROPERTIES ... 39
    3.1 INTRODUCTION ... 39
    3.2 GRADATION ... 39
    3.3 SPECIFIC GRAVITY ... 41
    3.4 COMPACTED UNIT WEIGHT ... 42
CHAPTER 4. SETTLEMENT ANALYSIS ... 47
    4.1 INTRODUCTION ... 47
    4.2 MATERIAL PROPERTIES ... 47
    4.3 METHODOLOGY ... 48
    4.4 RESULTS ... 52
CHAPTER 5. COMPRESSIBILITY ... 55
    5.1 INTRODUCTION ... 55
    5.2 APPARATUS ... 55
    5.3 CALIBRATION ... 58
    5.4 TESTING METHODOLOGY ... 66
    5.5 RESULTS ... 71
        5.5.1 Compressibility of Tire Chips Without Gravel ... 72
        5.5.2 Compressibility of Tire Chip and Gravel Mixtures ... 81
    5.6 SUMMARY ... 96

LIST OF TABLES

PAGE

Table 2.1 Dane County Landfill #2 Test Sections.........26

Table 3.1 Summary of compacted unit weights.............45

Table 5.1 Ko and Poisson's ratio from compressibility testing........................79

Table 5.2 Young's modulus from compressibility testing....................................80

Table 5.3 Ko and Poisson's ratio from compressibility testing of 2-in. minus MDOT type D gravel.............................85

Table 5.4 Young's modulus from compressibility testing of 2-in. minus MDOT type D gravel.......................................85

Table 5.5 Ko and Poisson's ratio from compressibility testing of 3/4-in. minus gravel.......................................94

Table 5.6 Young's modulus from compressibility testing of 3/4-in. minus gravel...............95

Table 5.7 Summary of tire chip compressibility results.....................................99

Table 6.1 Material properties used in finite element analysis............................111

Table 6.2 Results of 3 different meshes................113

Table 6.3 Equivalent axle load from deflection using AASHTO (1986b) method.................116

Table 6.4 Vertical stress in the tire chip layer for each case................................117

Table 7.1 Purchase prices of tire chips................135

BLANK

LIST OF FIGURES

PAGE

Figure 2.1 Load displacement curve of tire chips after Edil, et al. (1990) 14

Figure 2.2 Load displacement curve of 30% tire chips and 70% sand mixture by weight after Edil, et al. (1990) 15

Figure 2.3 Plate load test setup after Winters (1991) 17

Figure 2.4 Stress strain curve of plate load test after Winters (1991) 18

Figure 2.5 Cross section of Hedbom Forest Road after Geisler, et al. (1989) 20

Figure 2.6 Cross section of Eden Prairie road after Geisler, et al. (1989) 22

Figure 2.7 Cross section of U.S. Highway 10 in Rice, Minnesota after Palmer and Verdegan (1989) 25

Figure 2.8 Plan and sections through the test embankment at Dane County Landfill #2, Wisconsin after Edil, et al. (1990) (a) plan, (b) sections 27

Figure 2.9 Cross section through the Camas Valley Landslide - Oregon Highway 35 repair after Dodson (1990) 30

Figure 2.10 Plan and section through tire chip fill used in Putnamville, Vermont Rt. 12 slope flattening after Winters (1991) 31

Figure 2.11 Location and section through Georgia, Vermont town highway base after Frascoia (1991) 33

Figure 2.12 Section through Rt. I-76 near Denver, Colorado after Colorado Department of Highways (1991) 35

Figure 3.1 Gradation of tire chips 40

Figure 3.2 Specific gravity of tire chips 43

Preceding page blank

Figure 4.1 Coefficient of secondary compression versus moisture content after Batchelder Adams (1984) 50

Figure 4.2 Void ratio at end of primary consolidation versus moisture content after Batchelder Adams (1984) 51

Figure 4.3 Consolidation settlement on Presumpscot with and without tire chips 53

Figure 4.4 Consolidation settlement on peat with and without tire chips 54

Figure 5.1 Apparatus used for compressibility testing 59

Figure 5.2 Horizontal strain gage pressure calibration curve for compressibility testing 61

Figure 5.3 Effect of temperature on strain gage measurement for compressibility testing 63

Figure 5.4 Horizontal strain gage calibration check, using 12.5-in. long cylinder 64

Figure 5.5 Vertical strain gage load calibration curve for compressibility testing 65

Figure 5.6 Effect of side friction on vertical stress in sample during compressibility test 69

Figure 5.7 Typical vertical stress - strain load and unload curve for tire chips without gravel 73

Figure 5.8 Typical horizontal - vertical stress load and unload curve for tire chips without gravel 74

Figure 5.9 Typical vertical log stress - strain load and unload curve for tire chips without gravel 76

Figure 5.10 Five initial loading vertical stress - strain curves for tire chips without gravel 77

Figure 5.11 Five initial loading horizontal - vertical stress curves for tire chips without gravel 78

...

Figure 5.12 Vertical stress - strain initial loading curves of 50% (by weight) MDOT type D gravel and tire chip mix....................82

Figure 5.13 Horizontal stress - vertical stress initial loading curves for 50% (by weight) MDOT type D gravel and tire chip mix....................................83

Figure 5.14 Gradations of MDOT type D gravel and 50% mix by weight with tire chips................84

Figure 5.15 Gradations of 3/4-in. gravel and 25%, 50% and 75% mixes by weight with tire chips.....................................86

Figure 5.16 Vertical stress - strain initial loading curves for 25% (by weight) 3/4-in. gravel and tire chip mix....................87

Figure 5.17 Vertical stress - strain initial loading curves for 50% (by weight) 3/4-in. gravel and tire chip mix....................88

Figure 5.18 Vertical stress - strain initial loading curves for 75% (by weight) 3/4-in. gravel and tire chip mix....................89

Figure 5.19 Horizontal stress - vertical stress initial loading curves for 25% (by weight) 3/4-in. gravel and tire chip mix....................................90

Figure 5.20 Horizontal stress - vertical stress initial loading curves for 50% (by weight) 3/4-in. gravel and tire chip mix....................................91

Figure 5.21 Horizontal stress - vertical stress initial loading curves for 75% (by weight) 3/4-in. gravel and tire chip mix....................................92

Figure 6.1 Six road embankment stratigraphies used in finite element analysis of pavement deflection...............................104

Figure 6.2 Typical $\sigma3$ contour plot of wheel live load used for iterative modulus method, showing live load (LL), dead load (DL) from overburden, and the net $\sigma3$ stress..................................106

Figure 6.3 Principal stress angle versus distance from the load centerline for six elevations in case C........................108

Figure 6.4 Plot of iterative convergence of pavement deflection for case C..............110

Figure 6.5 Three different meshes used to check influence of model geometry.................112

Figure 6.6 Pavement deflections shown with the six road embankment stratigraphies..............114

Figure 6.7 Plot of pavement deflection versus soil cover thickness............................115

Figure 6.8 Increase in vertical stress contour plots for the six cases (a) Case A, (b) Case B, (c) Case C, (d) Case D, (e) Case E, (f) Case F..............................118

Figure 6.9 Deformed mesh plots for the six cases (a) Case A, (b) Case B, (c) Case C, (d) Case D, (e) Case E, (f) Case F..............125

Figure 6.10 Pavement deflection versus distance from axis of rotation for three 4-ft tire chip thicknesses and two 2-ft tire chip thicknesses with case without tire chips.....................................131

Figure 6.11 Effect of changing tire chip modulus on pavement deflection........................133

USE OF TIRE CHIPS AS LIGHTWEIGHT AND CONVENTIONAL EMBANKMENT FILL

By: William P. Manion and Dana N. Humphrey

Department of Civil Engineering
University of Maine
Orono, Maine

EXECUTIVE SUMMARY

In the State of Maine approximately 36 million discarded tires are heaped in open piles and an additional 1 million tires are discarded every year. One potential use for these tires is to chip them into 2-in. to 3-in. pieces and place these tire chips beneath paved roads as lightweight and conventional embankment fill. This use would have two major benefits.

- It would provide an economical source of lightweight fill for roads built on weak, compressible soils.
- An important contribution could be made to the disposal of waste tires. This would help the Maine Department of Transportation meet the state legislative mandate to investigate use of recycled materials in highway construction.

A literature search revealed that tire chips have been used successfully as fill in several road projects, however, very few reliable values of the engineering properties of tire chips were reported. Thus, the first goal of this project was to determined the following engineering properties of tire chips:

- Gradation
- Specific gravity
- Adsorption
- Compacted unit weight
- Compressibility

The tire chips used for this study were obtained from Sawyer Environmental Recovery Facility in Hampden, Maine. They had a uniform gradation with 90% of the particles larger than 0.5 in., and 50% between 1 and 1.5 in. The tire chips had a specific gravity of 1.05, which is slightly greater than the specific gravity of water. The tire chips adsorbed only 4% water by weight. The dry unit weight of compacted tire chips was about 40 pcf. This is about one-third the dry unit weight of conventional soil fill which clearly illustrates the potential of tire chips to be used for lightweight fill. Settlement analyses showed that when tire chip fill is substituted for

conventional soil fill in embankments built over the types of compressible soils found in Maine, settlements can be reduced by up to 40%.

The compressibility of tire chips was tested in a 12-in. diameter container that was custom designed to accommodate the large size and high compressibility of the tire chips. The tests showed that tire chips are much more compressible than conventional soil. The compressibility of mixtures of soil and tire chips was also investigated. Compressibility decreased as the percentage of soil increased. However, difficulty was encountered in obtaining a uniform blend of soil and tire chips since a significant portion of the soil particles, which are much heavier than tire chips, tended to settle to the bottom of the container during mixing and compaction. The results of the compressibility tests were used in a finite analysis to predict the effect of a layer of tire chips on pavement deflection.

The second goal of this project was to estimate the thickness of conventional soil needed between the top of the tire chip layer and the bottom of the pavement to keep pavement deflection to an acceptable level. This was investigated with a finite element analysis with a simulated 11-kip wheel load (22-kip equivalent single axle load). This showed that 2 ft to 6 ft of conventional soil fill is needed to minimize pavement deflection. These results will be used in a subsequent project to design a field trail.

The final goal was to investigate the economics of using tire chips as fill. The prices of tire chips quoted by the four tire chip producers in Maine ranged from $7.50/cy for 2-in. to 3-in. chips suitable for highway applications to $22/cy for smaller chips suitable for use as fuel in paper mill boilers. Placement would add about $4/cy to the cost. This price is very attractive when compared to other lightweight fills such as expanded shale, which must be imported from out of state at a cost of about $44/cy and have a unit weight of about 70 pcf. However, when compared to typical prices for granular borrow of $5 to $10/cy, it is likely that tire chips will be more expensive.

CHAPTER 1. INTRODUCTION

1.1 PROBLEM STATEMENT

It is estimated that 240 million used tires are generated every year in the United States (Maine DEP, 1989; Eaton, et al., 1991; Stark and Korte, 1988). According to Eaton, et al. (1991), 200 million are passenger car tires and 40 million are truck tires, creating roughly 2.1 million tons of scrap passenger tires and 1.9 million tons of scrap truck tires each year. Based on used tire accumulation rates between 0.8 to 1.5 tires per capita per year (Maine DEP, 1989), it is estimated that 1.2 million used tires are generated in the state of Maine every year. Tires covered by a thin layer of soil tend to "float" back to the ground surface, making burial an unacceptable disposal method. Consequently, tires are generally sent to large privately owned open piles, currently as large as 10 and 15 million tires in Maine. It is estimated that some 36 million tires have accumulated in piles throughout the state. These piles are a fire hazard, provide excellent breeding grounds for mosquitoes, and degrade the landscape.

According to the Maine DEP (1989), fire is a particularly important problem, since tire fires emit heavy black smoke into the air and petroleum and other chemical contaminants into surface and ground water.

With state pride, reputation, and tourism business based on scenic and environmental quality, the effects of a major tire fire could be devastating to large areas of Maine, both environmentally and economically. Once ignited, tire fires are extremely difficult to contain and extinguish, requiring large amounts of manpower and equipment.

Anyone who has ever handled an old tire realizes the impossibility of dumping all the water out of one. Such water creates breeding habitat for mosquitoes, known to carry yellow fever and many forms of encephalitis. According to the Maine DEP (1989), "In 1986, the U.S. Environmental Protection Agency estimated that health care costs for scrap tire related encephalitis totaled $5.4 million. This cost includes medical care as well as lost earnings due to illness."

To reuse these large quantities of tires, several potential uses have been explored in recent years, including highway uses of whole tires, recycled tire rubber in asphalt pavements and maintenance, tire derived fuel, and recycling tire materials into other petroleum derived products.

The California Transportation Laboratory has researched and used recycled whole tires for shoulder stabilization, channel slope protection as retaining walls, and protective barriers for seedlings (Williams and Weaver, 1987; Nguyen and Williams, 1989). Additionally, they have researched using tire sidewalls for fill stabilization (Hannon and Forsyth, 1973; Forsyth and Egan, 1976; Yee, 1979), and using whole tires for anchors in a timber wall system (Richman and Jackura, 1984). The California Transportation Laboratory has also performed research for using tire chips as permeable aggregate (Bressette, 1984). A reinforcing grid made of tire sidewalls has been used for a weather resistant flexible base for gravel roads in France (El Puente, 1990).

Two methods have been used to add scrap tire rubber to asphalt pavements, as outlined by Eaton, et al. (1991). Asphalt rubber concrete is made by adding finely ground rubber tire buffings to hot asphalt cement, making a rubberized asphalt binder, and subsequently adding this mixture to normal paving aggregates. Rubber tire buffings (crumb-rubber) are typically 1/64 in. in size and fall between the number 25 and 40 mesh sieves (0.425 mm or 0.017 in. to 0.710 mm or 0.028 in.) (Sikora, 1986). The second method uses larger rubber particles (1/16 in. to 3/8 in.) as part of the aggregate. Using rubber particles as aggregate in asphalt pavements, developed in Sweden in the late 1960s, is typically referred to as "PlusRide" in the United States. PlusRide contains granulated whole tires, including tire buffings and chopped cords. According to Eaton, et al. (1991), at least 18 states have built roadway test sections using PlusRide. The first type of asphalt rubber made using small particles is also used as a chip seal coat to prevent fatigue cracking, under asphalt concrete to absorb stress and reduce reflective cracking and as a crack and joint sealant (Sikora, 1986).

Tires have also been chipped finely enough to facilitate removal of most of the metals, making them suitable for use as fuel in boilers at paper mills and other industries. This tire derived fuel has a 25% higher energy output by weight than coal, and has been used in several states, such as Oregon, Texas and Georgia (Maine DEP, 1989). In Maine, according to Clark (1991), Champion Paper in Bucksport burns roughly 72 tons of tire chips each day, mixing them with waste wood, low sulfur coal and other fuels. Sawyer Environmental Recovery, Inc. of Hampden, Maine produces the chips burned by Champion.

In Minnesota, a company called Rubber Research Elastomerics, Inc. (RRE) has patented a process called TIRECYCLE, which uses a liquid polymer to surface treat finely ground vulcanized rubber into bonding with other rubber and plastic materials. The results, using every part of the tire, are products such as tire tread, molded mechanical items, carpet backing, roofing, railroad crossings and injection molded and extruded polypropylene and polyethylene parts (Stark and Korte, 1988). The existing TIRECYCLE facility was designed to process 3 million tires annually, but has not reached that level of production yet (Maine DEP, 1989). A new operation in Bradley, Oklahoma, turns tires into useful raw products with supposedly little or no pollution (Smith, 1991). It heats tire chips to 425°F, and chemically converts them into high grade oil, carbon black, steel and methane.

Another possible use of waste tires is the focus of this research, namely the use of waste tires which have been chipped to a 2-in. maximum size as conventional and lightweight embankment fill. In addition to using scrap tires, tire chips would provide Maine with a local source of lightweight fill. Currently lightweight fill such as expanded shale is purchased from other states at a fairly high cost. It is estimated, based on the cost of expanded shale purchased for a 1981 project in South Portland, that expanded shale would currently cost $44/cy. Furthermore, expanded shale typically has a unit weight of 70 pcf, (King, 1970) which is only moderately less than the unit weight of conventional soil (110 to 125 pcf typically). Tire chips have a unit weight of about 40 pcf, significantly less than soil and expanded shale, and could find many applications in Maine as embankment fill where foundation soils are soft and compressible. Another driving force for the use of tire chips in Maine is the mandate by the Maine State Legislature to the Maine Department of Transportation regarding use of recyclable materials in construction (Maine State Legislature, M.R.S.A., Ch. 26, Section 18, Department of Transportation Recycling Program).

1.2 OBJECTIVES OF THE STUDY

The major purpose of this research was to determine the basic engineering properties of tire chips and predict pavement deflections resulting from a layer of tire chips beneath a paved road. Major parts of the investigation were laboratory measurement of the compressibility of tire chips, and prediction of the minimum thickness of granular material required between the pavement and the tire chip layer to limit pavement deflection to acceptable levels.

1.3 ORGANIZATION OF REPORT

The results of this research are detailed in the following seven chapters. Chapter 2 is a literature review of available materials. The literature review is divided into sections on particle size, unit weight, compaction, compressibility, case histories, and environmental effects.

Testing methods and results of gradation, specific gravity and compacted density laboratory testing of tire chips are given in Chapter 3. Settlement analyses are presented for typical road embankments on Presumpscot formation and Maine peat deposits in Chapter 4.

Chapter 5 contains the laboratory testing methods and results of the large scale compressibility testing performed for this research.

Using data from the previous chapters, Chapter 6 presents the analysis method and results of finite element modeling of pavement deflection wich a layer of tire chips in the road embankment.

Chapter 7 provides a cost analysis for using tire chips in embankments and Chapter 8 summarizes the research findings.

Appendix A contains detailed compressibility results from the compressibility testing presented in Chapter 5.

BLANK

CHAPTER 2. LITERATURE REVIEW

2.1 INTRODUCTION

A summary of the limited published literature and work in progress by transportation agencies and universities on use of tire chips for lightweight and conventional road embankment fill is given below. The literature was gathered by contacting other researchers and by reviewing a TRB/HRIS "hot topics" bibliography on "use of recycled tires in highway maintenance and construction," dated May 1990. In addition, letters inquiring about tire chip usage were sent to all transportation agencies in the United States and Canada. Any agency indicating experience with tire chips was contacted by phone to obtain further information. The following relates properties of tire chips obtained from the literature and several case histories.

2.2 PARTICLE SIZES

The majority of published literature refers to the material as tire shreds. In general, tire shreds are larger particles than considered in this study, and are produced primarily for use as fill. In comparison, tire chips are smaller, currently being produced primarily for burning applications. Edil, et al. (1990), in their survey of four tire shredding operations in the state of Wisconsin, found tire chip sizes to range from 1 x 2 in.

to 4 x 18 in. The tire chip size depends on the nature of the shredding operation.

A typical material specification is the "Lightweight fill material specification," a project in Eden Prairie, Minnesota, copied from an unknown source. Parts E and F could be applied to all particle sizes.

> The lightweight fill material shall consist of chipped or shredded tire pieces meeting the following specifications:
> A. 80% of the material (by weight) must pass a six inch screen.
> B. A minimum of 50% of the material (by weight) must be retained on a four inch screen.
> C. All pieces shall have at least one sidewall severed from the face of the tire.
> D. The largest allowable piece is a quarter circle in shape or 12 inches in length, whichever is the lesser dimension.
> E. All metal fragments shall be firmly attached and 98% embedded in the tire sections from which they were cut. No metal particles will be allowed in the fill without being contained within a rubber segment. Ends of metal belts and beads are expected to be exposed only in the cut faces of some tire chips. If metal particles are found by the contractor, they will be placed off to the side and the supplier shall be called back to pick up this material along with any unused tire chips at no cost to the city.
> F. The tire chips supplied shall be free of any contaminates such as oil, grease, etc. that could leach into the ground water.
> G. The lightweight fill material supplied shall weigh less than 600 pounds per cubic yard (by truck measure).

The Vermont Agency of Transportation rebuilt a section of unpaved road using a 1:3 mixture of coarse to finer tire shreds (Frascoia, 1991). Coarse shreds of about 6-in. size were made using a single pass through the shredder, leaving pieces as large as one third of a tire. Finer shreds had been through the shredder two to three times, and were 2 to 3 in. in size.

Additionally, some applications used whole tires and parts of tires with and without a layer of tire chips, as a reinforcing layer at the base of an embankment. In these applications, the tires were not intended to serve as lightweight fill. Whole tires, half tires (cut into two donuts), and tire chips were used in different combinations and configurations on the Hedbom forest road, Floodwood, Minnesota (Geisler, et al., 1989).

2.3 UNIT WEIGHT

The unit weights reported in the literature for tire shreds are as follows: 20 pcf (Geisler, et al., 1989), 20.4 pcf (Palmer and Verdegan, 1989), 19 to 36 pcf (Edil, et al., 1990), 22 pcf loose to 34 pcf compacted (Dodson, 1990), and 28 to 30 pcf (Frascoia, 1991). The methods used in determination of the preceding values were not reported, but it can be inferred that "truck measure" (weighing a truck load of known volume) was the most usual. One case in Vermont reported in situ densities measured using Ottawa Sand of 47 to 56 pcf, a laboratory specific gravity of 1.21, and computed void ratio of compacted chips at 0.45 (Winters, 1991). In practice, Geisler, et al. (1989) found an individual tire to weigh approximately 20 lbs, allowing as many as 500 (whole) tires per truckload. Similarly, 100 cy of tire chips should fit in a 40-ft trailer.

2.4 COMPACTION

There were several suggested methods for compacting tire chips in the field. Palmer and Verdegan (1989) recommended placing tire chips in 2-ft lifts, and compacting each lift with a landfill type sheepsfoot roller or a fully loaded scraper. Edil, et al., (1990) used a vibratory sheepsfoot roller, with and without vibration. From measurements of surface settlement, it appeared that vibration may have helped compaction slightly. Dodson (1990) recommended compaction of 2 to 3-ft lifts by 3 or more "full coverage" passes by a D-8 or larger dozer (a "full coverage" pass is defined as at least one track of the dozer passing over every portion of the lift surface being compacted).

Generally, the angular shape of tire chips, combined with frictional forces, provides adequate shear strength to support construction equipment (Geisler, et al., 1989). Winters (1991) reported that "The tire chips were very workable with a five ton dozer." In this case, the tire chips were placed in maximum 18-in. loose lifts and compacted with a five ton dozer. During compaction, the chips would deflect 6 to 12 in. under the initial pass, and 3 to 4 in. under the second pass, but then rebound.

Overall, the site became spongy under the dozer after 4 ft of chips had been placed and compacted. In another case, a 9 to 12-in. layer of tire chips under an unpaved road were not compacted when placed (Frascoia, 1991). They were simply placed with dump trucks and leveled with a backhoe. Frascoia (1991) assumed that placing granular fill over the tire chip layer provided sufficient compaction.

2.5 COMPRESSIBILITY

In Wisconsin, Edil, et al. (1990) have done some preliminary compressibility testing using 6-in. and 12-in. diameter proctor molds, with either standard or modified compactive effort. Several different ratios of tire chips to sand or loam soil with various water contents were investigated. In some cases the soil and chips were layered while in others they were thoroughly mixed. Preliminary results using the 6-in. mold are shown in Fig. 2.1 for tire chips only and Fig. 2.2 for a mixture of 30% tire chips and 70% sand by weight. Results from the large mold and other mixtures were not yet available. At a maximum load of 2800 lb (99 psi), about 2.2 in. of deflection (36% strain) occurs for tire chips alone and 0.10 in. (2% strain) when mixed with sand. Stresses and strains were calculated using sample weights and unit weights given. Water contents were not reported.

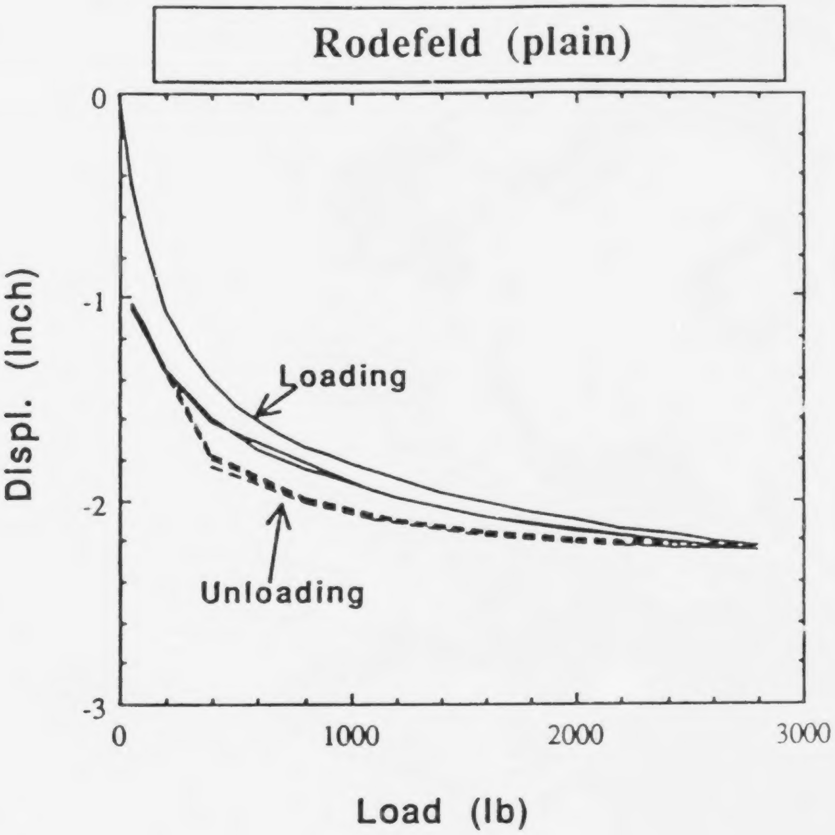

Figure 2.1 Load displacement curve of tire chips after Edil, et al. (1990)

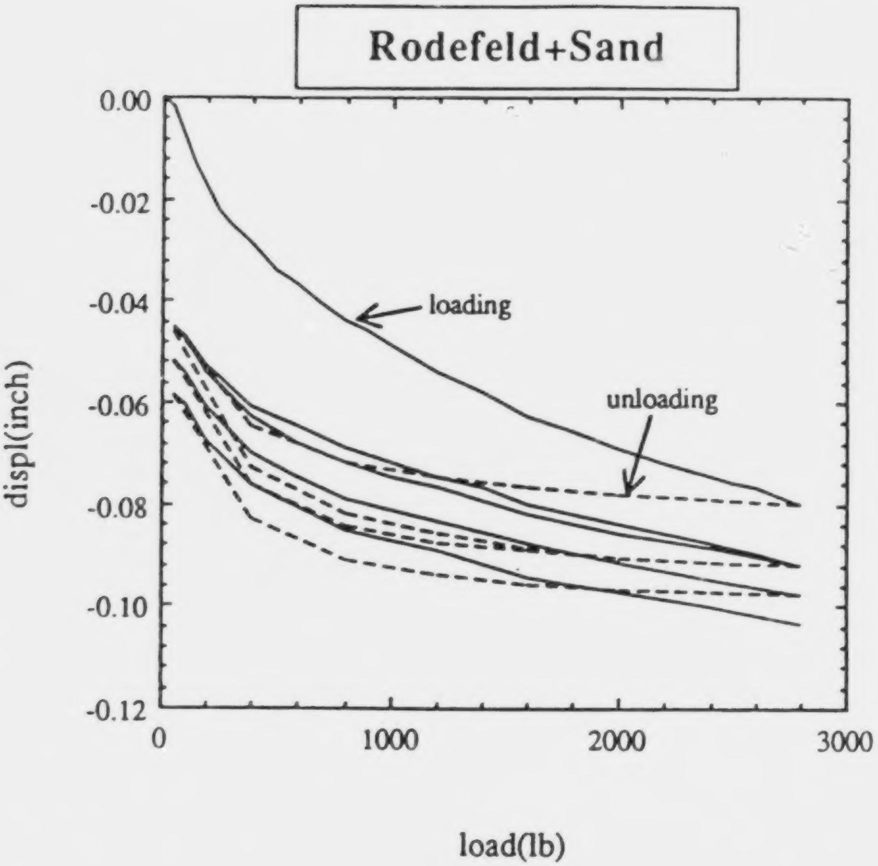

Figure 2.2 Load displacement curve of 30% tire chips and 70% sand mixture by weight after Edil, et al. (1990)

Winters (1991) reported results of a plate load test on an 18-ft thick tire chip embankment. As shown in Fig. 2.3, a 4.13 sf plate was loaded with a 55 gallon drum supporting 50 lb sand bags up to 2,028 lb for a maximum stress of 471.2 psf. Deflections were measured with survey equipment. Fig. 2.4 shows the resulting loading and unloading curves. A final permanent deflection upon unloading was reported as about 0.028 in. per foot of fill depth. The strain was computed by dividing the measured deflection by the full 18-ft thickness of the tire chip fill. Since the lower portion of the fill experienced a negligible change in stress, this definition of strain has little meaning. A modulus value was reported at 313 psf, based on a linear stress strain relationship at 600 lbs of load.

2.6 CASE HISTORIES

Several case histories were outlined in the literature. In many cases, details and engineering data were missing or not available, resulting in unfortunate ambiguities. The following is a summary and a diagram of each case history.

2.6.1 Hedbom Forest Road - Floodwood, Minnesota

The first recorded use of waste tires in road embankments was on the Hedbom forest logging road, in

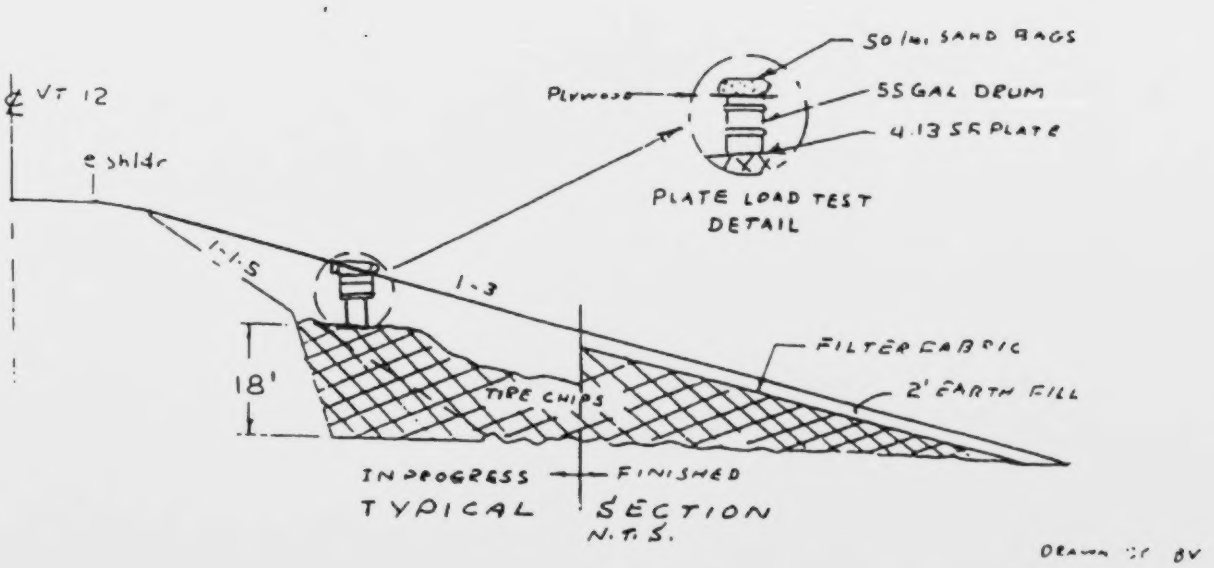

℄ VT 12
e shldr
1:1.5
1:3
18'
Plywood
50 lb. SAND BAGS
55 GAL DRUM
4.13 SF PLATE
PLATE LOAD TEST
DETAIL
FILTER FABRIC
2' EARTH FILL
TIRE CHIPS
IN PROGRESS
FINISHED
TYPICAL SECTION
N.T.S.
DRAWN BY BV

Figure 2.3 Plate load test setup after Winters (1991)

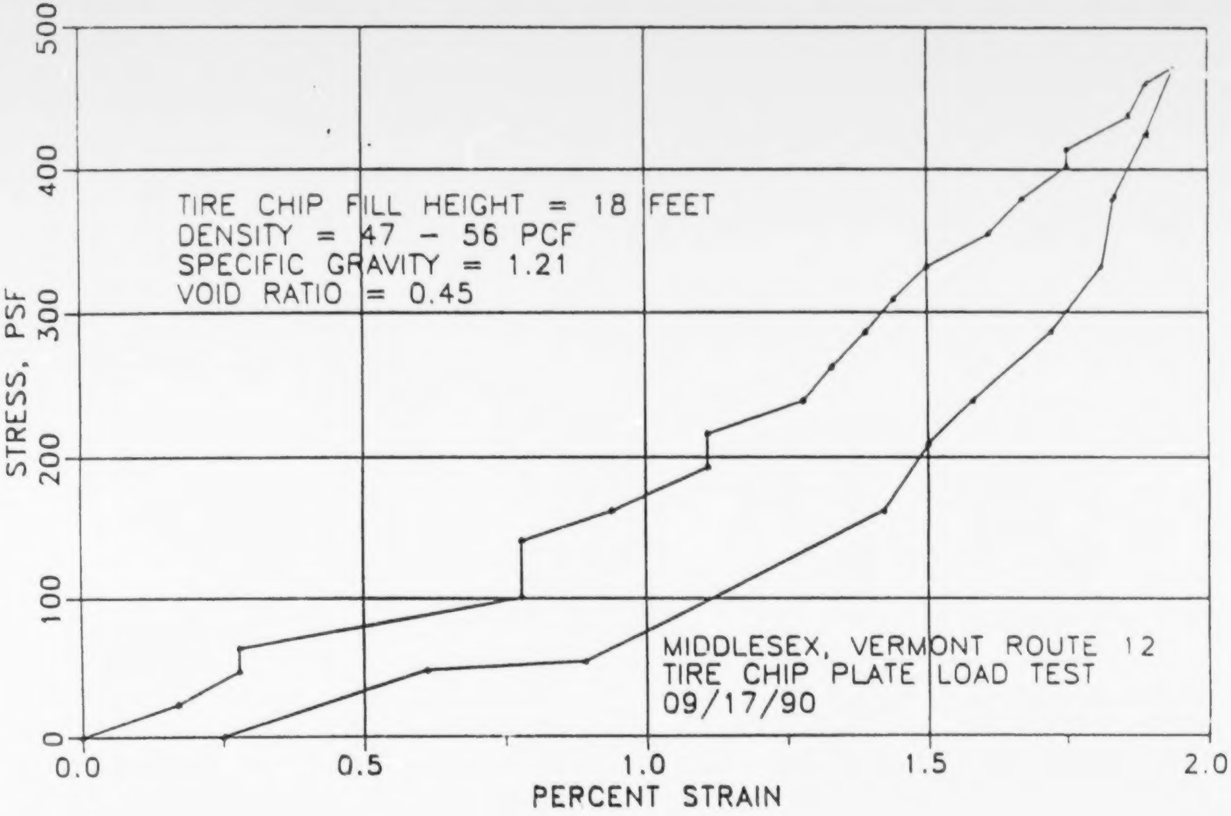

Figure 2.4 Stress strain curve of plate load test after Winters (1991)

Floodwood, Minnesota (Geisler, et al., 1989). The primary focus was using whole tires and half tires (donuts), tied in a mat to reinforce the embankment. The tires served as a replacement for the traditional corduroy log roads. Additionally, a turnout was constructed 10 ft wide and 120 ft long on undisturbed peat with 3 ft of shredded tires. However, no data or observations were presented for the shredded tire fill.

The work, designed by the Minnesota Department of Natural Resources - Forestry, was started in November of 1986. Site conditions of the existing old narrow road consisted of six miles of wet silty soil subgrade soil over 5 to 17 ft of peat. Eight 400-ft long test sections were built, on top of the existing narrow road and along one side, increasing the width of the embankment. Variables in the different sections were the following: single or double layer of tires, whole or half tires, cups up or down (half tires), and use of geotextiles. After filling the widened part of the embankment with silty sand common borrow to the original top of grade, the whole site was capped with 12 in. of compacted common borrow and 6 in. of 3/4-in. minus close graded aggregate. A generalized cross section is shown in Fig. 2.5. The road was used two years for three season logging and subsequently tested in the summer of 1989. Settlement plate readings showed that no one section had settled more than another, indicating that the variables

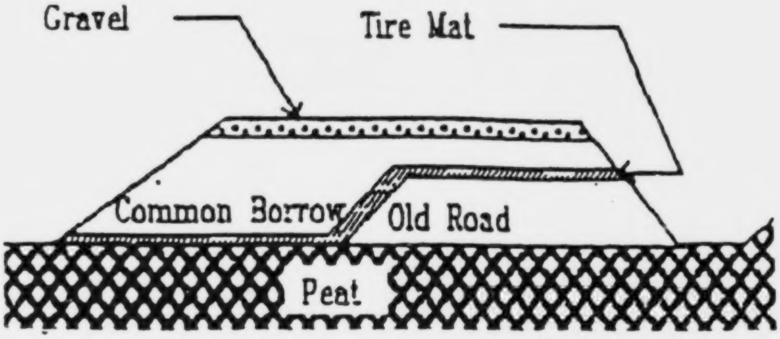
Gravel
Tire Mat
Common Borrow
Old Road
Peat

Figure 2.5 Cross section of Hedbom Forest Road after Geisler, et al. (1989)

of single or double layer of tires, whole or half tires, cups up or down (half tires), and use of geotextiles had little effect on settlement. Standard penetration test borings showed that the new widened section settled 12 to 18 in., 12 to 24 in. less than they calculated for a conventional soil embankment. The method of calculation was not given, and there was no data given for the control sections with a 400-lb woven slit film geotextile. Subgrade deflections with a six ton per axle truck were claimed to be indiscernible, but the method of observation was not reported.

2.6.2 Eden Prairie, Minnesota - Roadway

The Eden Prairie site was a 22-ft high fill for a municipal road constructed over a wetland. Foundation soils consisted of soft organic soil. When construction was attempted with conventional soil fill, failure due to excessive settlement occurred. Even after three years, settlement was still occurring at approximately one foot per year. Subsequently, 10 to 14 ft of the conventional soil fill was replaced with 30,000 cy of tire chips topped with a 4-ft layer of common borrow. The tire chips, 6 to 8 in. wide by 12 to 24 in. long, were placed in 2 to 3-ft thicknesses and compacted with several passes of a Caterpillar D-8 dozer. Geotextile was used between the tire chips and the common borrow fill. A generalized cross section is shown in Fig. 2.6.

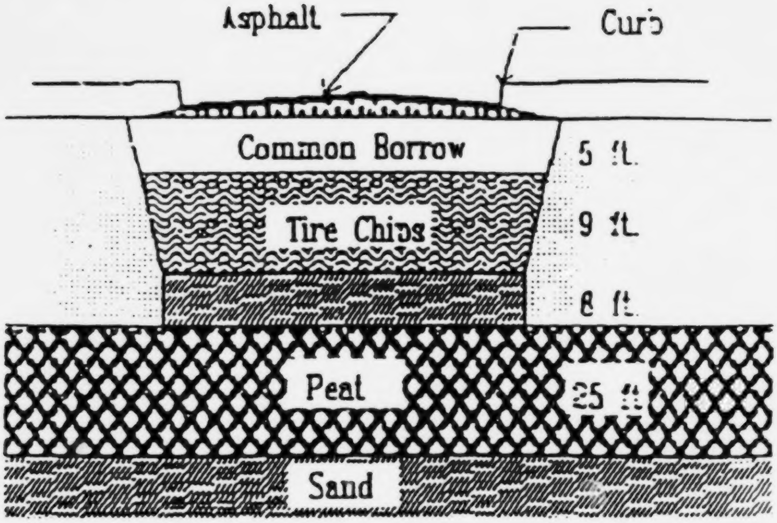
Asphalt
Curb
Common Borrow
5 ft.
Tire Chips
9 ft.
8 ft.
Peat
25 ft
Sand

Figure 2.6 Cross section of Eden Prairie road after Geisler, et al. (1989)

Settlement monitoring plates showed that the base of the subcut had stopped settling, but the tire chip layer itself was experiencing consolidation. It was decided to wait 3 weeks, allowing the shredded tires to consolidate between 8 and 10% of the total compacted thickness. The final construction steps were 12 in. of crushed limestone base, 3.5 in. of bituminous base course and a 1.5-in. bituminous wearing course. Settlement monitoring and pavement/subgrade strength determinations were to be performed as part of the study, but no results have been published.

2.6.3 Highway 10 in Rice, Minnesota

The embankment of U.S. Highway 10, which passes over saturated peat and muck in Rice, Minnesota, had been settling excessively for a number of years. In their report to the Benton County Highway Department, Palmer and Verdegan (1989) outline a repair option using tire chips. The following is the recommended construction procedure. Excavate the old embankment to 6 in. above the top of the adjacent marsh. Apply a layer of geotextile, such as Mirafi 500X. Place tire chips in 2-ft lifts, compacted with a landfill type sheepsfoot roller, to within 3.5 ft of the top of subgrade soil. Apply another layer of geotextile. Apparently, no geotextile was placed on the side slopes of the tire chip fill. Finally, backfill to final grade (an additional

3.5 ft) with clean granular fill compacted to 100% standard proctor. The section was to remain unpaved for several months to monitor performance and allow settlement to occur. It was expected that the subsequent lightening of load would be approximately equal to removal of 3 ft of fill from the top of the embankment. Approximately 52,000 tires were to be used in the 250-ft long section. A typical cross section is shown in Fig. 2.7. A report describing actual construction and performance of the tire chip fill has not been published.

2.6.4 Test Embankment - Dane County Landfill #2, Wisconsin

In Wisconsin, Edil, et al. (1990) have been researching the use of tire chips for roadway embankment fill. Their interim report, dated June 1990, relates information about their laboratory testing and a test embankment built at the Dane County Landfill #2. The test embankment was parallel to the entrance road at the landfill, so the quantity and severity of traffic could be varied and monitored simply by allowing refuse trucks to be diverted across the test section.

The 16-ft wide crest by 6-ft high embankment was bedded on 18 in. of compacted till covered with geotextile. The 2 (horizontal) : 1 (vertical) side slopes were also covered with geotextile before being finished with topsoil. The finish surface of the road

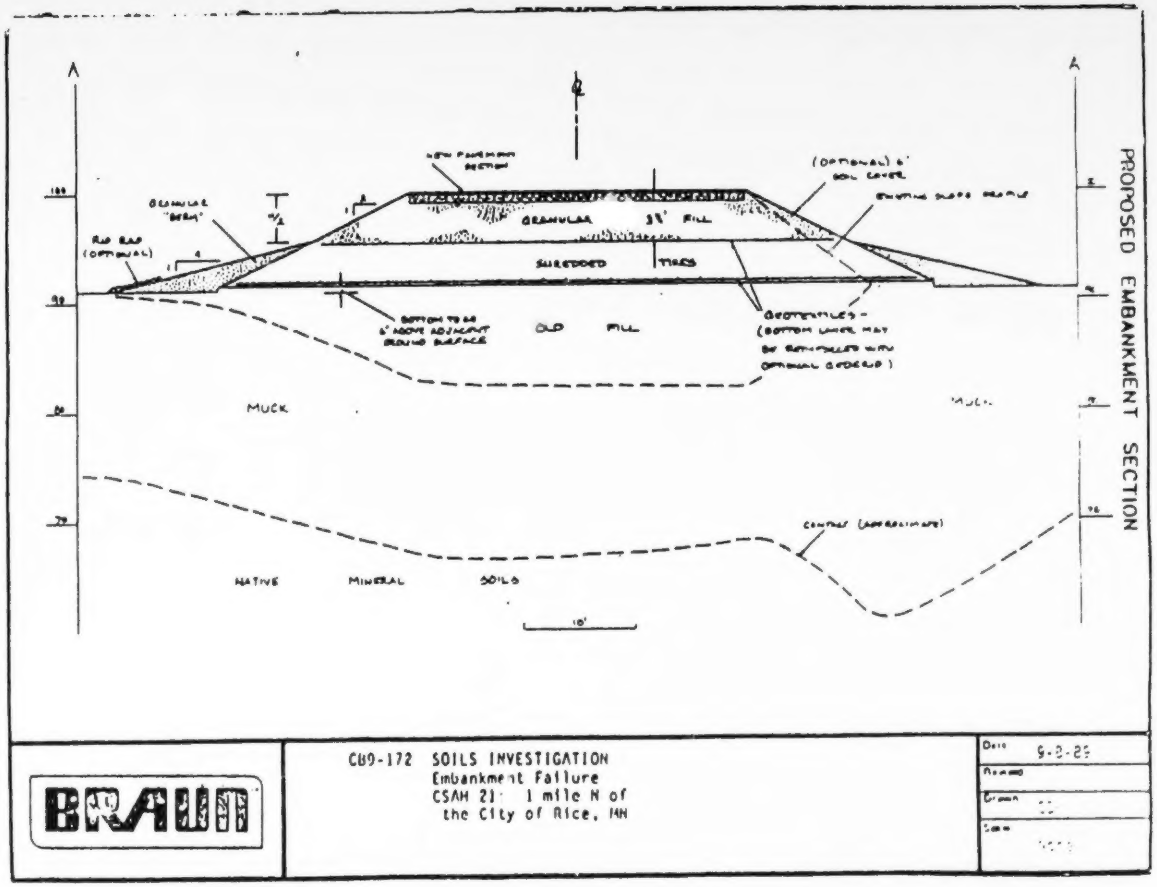
PROPOSED EMBANKMENT SECTION
A
A
℄
100
90
80
70
RIP RAP (OPTIONAL)
GRANULAR "BERM"
NEW PAVEMENT SECTION
GRANULAR
3½' FILL
SHREDDED
TIRES
BOTTOM TO BE 6' ABOVE ADJACENT GROUND SURFACE
OLD FILL
(OPTIONAL) 6' SOIL COVER
EXISTING SLOPE PROFILE
GEOTEXTILES - (BOTTOM LAYER MAY BE REINFORCED WITH OPTIONAL GEOGRID)
MUCK
MUCK
CONTACT (APPROXIMATE)
NATIVE MINERAL SOILS
10'
BRAUN
CB9-172 SOILS INVESTIGATION
Embankment Failure
CSAH 21: 1 mile N of
the City of Rice, MN
Date 9-8-89
Revised
Drawn
Scale

Figure 2.7 Cross section of U.S. Highway 10 in Rice, Minnesota after Palmer and Verdegan (1989)

was a 2.5-in. base course over 12 in. of conventional granular fill. Eight 20-ft long test sections were constructed as shown in Fig. 2.8 and as given in Table 2.1 below.

Table 2.1: Dane County Landfill #2 Test Sections

Section	Fill Material
1	12-in. thick alternating layers of loam and tire chips
2 & 3	3 ft of tire chips, 2 ft of loam, 12 in. conventional soil cap (using two different chip sources)
4 & 5	5 ft of tire chips, 12 in. conventional soil cap (using two different chip sources)
6	5 ft of 40% tire chips and 60% soil (by weight), 12 in. conventional soil cap
7 & 8	fiber and loam mixes (0.09 and 0.18% by weight)

Compaction of all materials, including the tire chips, was accomplished using a vibratory sheepsfoot roller in both vibratory and static modes. Settlement plates were installed to be monitored with surface surveys, but no settlement data was reported. Leachate water was collected for an environmental analysis using two leachate collection lysimeters.

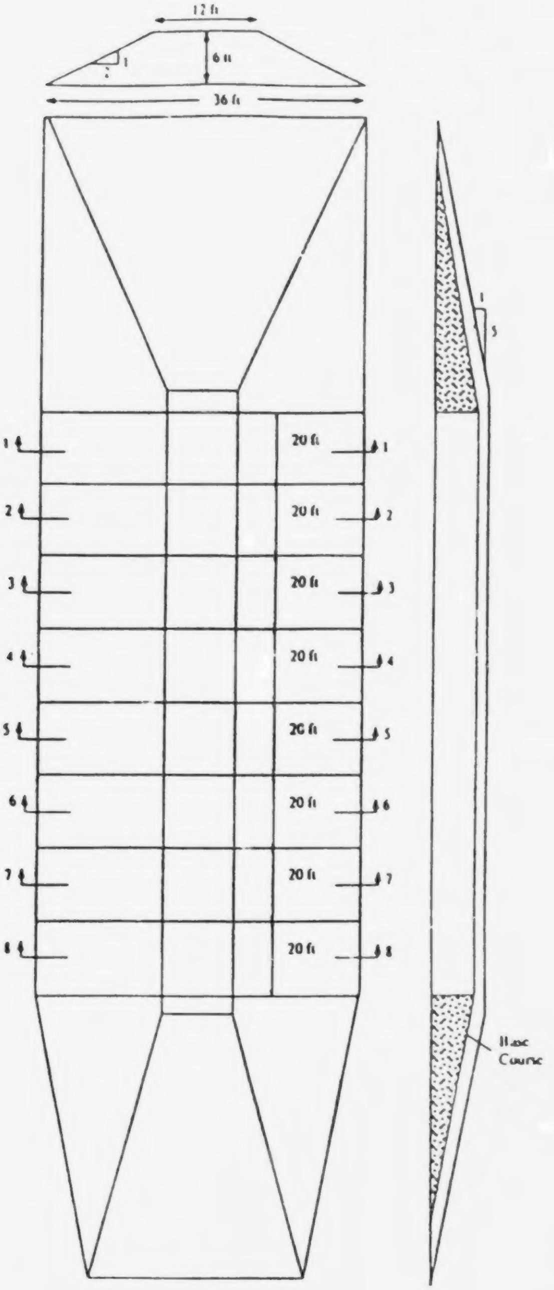
12 ft
6 ft
2
1
36 ft
1
2
3
4
5
6
7
8
20 ft
20 ft
20 ft
20 ft
20 ft
20 ft
20 ft
20 ft
1
2
3
4
5
6
7
8
1
5
Base Course

Figure 2.8(a) Plan of the test embankment at Dane County Landfill #2, Wisconsin after Edil, et al. (1990)

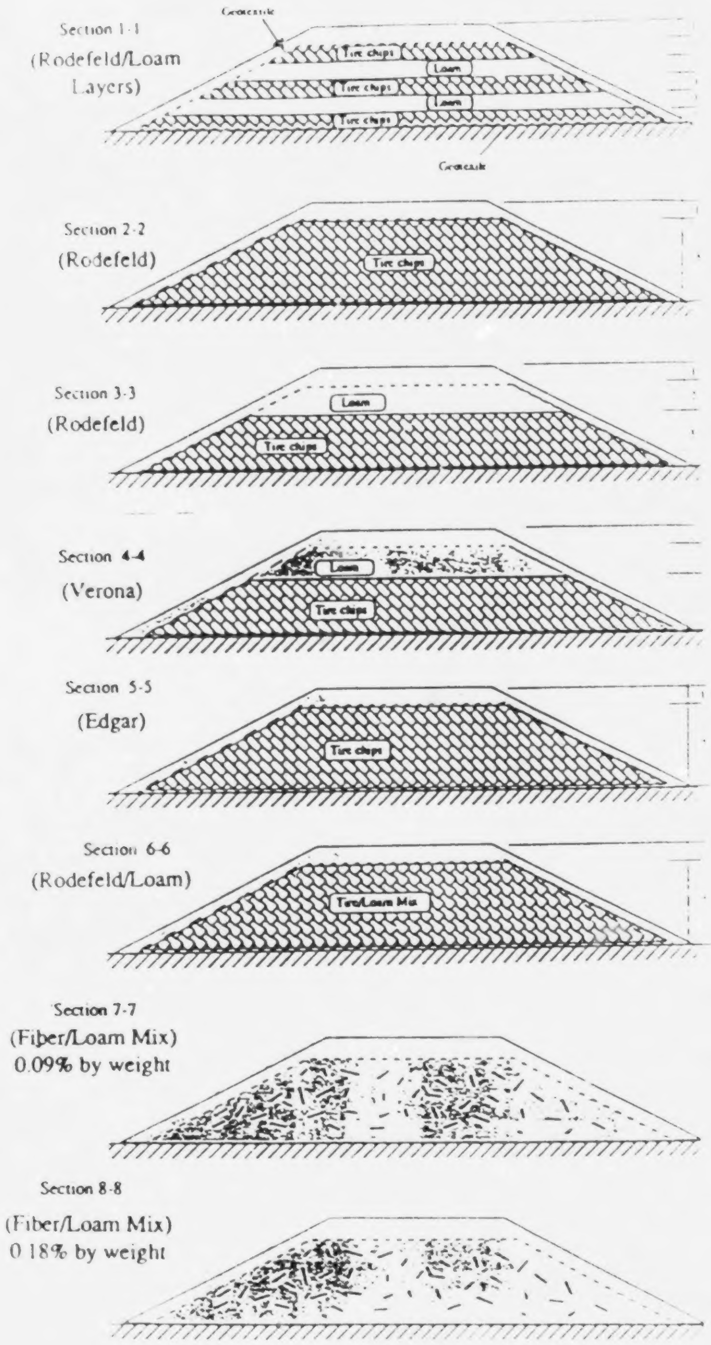
Section 1-1
(Rodefeld/Loam Layers)
Geotextile
Tire chips
Loam
Tire chips
Loam
Tire chips
Geotextile
Section 2-2
(Rodefeld)
Tire chips
Section 3-3
(Rodefeld)
Loam
Tire chips
Section 4-4
(Verona)
Loam
Tire chips
Section 5-5
(Edgar)
Tire chips
Section 6-6
(Rodefeld/Loam)
Tire/Loam Mix
Section 7-7
(Fiber/Loam Mix)
0.09% by weight
Section 8-8
(Fiber/Loam Mix)
0.18% by weight

Figure 2.8(b) Sections through the test embankment at Dane County Landfill #2, Wisconsin after Edil, et al. (1990)

2.6.5 Camas Valley Landslide- Oregon Highway 35

In Oregon, a 300-ft section of Highway 35 in the Camas Valley, along Muns Creek, was destroyed in a landslide (Dodson, 1990). To lighten the weight of the new embankment, tire chips were used as lightweight fill up to 16 ft in depth. Compaction of the tire chips was achieved in 2 to 3-ft lifts using 3 full coverage passes of a Caterpillar D-8 sized dozer. Drainage with geotextile and French drains were used below the fill, and a geotextile covered with 3 ft of granular fill was placed above the tire chips as shown in Fig. 2.9.

2.6.6 Putnamville, Vermont slope flattening

In the Town of Middlesex, Hamlet of Putnamville, Vermont, a project was undertaken to flatten side slopes along a portion of Route 12, to eliminate the need for a guardrail (Winters, 1991). The 2738 cy of shredded tires were placed as slope fill up to 18 ft deep, flattening the slope from 1.5(H):1(V) to 3(H):1(V). Tire chip compaction was accomplished in 18-in. lifts with several passes of a 5-ton dozer. The tire chips were purchased from suppliers in North Ferrisburg, Vt, and New Hampshire. As shown in Fig. 2.10 the tire chip fill was covered with filter fabric and 2 ft of earth fill. The finished site was then fine graded, seeded and mulched.

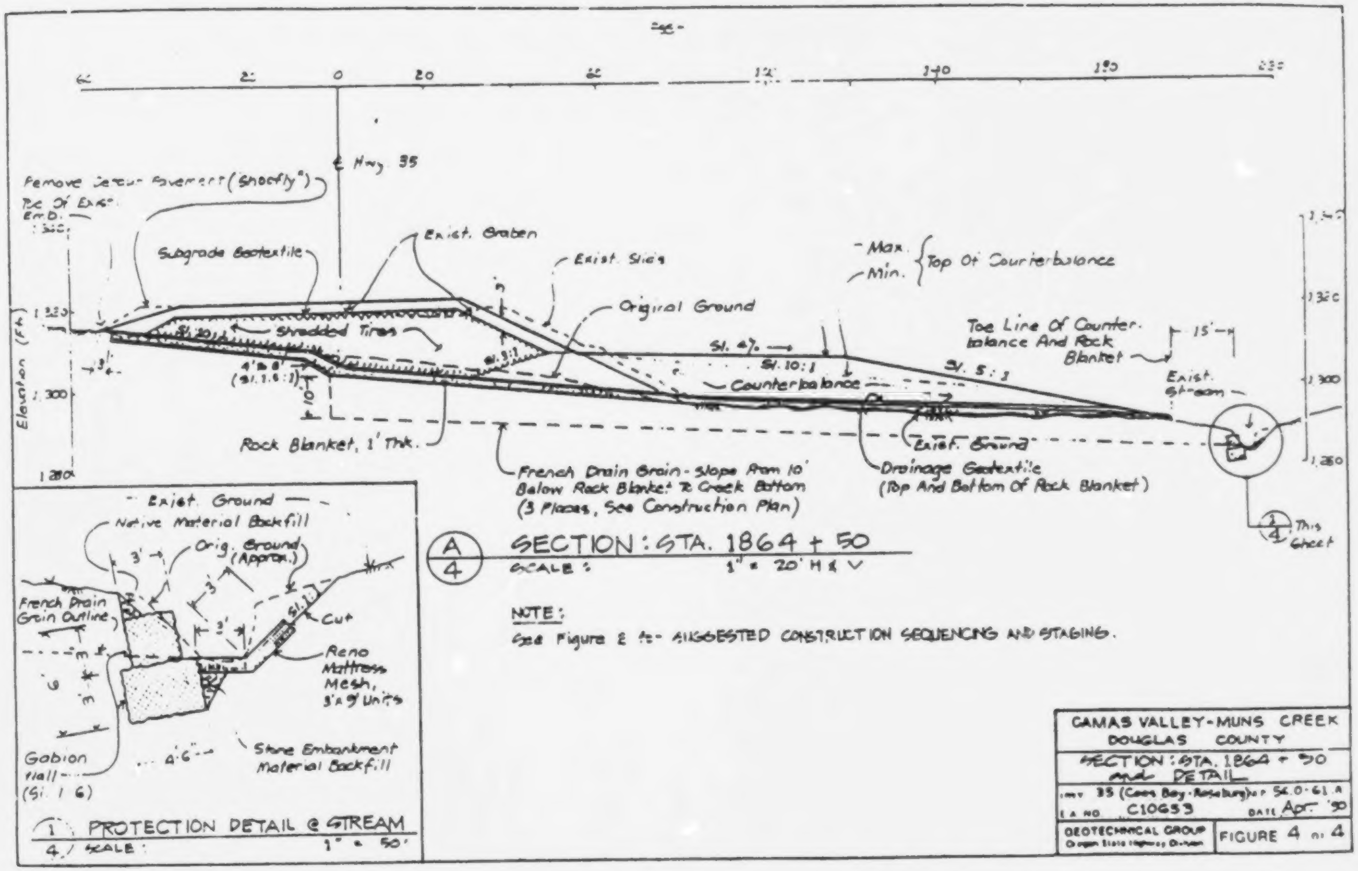
60
20
0
20
60
100
140
180
220
¢ Hwy. 35
Remove Detour Pavement ("Shoofly")
Toe Of Exist. Emb.
1,320
Subgrade Geotextile
Exist. Graben
Exist. Slide
Original Ground
Shredded Tires
Sl. 20:1
Sl. 3:1
4'± 8'
(Sl. 1.5:1)
3'±
Elevation (Ft.)
1,300
1,280
Rock Blanket, 1' Thk.
French Drain Grain - Slope From 10' Below Rock Blanket To Creek Bottom (3 Places, See Construction Plan)
- Max.
- Min.
Top Of Counterbalance
Sl. 4%
Sl. 10:1
Counterbalance
Sl. 5:1
Toe Line Of Counterbalance And Rock Blanket
15'
Exist. Stream
Exist. Ground
Drainage Geotextile (Top And Bottom Of Rock Blanket)
1,340
1,320
1,300
1,280
1/4 This Sheet
A/4 SECTION : STA. 1864 + 50
SCALE : 1" = 20' H & V
NOTE:
See Figure 2 for SUGGESTED CONSTRUCTION SEQUENCING AND STAGING.
Exist. Ground
Native Material Backfill
3'
Orig. Ground (Approx.)
3'
3'
French Drain Grain Outline
Cut
Sl. 1:1
Reno Mattress Mesh, 3'x 9' Units
Gabion Wall (Sl. 1:6)
4'6"
Stone Embankment Material Backfill
1/4 PROTECTION DETAIL @ STREAM
SCALE : 1" = 50'
CAMAS VALLEY-MUNS CREEK
DOUGLAS COUNTY
SECTION : STA. 1864 + 50 and DETAIL
HWY 35 (Coos Bay-Roseburg) M.P. 56.0-61.A
E.A. NO. C10653
DATE Apr. '90
GEOTECHNICAL GROUP
Oregon State Highway Division
FIGURE 4 of 4

Figure 2.9 Cross section through the Camas Valley Landslide - Oregon Highway 35 repair after Dodson (1990)

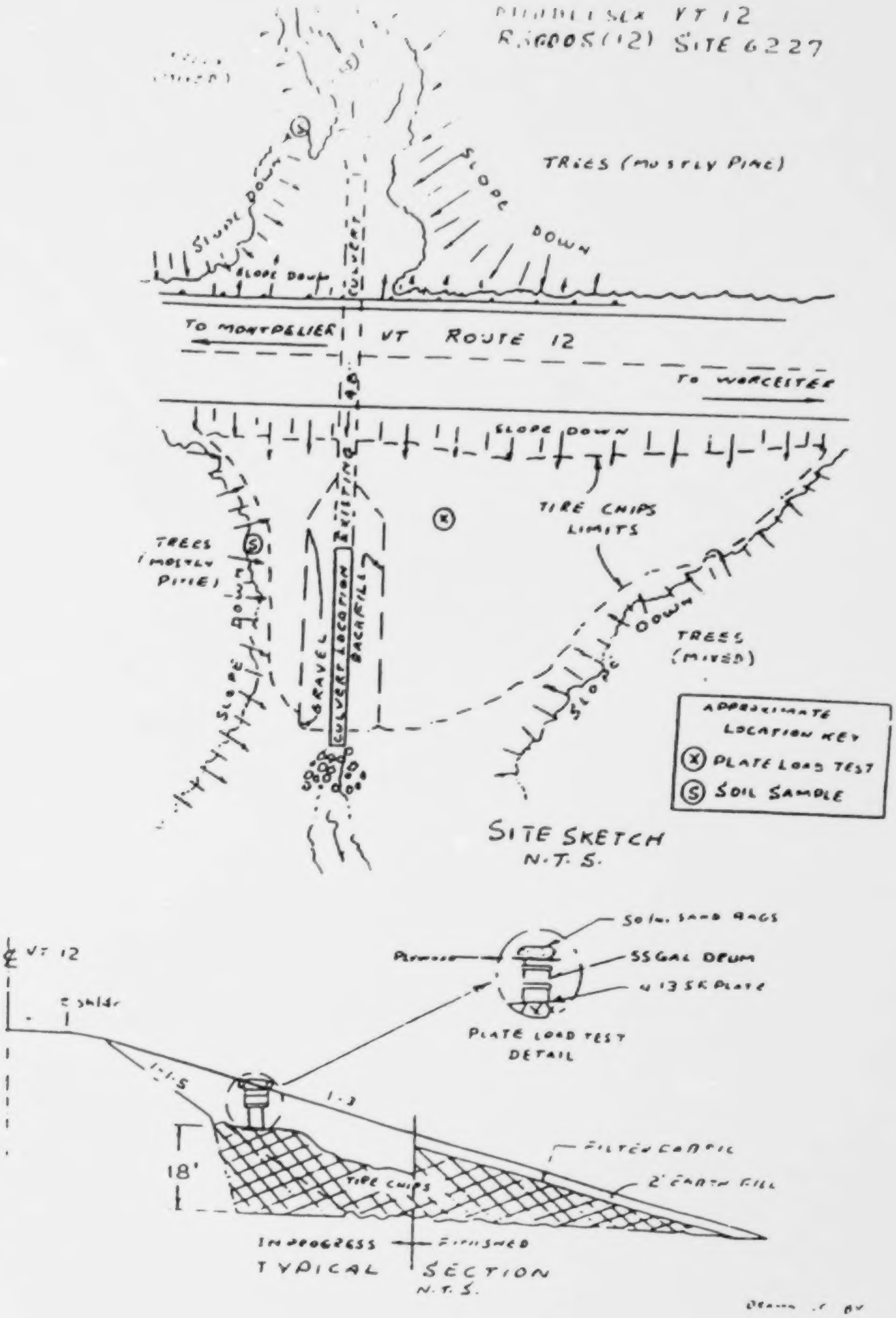
MIDDLESEX VT 12
RS 6005(12) SITE 6227
TREES (MOSTLY PINE)
SLOPE DOWN
SLOPE DOWN
SLOPE DOWN
CULVERT
TO MONTPELIER
VT ROUTE 12
TO WORCESTER
SLOPE DOWN
TIRE CHIPS LIMITS
TREES (MOSTLY PINE)
SLOPE DOWN
EXISTING
GRAVEL
CULVERT LOCATION
BACKFILL
SLOPE DOWN
TREES (MIXED)
APPROXIMATE LOCATION KEY
Ⓧ PLATE LOAD TEST
Ⓢ SOIL SAMPLE
SITE SKETCH
N.T.S.
℄ VT 12
℄ shldr
1:1.5
1:3
50 lb. SAND BAGS
55 GAL DRUM
12 SK PLATE
PLATE LOAD TEST DETAIL
18'
TIRE CHIPS
FILTER FABRIC
2' EARTH FILL
IN PROGRESS
FINISHED
TYPICAL SECTION
N.T.S.

Figure 2.10 Plan and section through tire chip fill used in Putnamville, Vermont Rt. 12 slope flattening after Winters (1991)

2.6.7 Georgia, Vermont town highway base

On Town Highway 4, known as the Oakland Station Road, a 300-ft long test section was constructed, starting 1.7 miles north of the junction with Route 7 (Frascoia, 1991). The roadway consisted of 2 ft of gravel over a silty sand subgrade soil containing 24 to 43% fines. In the spring mud season, a high water table typically made the road almost impassible, due to contamination of the gravel with fines from the silty sand. Construction involved the removal of about 24 in. of existing base material and 6 in. of subgrade soils and placement of 9 to 12 in. of loose tire chips. Tire chips were hauled to the site in dump trucks and placed with a backhoe. Additional compaction and measurement of compression after backfilling with granular fill were not performed. A typical section through the roadway as in Fig. 2.11 shows the 6-in. compressed layer of tire chips beneath a maximum of 22 in. of clean gravel. About 200 cy of mixed size tire chips were utilized from a plant in Ferrisburg, Vt. One month after construction was completed, an inspection of the test section revealed some fine longitudinal cracks in the gravel surface in or near the right wheel path of the southbound lane. Some transverse cracks were also noted but rutting was not evident. About 3 months after construction, no distress was noted in the test section or adjacent roadway. It

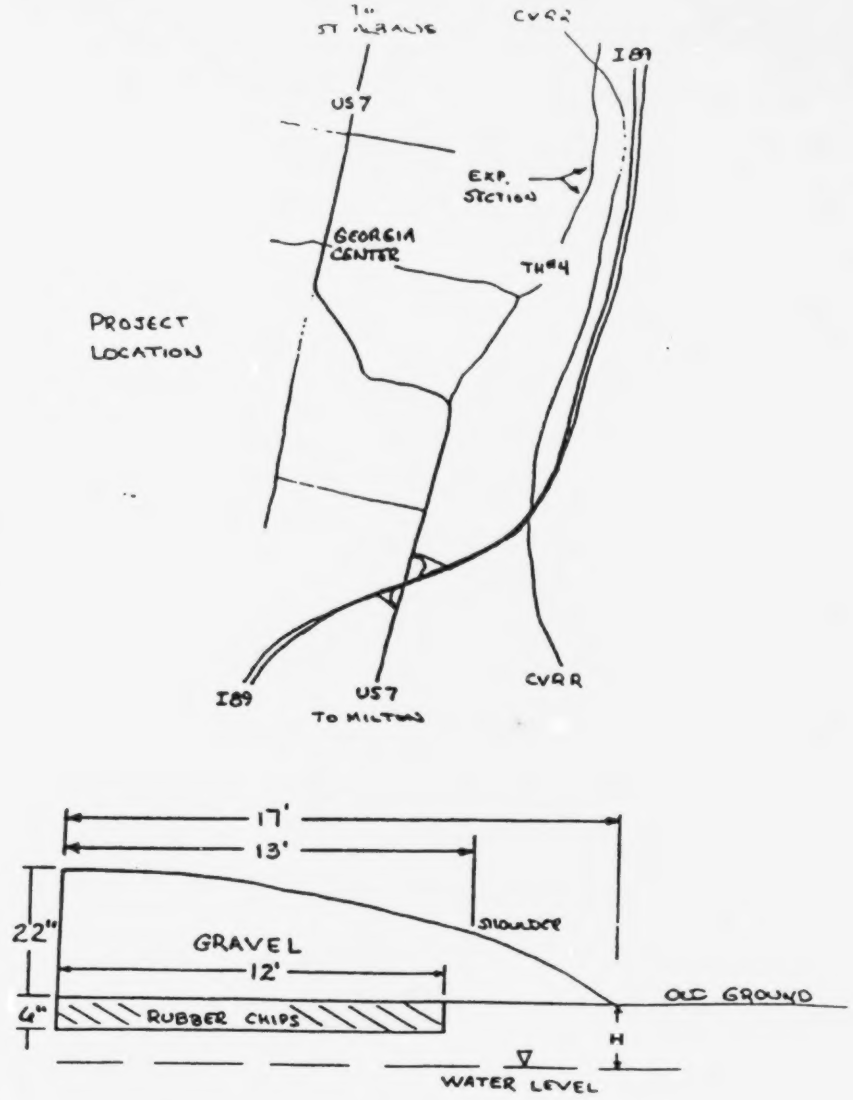
TO ST ALBANS
CVRR
I89
US7
EXP. SECTION
GEORGIA CENTER
TH#4
PROJECT LOCATION
I89
US7
TO MILTON
CVRR
17'
13'
22"
SHOULDER
GRAVEL
12'
4"
RUBBER CHIPS
OLD GROUND
H
WATER LEVEL

ROADWAY TYPICAL

Figure 2.11 Location and section through Georgia, Vermont town highway base after Frascoia (1991)

was noted that the test section froze several days after the rest of the road. The following spring, some 7 months after construction, a few fine longitudinal and transverse cracks were evident, with most in the southbound lane. To maintain drivability on the adjacent road, the surface had been graded about 7 times in the previous month. Compared to the nearby road, which was wet, cracked, and rutted, the test section was in good shape, being dry and free of ruts. It is possible that the comparatively milder winter, dry spring season and the clean gravel over the test section may have contributed to the noted differences in performance. The author concluded that the tire chips prevented the capillary rise of the ground water, and provided drainage for the gravel layer, preventing the typical mud season conditions that occurred on the adjacent roadway.

2.6.8 New Route I 76, Denver, Colorado

The Colorado Department of Highways used tire chips for embankment fill over a section of landfill in the construction of I 76 in northwest Denver (Colorado Dept. of Highways Research Newsletter, 1991). The 300-ft long embankment surrounded a 5-ft thickness of tire chips contained on all sides with geotextile and covered with about 3 ft of conventional soil fill on the top and side slopes. A cross section is shown in Fig. 2.12. Performance results are not yet available.

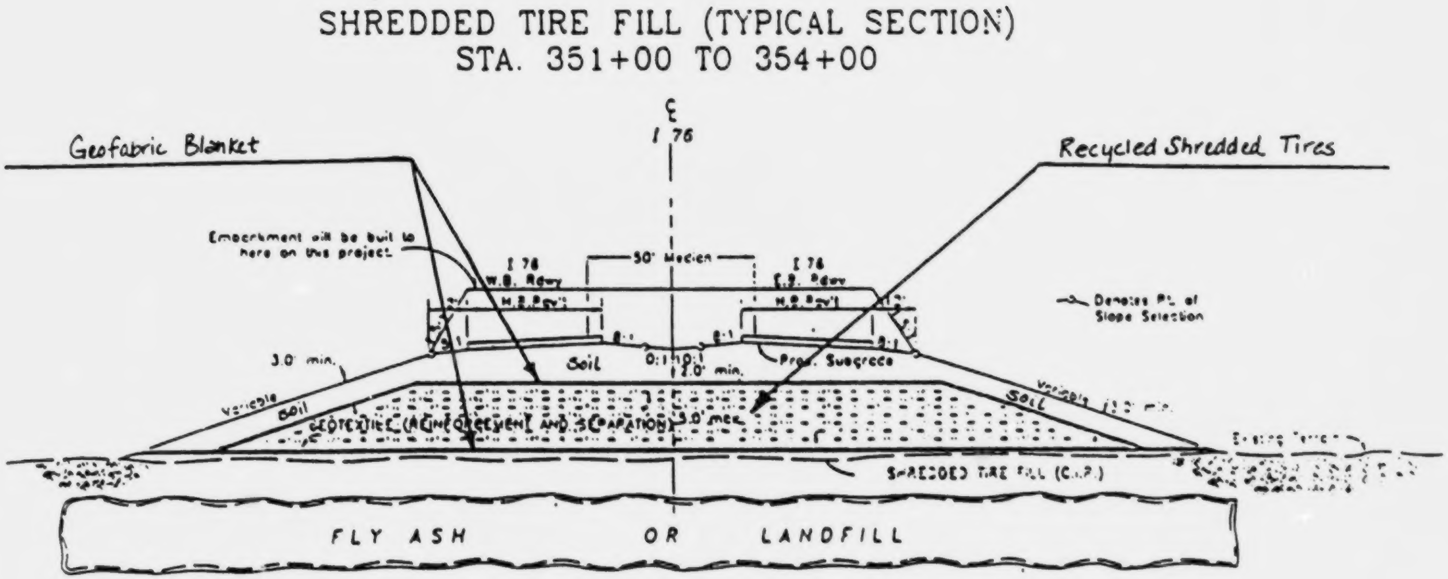
SHREDDED TIRE FILL (TYPICAL SECTION)
STA. 351+00 TO 354+00
℄
I 76
Geofabric Blanket
Recycled Shredded Tires
Embankment will be built to here on this project
50' Median
I 76
W.B. Rdwy
I 76
E.B. Rdwy
Denotes Pt. of Slope Selection
3.0' min.
Soil
2.0' min.
Prop. Subgrade
Variable
Soil
GEOTEXTILE (REINFORCEMENT AND SEPARATION)
3.0' max.
Soil
Variable
Existing Terrain
SHREDDED TIRE FILL (C.I.P.)
FLY ASH OR LANDFILL

Figure 2.12 Section through Rt. I-76 near Denver, Colorado after Colorado Department of Highways (1991)

2.7 ENVIRONMENTAL EFFECTS

The use of tire chips in road embankment construction may have the potential to cause environmental damage, although currently it is believed to be minimal. Edil, et al. (1990) found that tire chips show no likelihood of being a hazardous waste, and further state that "By comparison to other wastes for which leach test and environmental monitoring data are available, the tire leach data indicate little or no likelihood of shredded tires to have effects on ground water." Their findings were based on duplicate EP toxicity and AFS leaching tests performed by the Wisconsin State Laboratory of Hygiene. Metals concentration testing showed the highest iron and manganese concentrations at or above applicable drinking water standards and barium and zinc well below allowable concentrations. Overall, Edil, et al. (1990) concluded that "shredded tires leach very small amounts of substances compared to other wastes."

A report published by the Minnesota Pollution Control Agency (1990) contained a number of conclusions relating to the results of their laboratory and field studies. They found that leaching of metals from tire materials is highest under acid conditions while polynuclear aromatic hydrocarbons (PAHs) and total petroleum hydrocarbons leach in higher concentrations in basic environments. In comparison, asphalt materials may leach more pollutants than tire materials in some environments. Worst case conditions may cause drinking water Recommended Allowable Limits (RALs) to be exceeded. Limits for Co-disposal and E.P. Toxicity are not typically exceeded. Field studies were basically inconclusive, indicating the need for further work in this area. Their overall recommendation was to use tire chips above the water table and somehow keep water from moving through them.

During this research, the Maine Department of Environmental protection was contacted for their concerns about using tire chips either above or below the ground water table. They responded with verbal approval to use tire chips above the ground water table, but were more concerned with using tire chips below the ground water table.

2.8 SUMMARY

The limited literature available on the use of tire chips as conventional or lightweight fill contained mostly qualitative observations. Those observations indicated that road embankments made with tire chips have been successful in a wide variety of situations, from county roads to interstate highways. Thickness of soil cover between a tire chip layer and road surface ranged between 1 and 5 ft. However, engineering data and specific construction procedures were not generally available. Researchers have recently begun to investigate the actual engineering properties of tire chips for use as lightweight fill.

CHAPTER 3. BASIC ENGINEERING PROPERTIES

3.1 INTRODUCTION

The gradation, specific gravity, and compacted unit weight of tire chips were determined using slightly modified conventional test procedures. Samples were obtained on two separate occasions from a stockpile at the Sawyer Environmental Recovery facilities in Hampden, Maine. The tire chips are a mix of steel and fiberglass belted tires, chipped to a maximum size of 2 in. by a hydraulic chipping machine. Chips which contained a large portion of steel belt had been removed with a magnetic separator.

3.2 GRADATION

The gradation of the tire chips was determined using AASHTO designation T 27-84, "Sieve analysis of fine and coarse aggregates" (AASHTO, 1986a). The samples were air dried prior to testing. Sieve opening sizes, in inches, were 2, 1-1/2, 1, 3/4, 1/2, 3/8, 1/4, and standard #8. Individual sample sizes ranged from 12 to 18 lbs.

The results of the gradation analysis are presented in Fig. 3.1. It is seen that the tire chips are nearly 90% larger than 1/2-in. (12.7 mm), and 50% between 1 and 1-1/2 in. (25.4 and 38.1 mm). Curves for the 6 samples from mixed steel and glass belted tires plot in a relatively narrow band. The other two samples

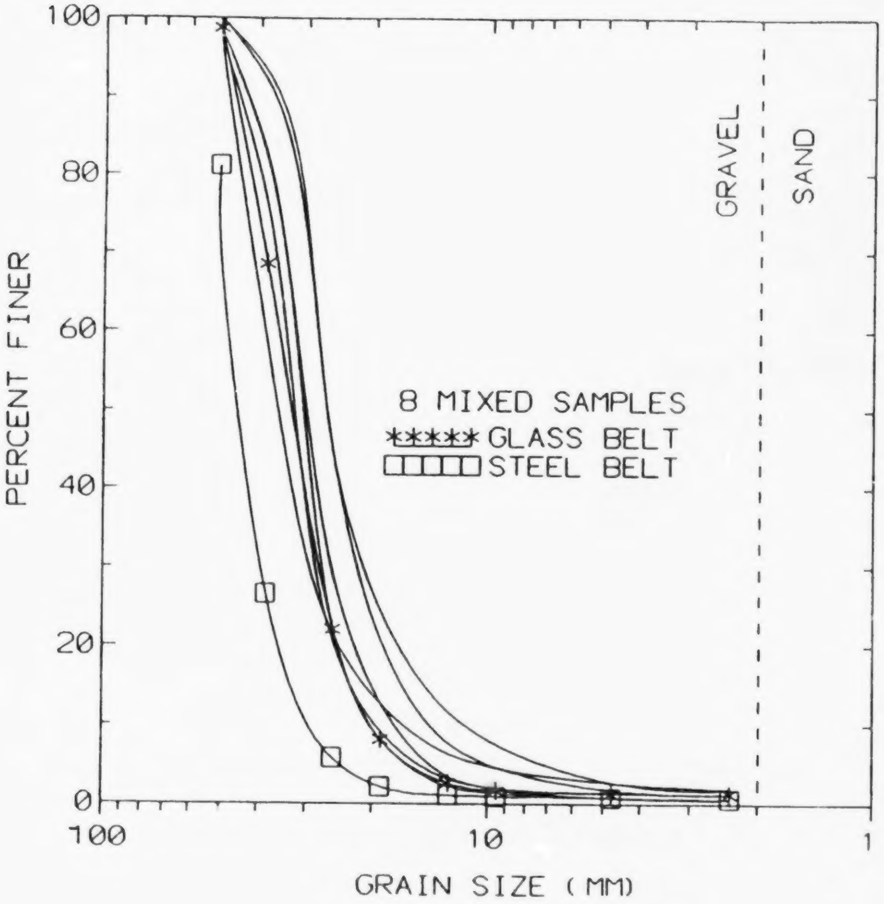

Figure 3.1 Gradation of tire chips

were composed entirely of steel belted tire chips or glass belted tire chips, separated by hand. The fiber belt sample gradation plots within the same range as the standard mixed samples, but the steel belt curve indicates larger overall particle sizes. Small size particles of steel belted tire chips are probably removed with the steel removal magnet in the manufacturing process. Smaller (0.5 in.) diameter tire chips from steel belted tires generally had a lot of protruding steel belt. Very few of these particles were noticed, since the magnetic separator probably removed most of them.

3.3 SPECIFIC GRAVITY

The specific gravity of the tire chips was determined using AASHTO designation T 85-85, "Specific gravity and absorption of coarse aggregate," (AASHTO, 1986a). However, the samples were air dried rather than oven dried prior to beginning the test. Three types of samples were tested: steel belts only, glass belts only, and mixed. Bulk, saturated surface dry, and apparent specific gravities were calculated. The applicability of each specific gravity depends on moisture condition of the aggregate as described by AASHTO (1986a): "bulk specific gravity (oven dry) is used for computations when the aggregate is dry or assumed to be dry ... bulk specific gravity (SSD) is used if the aggregate is wet, that is, if its absorption has been satisfied ... apparent specific gravity pertains to the relative density of the solid material making up the constituent particles not including the pore space within the particles which is accessible to water."

Two samples each of steel and glass belts and four samples of mixed steel and glass belts were tested. Results are summarized in Fig. 3.2. It is seen that the specific gravities of the steel belt mixture are the highest, while they are the lowest for fiber belts. The saturated surface dry specific gravities of each mixture are greater than one so they sink when placed in water. Absorption capacities were also determined at about 4% for all samples.

3.4 COMPACTED UNIT WEIGHT

The compacted unit weight of tire chips was determined using a procedure similar to AASHTO designation T 180-86, "Moisture density relations of soils using a 10-lb rammer and an 18-in drop," (AASHTO, 1986a). Method D, using the 6-in. diameter mold and material passing a 3/4-in. sieve and retained on a #4 sieve, was used initially. However, less than 25% of any sample passes a 3/4-in. sieve so this test was not representative of the entire sample.

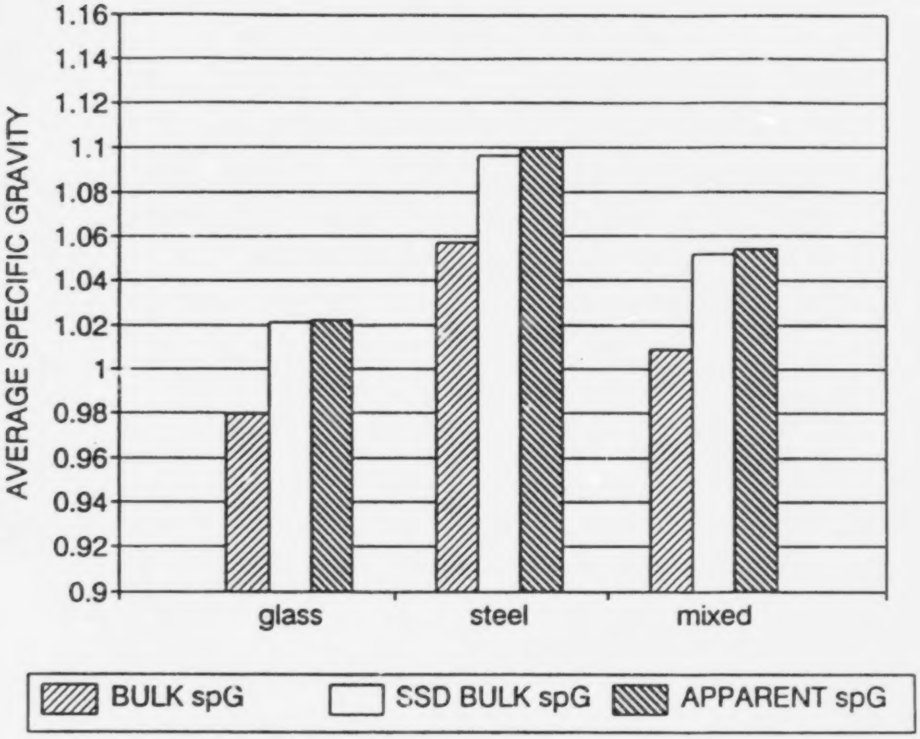

Figure 3.2 Specific gravity of tire chips

To accommodate the larger particle sizes, a 10-in. diameter by 10-in. high mold was used. The volume of the mold was determined to be 0.44 cf using a graduated cylinder to fill the mold with water. The new test used the modified proctor 10-lb hammer with an 18-in. drop, five compaction layers, and with the number of blows per layer adjusted to give equivalent compacted energy.

Tests were made using three different levels of energy, to determine the effect of energy level on unit weight. The energy levels correspond to modified proctor, standard proctor and 60% of standard proctor. The energy per unit volume and the required number of blows per layer for each energy level are shown in Table 3.1. Compacted unit weight of air dried samples was found to decrease only slightly with decreasing energy level, as shown in Table 3.1. This suggests that energy level has only a small effect on compacted unit weight. Therefore, for convenience, subsequent testing was done using the 44 blow per layer, 60% standard proctor energy. The effect of moisture content was investigated by testing samples both air dried and saturated surface dry. The values contained in Table 3.1 indicate that the addition of moisture has a negligible effect, so subsequent samples were tested air dried.

Table 3.1: Summary of compacted unit weights

Test Standard	Energy per unit volume (ft-lb/ft^3)	Blows per layer	Dry unit weight
Modified	56,250	330	41
Standard	12,375	73	40
60% Standard	7,425	44	39 *
60% Standard (compacted SSD)	7,425	44	38
Loose	0	0	25

* average of three tests

The unit weights for three samples compacted dry with 60% of standard proctor energy ranged from 38 and 40 pcf showing the effects of sample variability. When moisture was added to a saturated surface dry condition, the dry unit weight was determined to be 38 pcf, indicating that moisture content does not have a significant effect on the compacted unit weight of tire chips. Samples for subsequent tests were compacted using air dried samples. For comparison, an uncompacted unit weight of 25 pcf was determined by pouring a sample into the compaction mold. Compacted unit weights of glass belt and steel belt chips alone, separated by hand, did not significantly vary from the 39 pcf mixed average.

BLANK

CHAPTER 4. SETTLEMENT ANALYSIS

4.1 INTRODUCTION

Since one of the major benefits of using tire chips is their low unit weight, two representative groups of settlement analyses were performed to estimate potential decrease in consolidation settlement. Consolidation settlement analyses were performed for three heights (10, 20, and 30 ft) of road embankment section over three different thicknesses (10, 25, and 50 ft) of native Maine peat or Presumpscot clay formation with and without tire chip fill for a total of 36 cases.

4.2 MATERIAL PROPERTIES

Specific engineering properties of the Presumpscot clay formation were derived from the soils report "A Subsurface Investigation for the Proposed Replacement for the Maine Turnpike-Falmouth Spur (I-95) Bridges over the Canadian National Railroad in Falmouth," by the Maine Department of Transportation (King, et al., 1988). Based on this report, a saturated unit weight of 120 pcf and $C_c/(1+e_o)$ of 0.149 were used.

Specific engineering properties of the peat were derived from a soils report by the Maine Department of Transportation on the "Subsurface Investigation for the proposed Reconstruction of a portion of Route 77, Cape Elizabeth, Cumberland County," Maine (Beniwal, et al.,

Preceding page blank

1971) Based on this report a water content of 600% and unit weight of 67 pcf were used.

4.3 METHODOLOGY

The crest width of the embankment was assumed 44 ft, with 3 horizontal to 1 vertical side slopes. A 4-ft thick layer of conventional fill was used directly below the road surface in all cases. Water table elevation was maintained at the original ground surface. Settlement calculations for the Presumpscot formation followed conventional cohesive soil consolidation settlement analysis methods (Das, 1990). Secondary consolidation settlement was not included.

A slightly modified conventional technique as proposed by the New York State Department of Transportation (Batchelder Adams, 1984) was used for the peat. This technique includes both primary and secondary consolidation settlements, and is essentially the same as presented in Das (1990) with the following exceptions. The compression index C_c is determined using the relationship

$$C_c = 0.01(w_c)$$

where w_c is the natural water content. The initial void ratio e_o is determined using the relationship

$$e_o = 0.02(w_c)$$

The coefficient of secondary compression C_α is determined from Fig. 4.1, a plot of C_α versus w_c. The void ratio at the end of primary consolidation e_f is calculated using

$$e_f = e_o - C_c \log (P_f/P_o)$$

where P_f is the final effective stress and P_o is the initial effective stress. The change in void ratio during secondary consolidation Δe_{sc} is computed using

$$\Delta e_{sc} = C_\alpha \log (t_{sc}/t_o)$$

where t_{sc} is the field time after primary consolidation under consideration, measured from the time of load application and t_o is the time at the end of primary consolidation, measured from the time of load application. Finally the secondary consolidation S_s is calculated using

$$S_s = (H \Delta e_{sc})/(1 + e_f)$$

where e_f is the void ratio at the end of primary consolidation, found using a chart from Batchelder Adams (1984) showing e_f versus w_c for a number of ratios P_f/P_o as shown in Fig. 4.2.

Since many of the original computed settlements over the peat were in excess of 6 ft, an iterative circular spreadsheet calculation was implemented to keep the

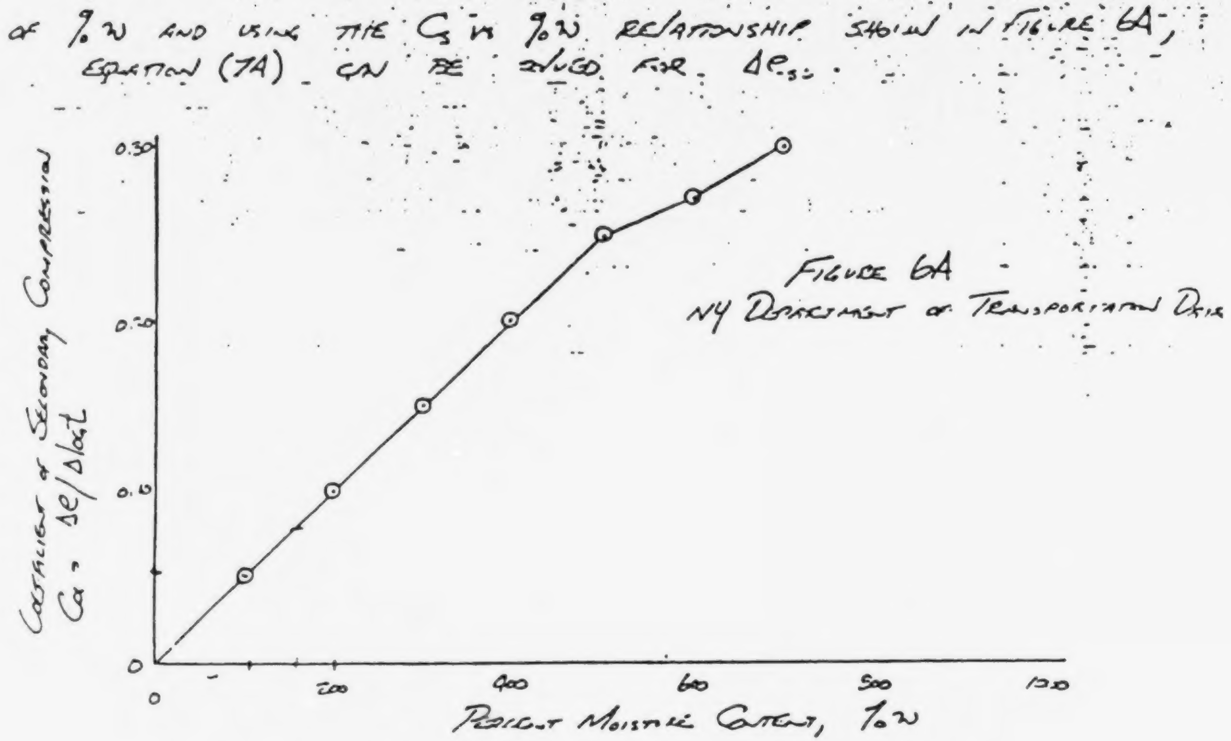

OF %W AND USING THE C_s VS %W RELATIONSHIP SHOWN IN FIGURE 6A, EQUATION (7A) CAN BE SOLVED FOR Δe_{s}.

Figure 4.1 Coefficient of secondary compression versus moisture content after Batchelder Adams (1984)

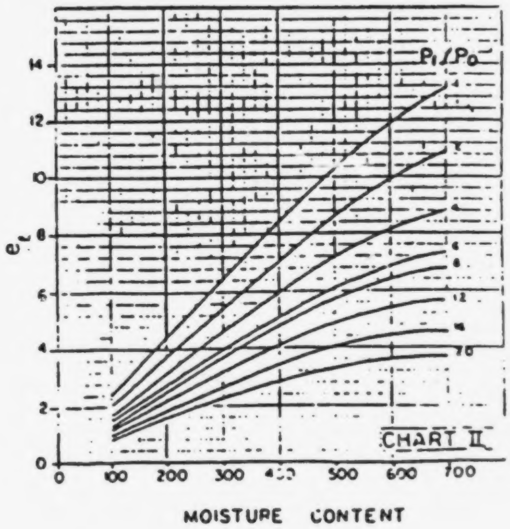

Figure 4.2 Void ratio at end of primary consolidation versus moisture content after Batchelder Adams (1984)

original road surface elevation constant. Basically, in each iteration, tire chip fill or granular fill was added to the base of the embankment, to compensate for calculated settlement, and then a new settlement was computed. The amount of fill added was equal to the computed primary settlement. The buoyant unit weight of the fill material was used for fill which settled below the ground water table. Roughly ten iterations were required to reach equilibrium.

4.4 RESULTS

Computed settlements with and without using tire chips were compared in graphical form as shown in Figs. 4.3 and 4.4. Over the Presumpscot formation, settlements using tire chips were reduced 26 to 42% from settlements without tire chips. For the peat, similar (25 to 43%) reductions in settlement can be achieved. These reductions in settlement are significant, as illustrated by the case with 50 ft of peat and a 30-ft embankment, where the computed settlements were reduced from 36 ft without tire chips to 22 ft with tire chips.

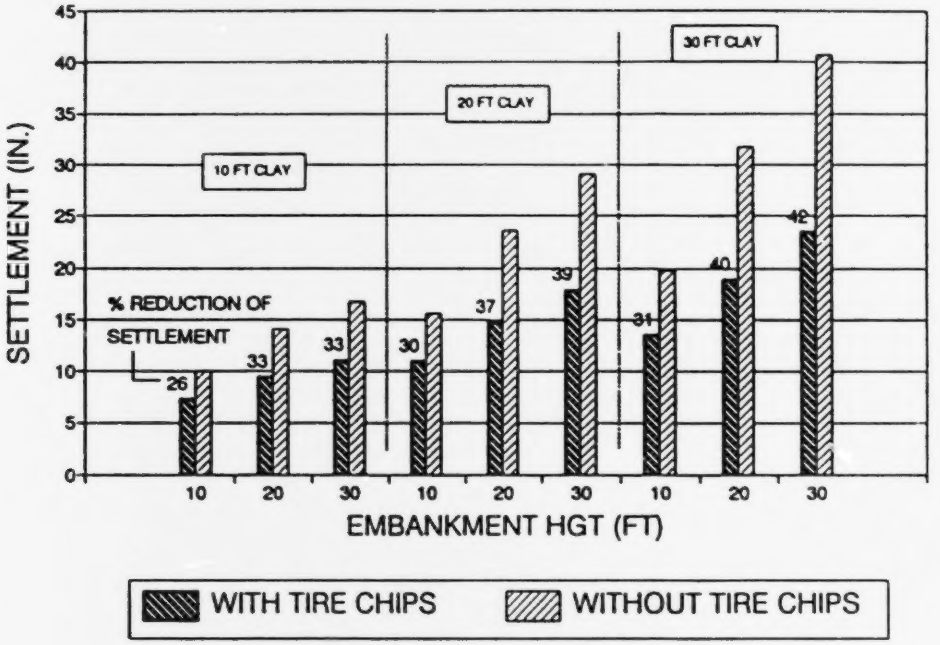

Figure 4.3 Consolidation settlement on Presumpscot with and without tire chips

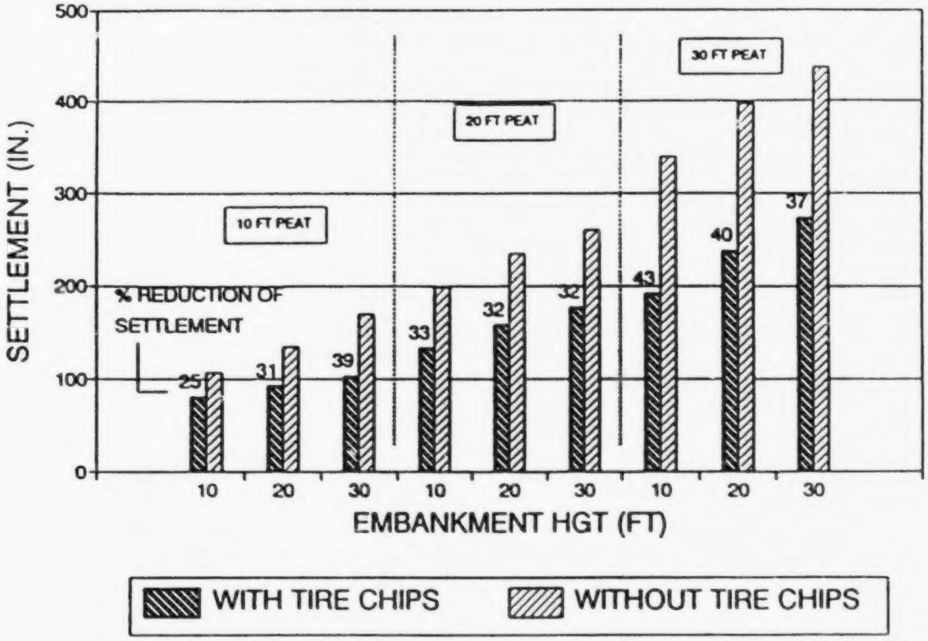

Figure 4.4 Consolidation settlement on peat with and without tire chips

CHAPTER 5. COMPRESSIBILITY

5.1 INTRODUCTION

One of the key goals of this research was to predict pavement deflections under load, when tire chips are used as fill in an embankment. To do this, the compressibility properties of tire chips, namely Young's modulus and Poisson's ratio, were required. Due to the large particle sizes and high compressibility of tire chips, small conventional compressibility and consolidation equipment, designed for use with cohesive fine grained soils, could not be used. A large scale custom apparatus was designed and built to accommodate the special characteristics of tire chips, as described below.

5.2 APPARATUS

Preliminary testing of 10-in. diameter by 6 to 8-in. high samples of compacted tire chips showed that vertical strains approaching 50% were possible. Thus, the compressibility apparatus had to accommodate large volume changes. Additionally, to obtain a value of Poisson's ratio, it was necessary to measure horizontal stress in the sample. To accommodate these requirements, the final design consisted of a 12.5-in. long piece of schedule 40 PVC pipe, with a nominal inside diameter of 12 in. and wall thickness of 0.32 in. Strain gages were used to measure circumferential and vertical strains in the container resulting from stresses in the sample during testing. Micro Measurements 0.25-in. long single axis bonded 1000 ohm resistance strain gages, model EA-13-250BK-10C were selected, based on recommendations by the Micro Measurements company and available stock.

It was theorized that the pipe, with an elastic modulus in tension of about 440,000 psi would expand sufficiently under horizontal stress imposed by the sample to be measured by circumferentially mounted strain gages. Strain gage equipment and economic constraints limited this measurement to four gages. In anticipation of an average sample height during testing of 7 in., the four circumferential gages were mounted 3.5 in. from the base. The bottom of the cylinder was supported on a 0.75-in. thick smooth steel plate, allowing the base of the cylinder to expand as freely as possible. To eliminate problems with inconsistencies in the pipe dimensions and elastic properties, a direct calibration was made between the horizontal stress applied to the inside of the pipe and resultant strains measured by the strain gages, as discussed in the next section.

The friction between the tire chips and the wall of the pipe was expected to be significant due to the high sliding friction of rubber and the pieces of steel belt protruding from the tire chips. To measure the load transferred by friction from the sample to the cylinder wall, two strain gages were mounted vertically 3.5 in. above the base on opposite sides of the pipe. This was at the same height as the circumferential gages so that the vertical and horizontal stress in the sample were known at the same location, giving better data for calculation of Poisson's ratio. A direct calibration was made for the vertical gages. The following section details the calibration procedures and results.

The vertical load was applied using an Instron 4204 universal testing machine controlled by an IBM compatible 286 computer through an IEEE-488 port. The IEEE-488 port provided computer control of the deformation rate, as well as obtaining load and deflection measurements. To measure strains from the strain gages mounted on the cylinder, wheatstone bridge completion circuits were fabricated using high precision Micro Measurements resistors. A nominal excitation voltage of 4 volts was input into the bridge. Electronic resistance strain gages work by changing resistance when being strained and wheatstone bridges transfer that change in resistance to a change in voltage. The excitation voltage (input) and the output voltages from the six strain gages were read by a Strawberry Tree 16 bit analog to digital board (model ACPC-16) installed in the computer. The analog to digital board was rated as accurate to within 0.00076 millivolts over a 50 millivolt range. To partially compensate for electronic noise and imbalance, ten voltage readings were taken and averaged each time a strain reading was taken. The general layout of the apparatus is shown in Fig. 5.1.

The first test revealed a design defect. Upon unloading of the sample, the friction from the swelling sample moved the cylinder several inches off the base. Consequently, clamps were fabricated to hold the cylinder against the baseplate during unloading cycles only. The force produced by clamping increased the strain in the cylinder, causing strain readings to show increased force in the cylinder and thus an apparent decrease in the vertical stress carried by the sample. This effect was considered in evaluation of the unloading cycles.

5.3 CALIBRATION

Extensive calibrations were performed to determine relationships between circumferential strain and internal pressure, strain versus ambient temperature, and vertical strain versus vertical load. To develop the relationship between circumferential strain and horizontal stress, a 30-in. length of pipe was used to minimize end effects. The portion that was used for the test cylinder and the circumferential strain gages were at the center of the

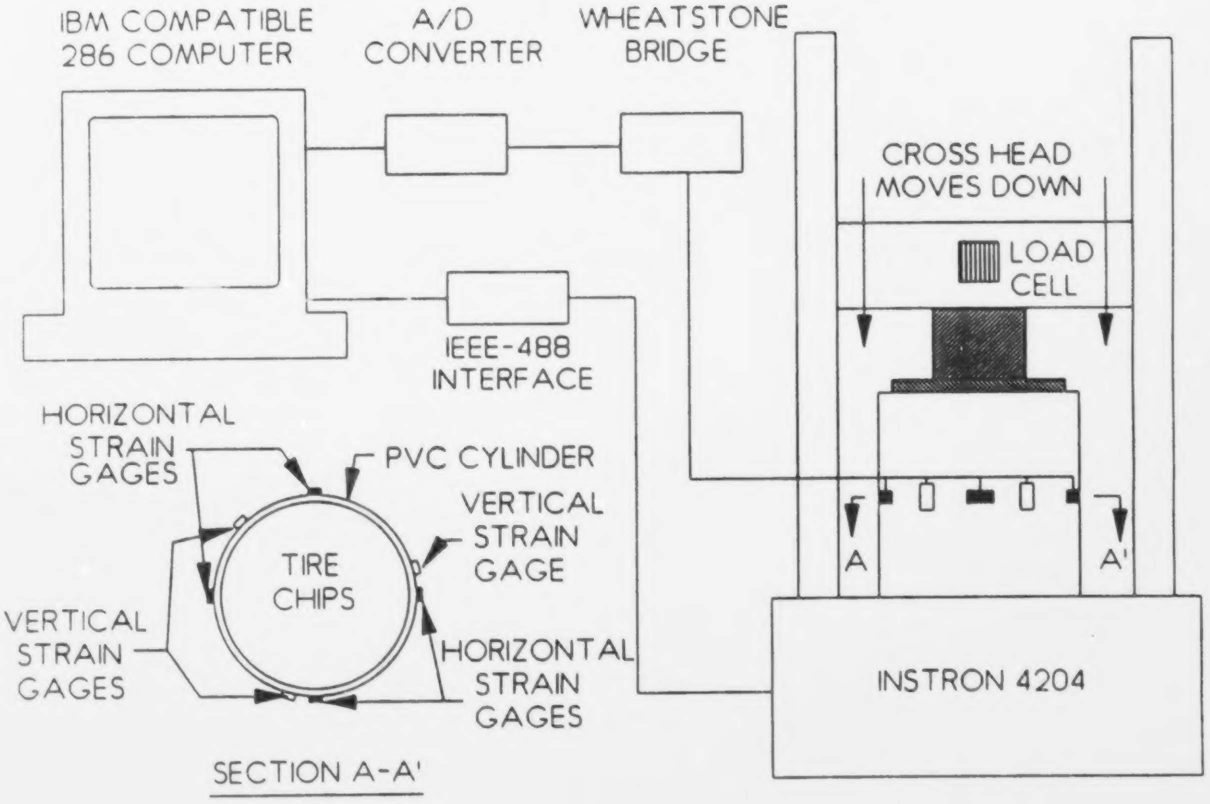
IBM COMPATIBLE
286 COMPUTER
A/D
CONVERTER
WHEATSTONE
BRIDGE
CROSS HEAD
MOVES DOWN
LOAD
CELL
IEEE-488
INTERFACE
HORIZONTAL
STRAIN
GAGES
PVC CYLINDER
VERTICAL
STRAIN
GAGE
TIRE
CHIPS
VERTICAL
STRAIN
GAGES
HORIZONTAL
STRAIN
GAGES
A
A'
INSTRON 4204
SECTION A-A'

Figure 5.1 Apparatus used for compressibility testing

30-in. length. The pipe was capped with gasketed 0.75-in. thick PVC plate backed by 0.75-in. thick structural plywood. Eight 0.5-in. diameter threaded rods spaced around the outside diameter of the pipe provided the capping pressure. The capped pipe was filled with water, incremental pressures from 10 to 70 psi were applied, and circumferential strains were measured through the strain gages. The stress imposed by capping caused some bulging of the pipe and thus circumferential strain, which was deducted from the calibration. After many repetitions, an average curve of circumferential strain vs. pressure was prepared, and a second order equation relating internal pressure from given circumferential strain was determined through regression analysis. The final calibration curve, with an R squared value of 0.999971 is shown in Fig. 5.2. However, at pressures less than 10 psi there was insufficient strain to exceed the precision of the calibration setup, and a meaningful regression was impossible. Therefore, below 10 psi, the relationship was assumed to be linear to the origin.

There was some concern about creep in the pipe under long term loading and temperature changes causing strain. Therefore, long term tests of up to 60 hours were conducted at moderate pressures (30-40 psi), monitoring change in strain of the cylinder gages. Ambient temperature was measured at the cylinder gages and at an unstrained dummy gage mounted to a scrap piece of pipe.

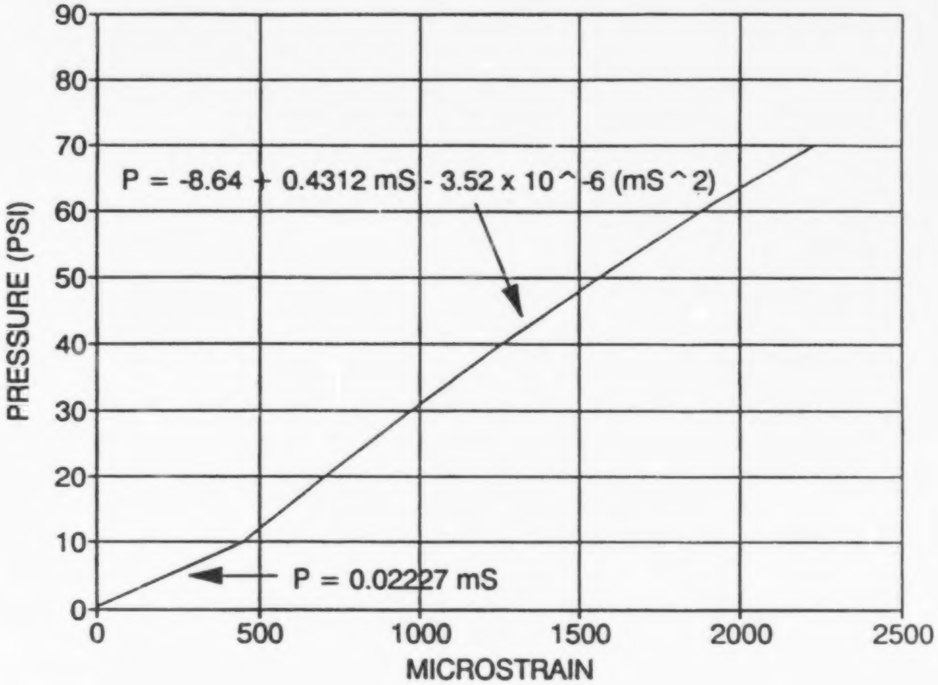

Figure 5.2 Horizontal strain gage pressure calibration curve for compressibility testing

A linear relationship was developed between temperature and induced strain with an R squared value of 0.869, as shown in Fig. 5.3. Long term creep of the pipe under pressure was determined to be negligible.

Due to concerns about end restraint effects, a horizontal stress calibration using the same system as described above was performed on the cylinder at its final 12.5-in. height. The resulting curve plotting water pressure applied against the stress measured by the strain gages is plotted in Fig. 5.4. The plot shows a small amount of deviation from the straight line, indicating an effect of further restraining the ends of the cylinder. Since the end restraint during testing was significantly less than that applied with the capping, end end restraint effects should have had a negligible influence on the results.

The relationship between vertical load and vertical strain was developed after cutting the cylinder to its final height simply by applying a vertical load to the top of the cylinder and measuring the resultant vertical strains. The vertical load to vertical strain calibration, with an R squared value of 0.99995 is shown in Fig. 5.5. Due to imperfect fit between the bottom of the cylinder and the steel baseplate, the cylinder had to be placed in the exact same position for testing as in calibration.

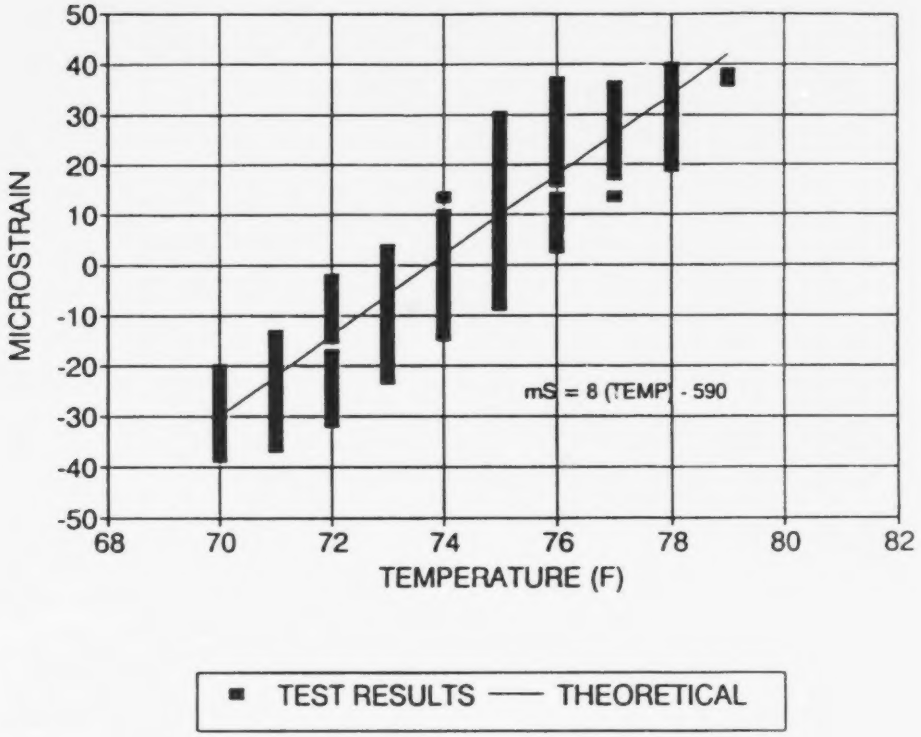

Figure 5.3 Effect of temperature on strain gage measurement for compressibility testing

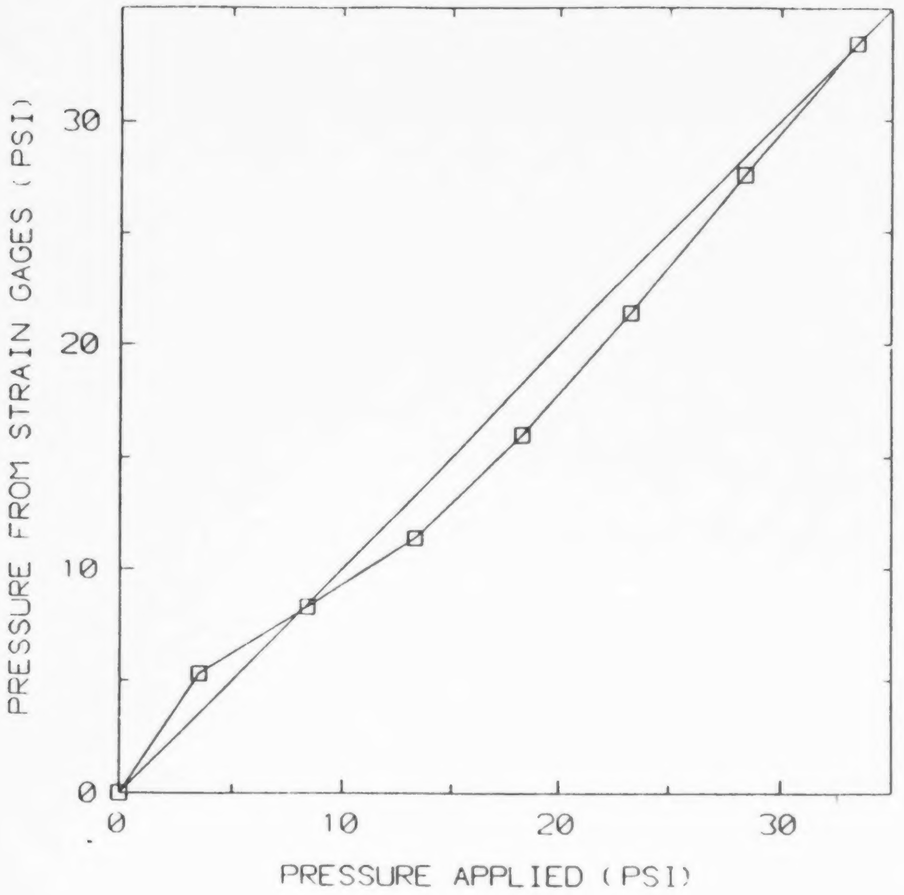

Figure 5.4 Horizontal strain gage calibration check, using 12.5-in. long cylinder

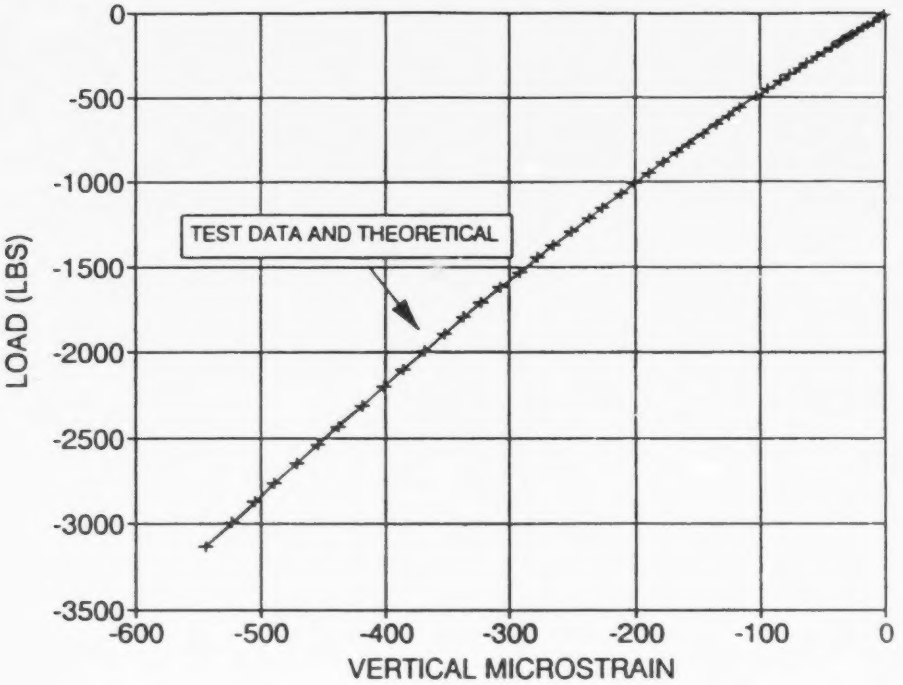

$$P = -11.75 + 4.41\ mS - 0.003\ mS^2 - 1 \times 10^6\ mS^3$$

Figure 5.5 Vertical strain gage load calibration curve for compressibility testing

The relationships between circumferential strain and internal pressure, and vertical strain and vertical load were input as calibrations into the computer program controlling testing and compiling data, as described in Section 5.4.

5.4 TESTING METHODOLOGY

A program was written in BASIC to record and compile the data. The operating scheme of the program, called LMTCC (Laboratory Measurement of Tire Chip Compressibility), is as follows:

1. The interface boards are initialized.
2. General data is input such as the date, test number, mixture type, output mode, and initial sample height.
3. The initial data arrays are created for storage of strain gage readings and the initial ten unstrained voltage readings are taken, averaged, and stored.
4. Load application is begun at 0.5 in. per minute.
5. The computer takes readings of applied load, crosshead movement, and ten voltage readings of each strain gage channel at 10 second intervals. Thus a set of readings is taken every 0.083 in. of deformation. For each set of readings the following steps occur.

a. Current load and crosshead movement are read from the Instron through the IEEE-488 interface.

b. Ten voltage readings are taken through the analog to digital board for each channel. The average for each channel is computed and used with the initial readings to calculate the strain for each gage with the following relationships.

$V_r = V_{out}/V_{in}$ strained - V_{out}/V_{in} unstrained

Strain = $(-4\ V_r)\ /\ [GF \times (1 + 2\ V_r)]$

where: V_{out} = voltage output from wheatstone bridge

V_{in} = voltage input to wheatstone bridge

GF = gage factor given with strain gages

The circumferential strain is calculated as the average strain from the four circumferential gages. The correlation of horizontal stress with circumferential strain (see Section 5.3) is used to compute the horizontal stress (σ_h at gage). Similarly, the two vertical strains are used with the correlation of load in the cylinder with vertical strain to calculate the load transferred to the cylinder through friction at the gage height.

c. The vertical strain (ϵ_v) of the sample is computed using the crosshead movement and initial sample height.

d. The vertical stress in the sample at the gage height (σ_v at gage) is calculated by subtracting the load carried by the cylinder at gage height from the applied load and then dividing by the sample area.

e. The average vertical stress (σ_v avg) is a more complicated process. The force transferred by friction to the cylinder was assumed to increase linearly from zero at the top to a maximum at the bottom but it is only measured at 3.5 in. from the base as shown in Fig. 5.6. The average stress carried by the sample (σ_{avg}) should occur at the mid height of the sample, and is calculated using the following relationship.

$$P_{avg} = P_{applied} - [(hgt/2) \times P_{frict}/(hgt-3.5)]$$

where: P_{frict} = friction load measured by gages

$P_{applied}$ = current applied load

hgt = sample height when readings were taken

The average vertical stress (σ_v avg) is then computed by dividing P_{avg} by the sample area.

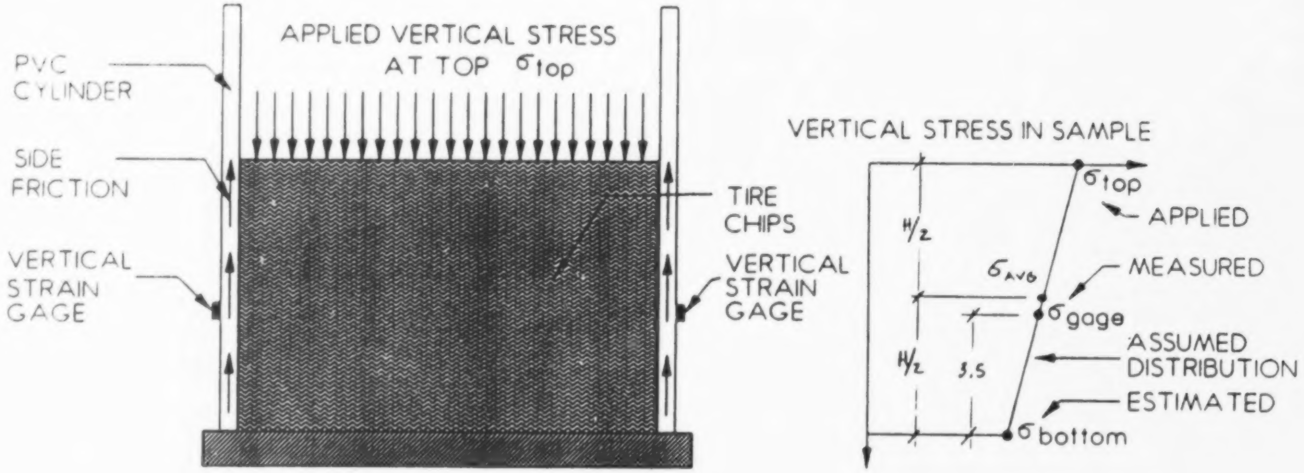
APPLIED VERTICAL STRESS
AT TOP σ_{top}
PVC CYLINDER
SIDE FRICTION
VERTICAL STRAIN GAGE
TIRE CHIPS
VERTICAL STRAIN GAGE
VERTICAL STRESS IN SAMPLE
σ_{top}
APPLIED
H/2
σ_{AVG}
MEASURED
σ_{gage}
ASSUMED DISTRIBUTION
H/2
3.5
ESTIMATED
σ_{bottom}

Figure 5.6 Effect of side friction on vertical stress in sample during compressibility test

f. Data is printed to the output files. One file contains the average vertical strain (ε_V), average vertical stress (σ_V avg), vertical stress at gage height (σ_V at gage) and horizontal stress at gage height (σ_h at gage) for plotting. Another file contains more detailed information to be used as backup.

6. When maximum applied load is reached, near the 10,000 lb capacity of the testing machine, loading is stopped automatically and the user is prompted for the next test cycle.
7. For an unloading cycle, the load is removed at 0.5 in. per minute and the same process as in step 5 is used to take measurements.
8. Upon termination of the test, the standard format ASCII data output files can be imported into graphing software packages for plotting and analysis.

Specimens were prepared by compacting the tire chips using 60% of standard proctor energy into the cylinder clamped to the baseplate. Sample identification, general data and initial sample height were then input into the LMTCC computer program, the clamps were removed and the test was begun. As discussed in Section 5.2, the rate of loading used was 0.5 in. per minute, and readings of load, deflection, circumferential strains and vertical strains were taken every 10 seconds, and converted to average vertical strain (ϵ_v), average vertical stress (σ_v avg), vertical stress at gage height (σ_v at gage) and horizontal stress at gage height (σ_h at gage). At a vertical load of between 9 and 10 kips including load carried in the sample and load carried through friction in the cylinder, the computer program stopped the crosshead, clamps were applied to hold the cylinder to the baseplate, and unloading began at the same deformation rate of 0.5 in. per minute with the same readings at 10 second intervals. Typical tests involved two to three loading and unloading cycles.

Initial tests showed friction carrying 54% of maximum total load. Consequently, the sides of the cylinder were lubricated with pump grease, decreasing maximum friction to a maximum of about 40% of applied vertical load.

5.5 RESULTS

Three groups of tests were performed: compacted tire chips only, compacted mixtures of 50% (by weight) 2-in. minus MDOT type D gravel and tire chips, and compacted mixtures of 25%, 50%, and 75% 3/4-in. minus gravel with tire chips. The tire chip samples were obtained on several occasions from Sawyer Environmental Recovery in Hampden, Maine. Test results were used to calculate elastic parameters for use in pavement deflection analysis. Plots of all test results are presented in Appendix A and a summary of results is presented below.

5.5.1 Compressibility of Tire Chips Without Gravel

Average vertical strain (ϵ_v) versus average vertical stress (σ_v avg) and horizontal stress at gage height (σ_h at gage) versus vertical stress at gage height (σ_v at gage) for a typical test on compacted tire chips is shown in Figs. 5.7 and 5.8 respectively. The vertical stress-strain curve transitions smoothly from steep at low stress to flatter at higher stress. The gap between the unloading and reloading parts of the curve was caused at least in part by forces applied by the clamps, as described previously.

The plot of horizontal stress versus vertical stress shows a flatter slope at lower stresses and becomes linear at higher stresses with a slope of about 45 degrees. A similar behavior was observed for all tests. It is theorized that the flatter initial slope indicates the compression of voids in the sample, and that the steeper slope at higher stresses indicates primarily compression of the rubber. The unloading and reloading curves roughly parallel the initial loading curve. Although there appears to be an abrupt change in slope at a horizontal stress of 10 psi, it is really caused by the two different horizontal stress to circumferential

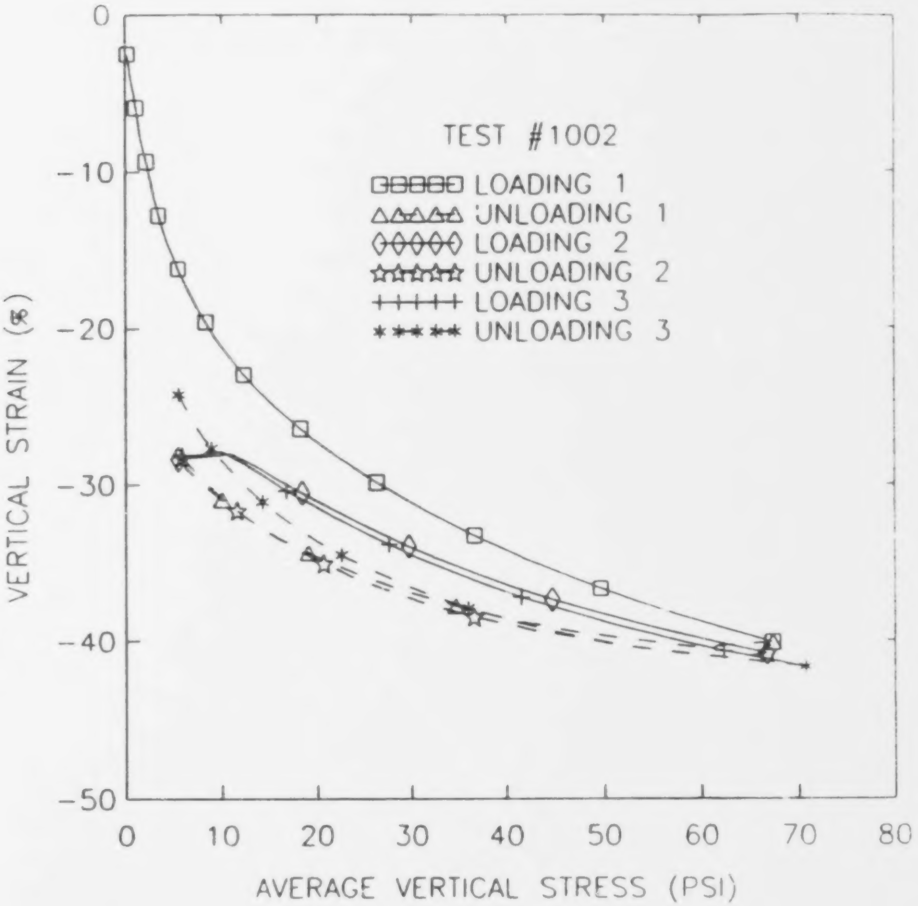

Figure 5.7   Typical vertical stress - strain load and unload curve for tire chips without gravel

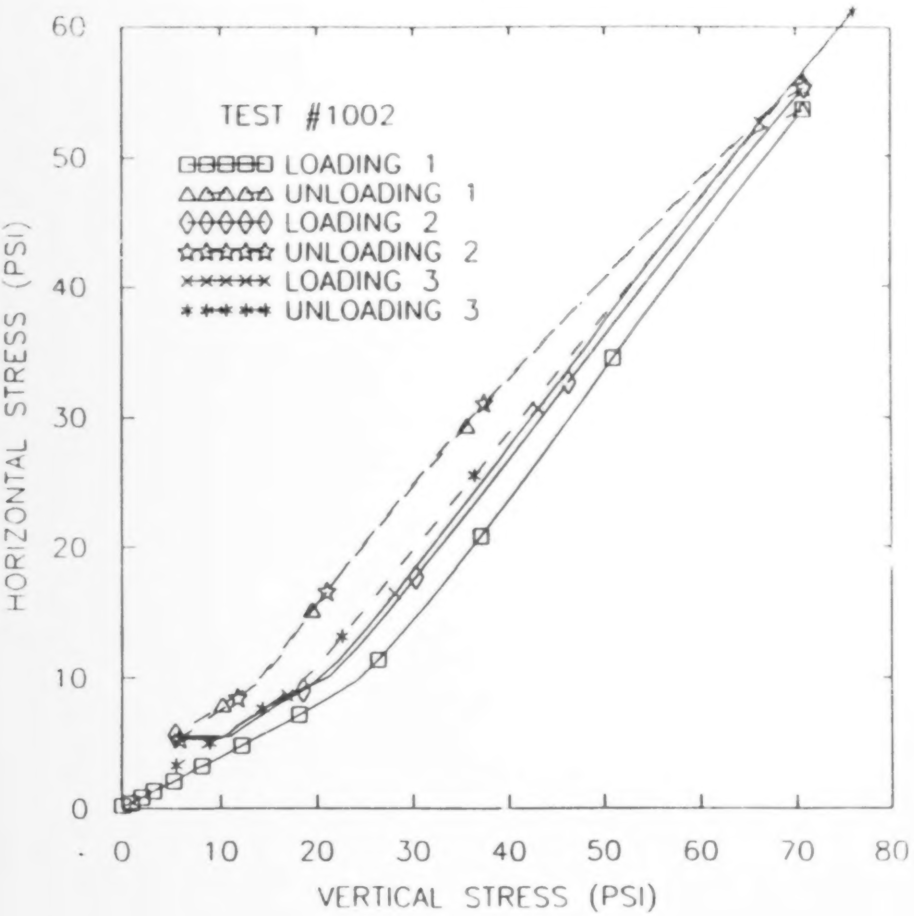

Figure 5.8 Typical horizontal - vertical stress load and unload curve for tire chips without gravel

strain calibrations. As shown previously in Fig. 5.2, at stresses increasing past 10 psi the correlation changes from linear to a second order polynomial. For comparison to conventional consolidation testing of soils, Fig. 5.9 shows a plot of vertical strain versus the logarithm of vertical stress.

For purposes of comparison, the initial loading portion of five tests are plotted together on Figs. 5.10 and 5.11. It is seen that all five test results follow the same general trend. A vertical stress of 10 psi will cause about 20% vertical strain and vertical strains reach 40% at average vertical stresses of about 60 psi. Overall, the results indicate high compressibility at low stresses, but decreasing significantly upon loading to higher stresses. The horizontal stress versus vertical stress curves follow the same general trend, as discussed above for Fig. 5.7.

Elastic parameters were calculated using the following methods and relationships. The coefficient of earth pressure at rest K_o was obtained from the slope of the vertical-horizontal stress curve.

$$K_o = \delta\sigma_h / \delta\sigma_v \text{ at gage height}$$

Values of K_o were computed separately for σ_v less than 23 psi and σ_v greater than 23 psi. K_o averaged 0.44 for the

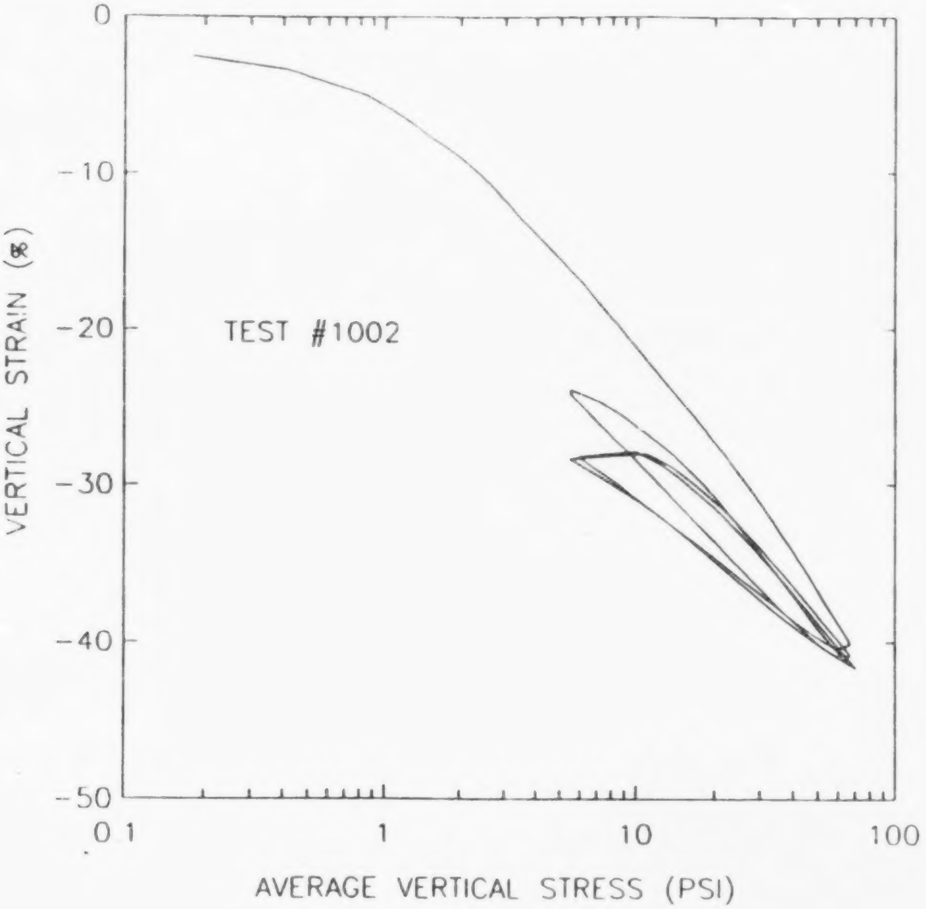

Figure 5.9 Typical vertical log stress - strain load and unload curve for tire chips without gravel

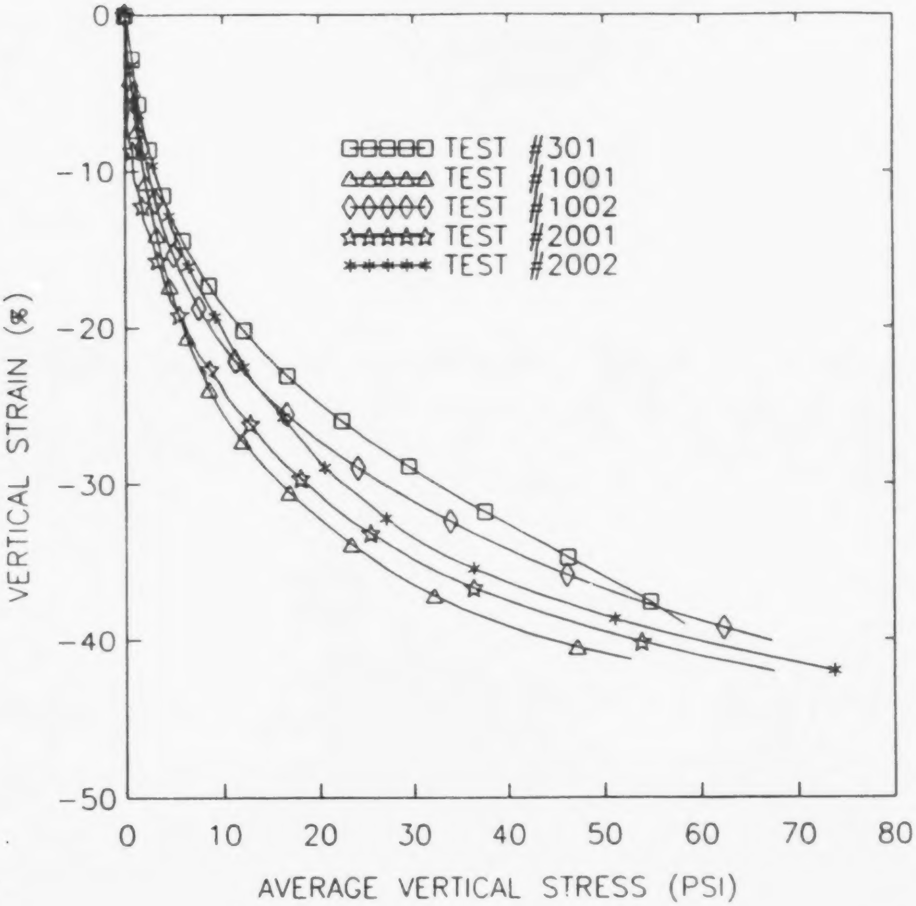

Figure 5.10 Five initial loading vertical stress - strain curves for tire chips without gravel

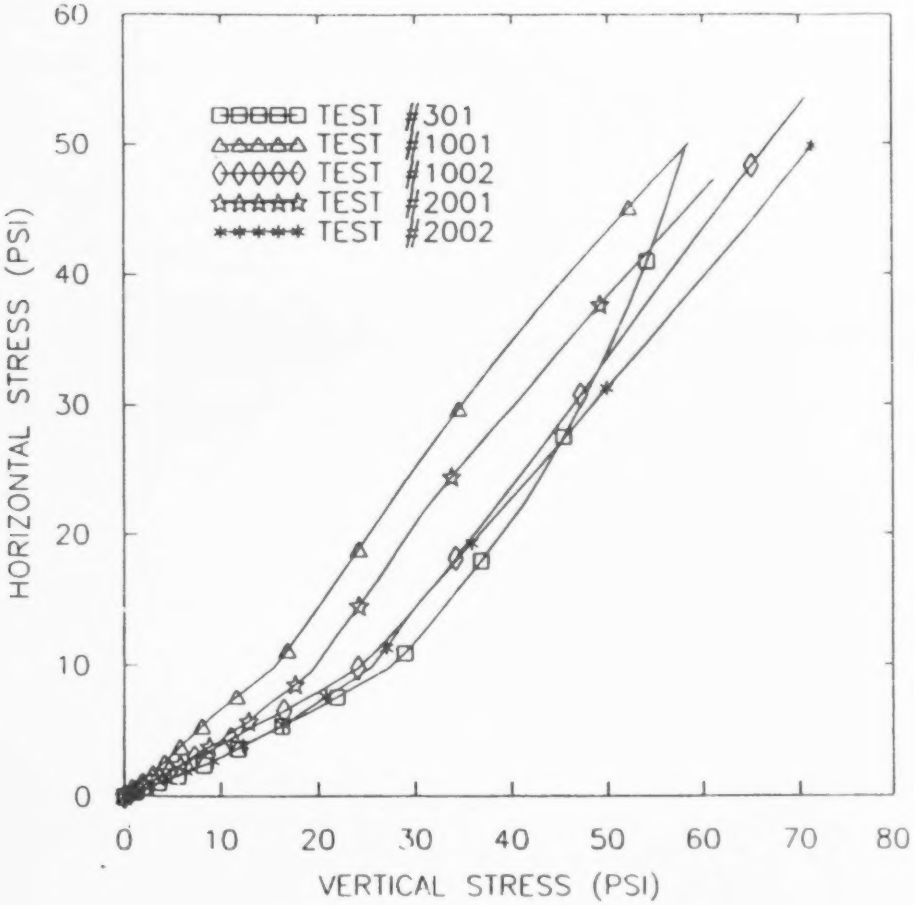

Figure 5.11 Five initial loading horizontal - vertical stress curves for tire chips without gravel

lower stress range and 0.98 for the higher stress range as shown in Table 5.1.

Table 5.1: K_o and Poisson's ratio from compressibility testing

test	part of curve	K_o	Poisson's ratio
301	$\sigma_v > 23$ psi	1.19	0.54
	$\sigma_v < 23$ psi	0.33	0.25
1001	$\sigma_v > 23$ psi	1.00	0.50
	$\sigma_v < 23$ psi	0.65	0.39
1002	$\sigma_v > 23$ psi	0.94	0.48
	$\sigma_v < 23$ psi	0.40	0.29
2001	$\sigma_v > 23$ psi	0.91	0.48
	$\sigma_v < 23$ psi	0.45	0.31
2002	$\sigma_v > 23$ psi	0.86	0.46
	$\sigma_v < 23$ psi	0.35	0.26
avg	$\sigma_v > 23$ psi	0.98	0.49
	$\sigma_v < 23$ psi	0.44	0.30

Poisson's ratio (μ) was computed with the following relation from Jaky (1948).

$$\mu = K_o \,/\, (1 + K_o)$$

Results for the lower and higher stress levels are shown in Table 5.1. It is seen that μ ranges between 0.25 and 0.39 for the lower stress levels with an average of 0.30. At higher stress levels μ averaged 0.49 which is the same as would be expected for rubber. For tire rubber, Poisson's ratio is about 0.5 and static Young's modulus ranges between 180 and 750 psi, depending on the part of the tire tested (Beatty, 1981). Since stress levels in the tire chips under field conditions were not likely to exceed 23 psi, the K_o and μ values for the upper part of the curve were not utilized further.

The slope of the vertical stress strain plot is equal to the constrained modulus D.

$$D = \delta\sigma_{v\ avg} / \delta\epsilon_{v}$$

Using Poisson's ratio and the constrained modulus, Young's modulus (E) can be calculated from (Lambe and Whitman, 1969)

$$E = (1 + \mu)(1 - 2\mu)D / (1 - \mu)$$

Young's modulus was calculated from constrained moduli at an initial tangent and secant values at 10% and 20% vertical strain. The results shown in Table 5.2 indicate a fairly wide range for each type of E.

Table 5.2: Young's modulus from compressibility testing

			Young's Modulus (psi)		
test	part of curve	Poisson's ratio	initial tangent	secant @ 10%	secant @ 20%
301	$\sigma_v < 23$ psi	0.25	18.0	25.0	50.1
1001	$\sigma_v < 23$ psi	0.39	3.4	9.0	14.4
1002	$\sigma_v < 23$ psi	0.29	12.9	21.6	37.3
2001	$\sigma_v < 23$ psi	0.31	3.6	10.1	24.5
2002	$\sigma_v < 23$ psi	0.26	17.2	24.5	40.5
avg	$\sigma_v < 23$ psi	0.30	11.0	18.1	33.4

Following is an example calculation of μ and E for test number 1002. K_o is taken from the lower part of the vertical-horizontal stress curve and D is taken as the 10% secant value.

$$K_o = \delta\sigma_h / \delta\sigma_v = 0.4 \text{ (from plot)}$$

$$\mu = K_o / (1 + K_o) = 0.4 / (1 + 0.4) = 0.285$$

$$D = \delta\sigma_{v\,avg} / \delta\varepsilon_v = 28.0 \text{ psi (from plot)}$$

$$E = (1 + \mu)(1 - 2\mu)D / (1 - \mu)$$

$$= (1 + 0.285)[1 - 2(0.285)](28.0 \text{ psi}) / (1 - 0.285)$$

$$= 21.6 \text{ psi}$$

5.5.2 Compressibility of Tire Chip and Gravel Mixtures

Figures 5.12 and 5.13 show vertical stress strain and horizontal versus vertical stress for three test mixtures of 50% by weight 2-in. minus MDOT type D subbase and 50% tire chips (about 3:1 tire chips:gravel by volume). The gravel had a low water content at the time of mixing. However, the actual water content was not determined. Vertical strain was reduced to about 28% at a maximum stress of roughly 60 psi, less than the 40% maximum strain without gravel. The horizontal-vertical stress curves plot slightly below those without gravel, indicating somewhat lower values of K_o and Poisson's ratio. The gradation of the MDOT type D gravel and the 50% gravel and tire chip mix are shown in Fig. 5.14. Values of K_o, Poisson's ratio and Young's Modulus are summarized in Tables 5.3 and 5.4.

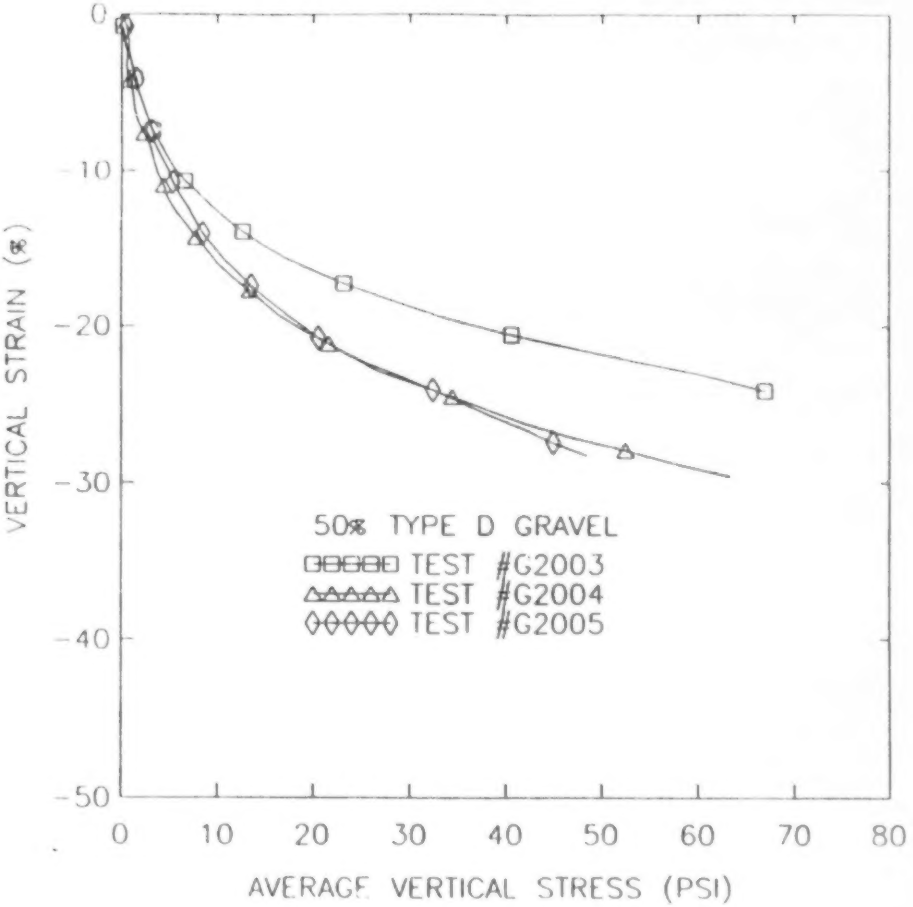

Figure 5.12 Vertical stress - strain initial loading curves of 50% (by weight) MDOT type D gravel and tire chip mix

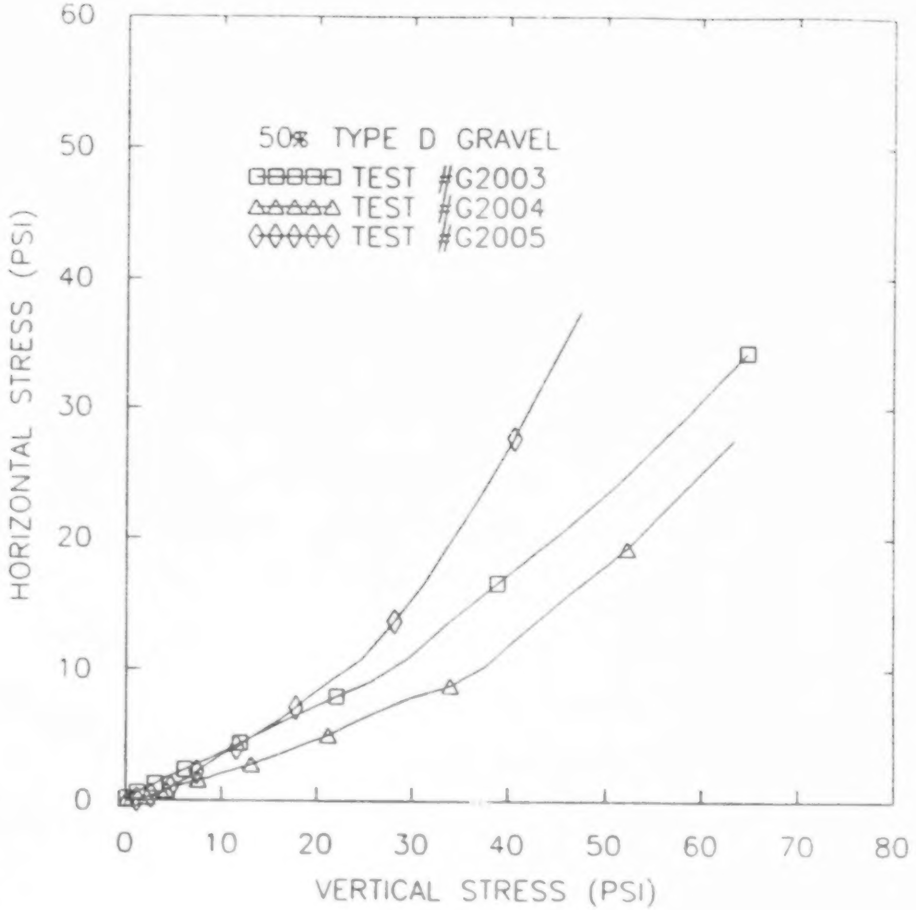

Figure 5.13 Horizontal stress - vertical stress initial loading curves for 50% (by weight) MDOT type D gravel and tire chip mix

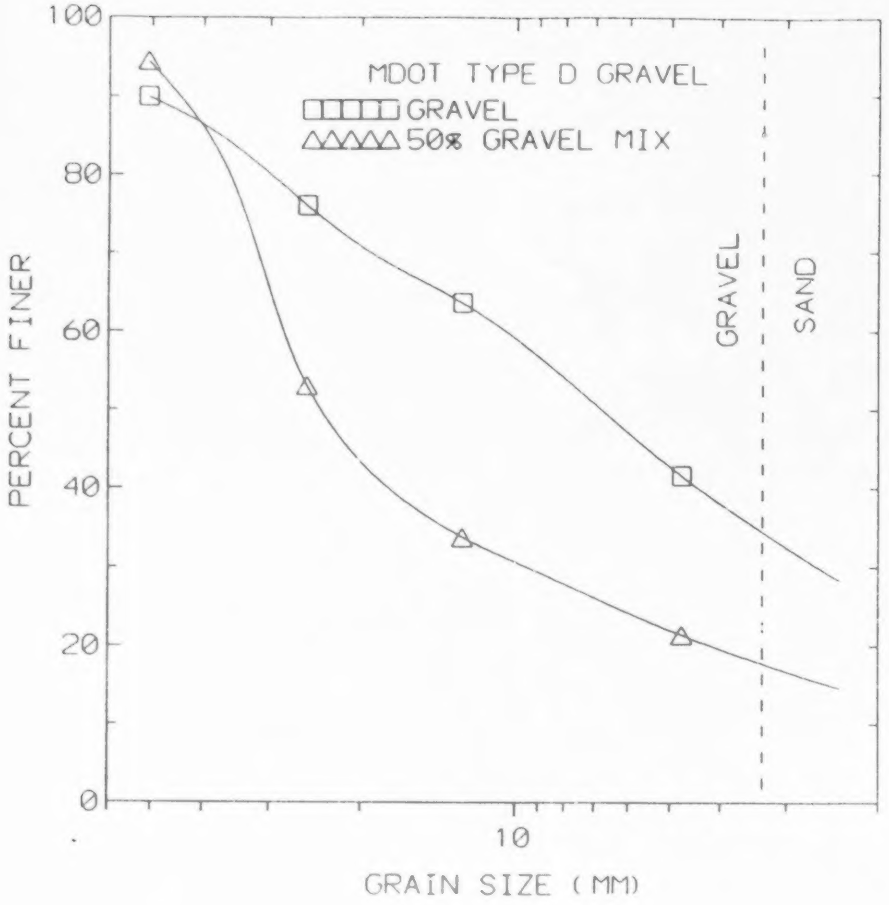

Figure 5.14 Gradations of MDOT type D gravel and 50% mix by weight with tire chips

Table 5.3: K_o and Poisson's ratio from compressibility testing of 2-in. minus MDOT type D gravel

test	part of curve	K_o	Poisson's ratio
2003	$\sigma_v > 23$ psi	0.66	0.40
	$\sigma_v < 23$ psi	0.36	0.27
2004	$\sigma_v > 23$ psi	0.68	0.41
	$\sigma_v < 23$ psi	0.25	0.20
2005	$\sigma_v > 23$ psi	1.16	0.54
	$\sigma_v < 23$ psi	0.40	0.29
avg	$\sigma_v > 23$ psi	0.83	0.46
	$\sigma_v < 23$ psi	0.34	0.25

Table 5.4: Young's modulus from compressibility testing of 2-in. minus MDOT type D gravel

			Young's Modulus (psi)		
test	part of curve	Poisson's ratio	initial tangent	secant @ 10%	secant @ 20%
2003	$\sigma_v < 23$ psi	0.27	17.4	24.3	48.6
2004	$\sigma_v < 23$ psi	0.20	6.3	16.7	26.6
2005	$\sigma_v < 23$ psi	0.29	12.9	21.6	37.3
avg	$\sigma_v < 23$ psi	0.25	12.2	20.8	37.5

Additionally, a well graded 3/4-in. minus gravel obtained from Cummings Concrete in Alton, Maine was mixed with tire chips and tested at mixtures of 25%, 50% and 75% gravel by weight (about 9:1, 3:1, and 1:1 tire chips:gravel by volume). Water was also added to the gravel to give it a moisture content of about 6%. The gradations of the gravel and the mixtures tested are shown in Fig. 5.15. As shown in Figs. 5.16 through 5.18, increasing the gravel content decreases the slope and strain at peak stress, indicating a corresponding modulus increase. The horizontal-vertical stress curves shown in Figs. 5.19 through 5.21 do not reveal

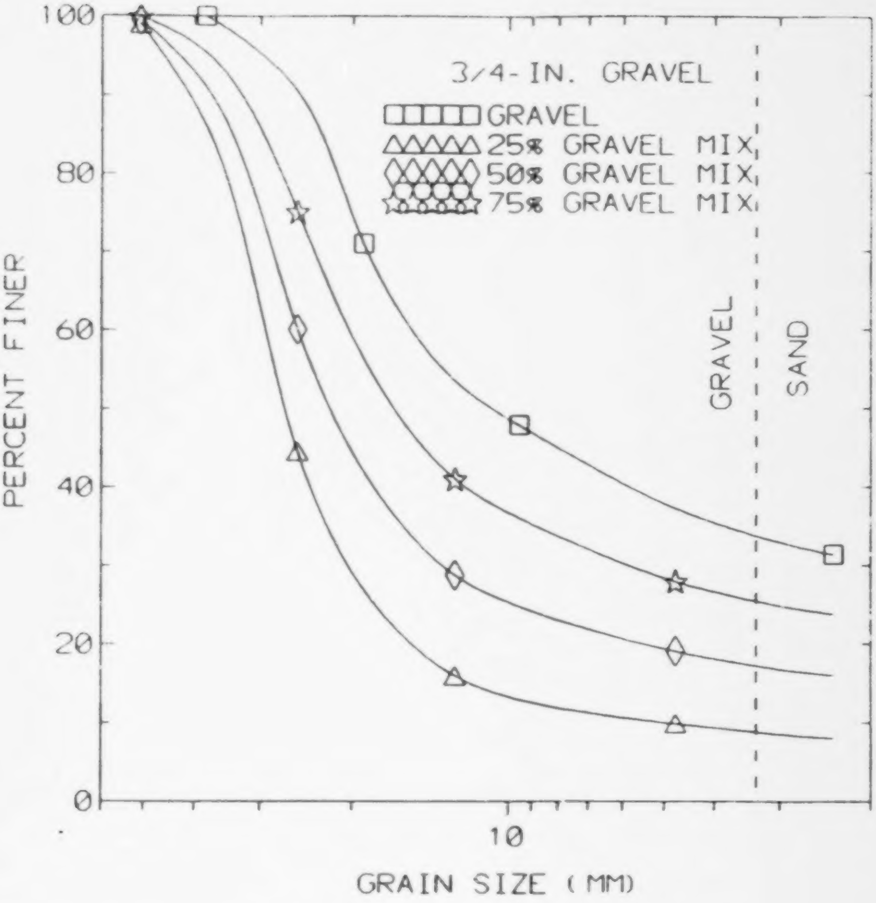

Figure 5.15 Gradations of 3/4-in. gravel and 25%, 50% and 75% mixes by weight with tire chips

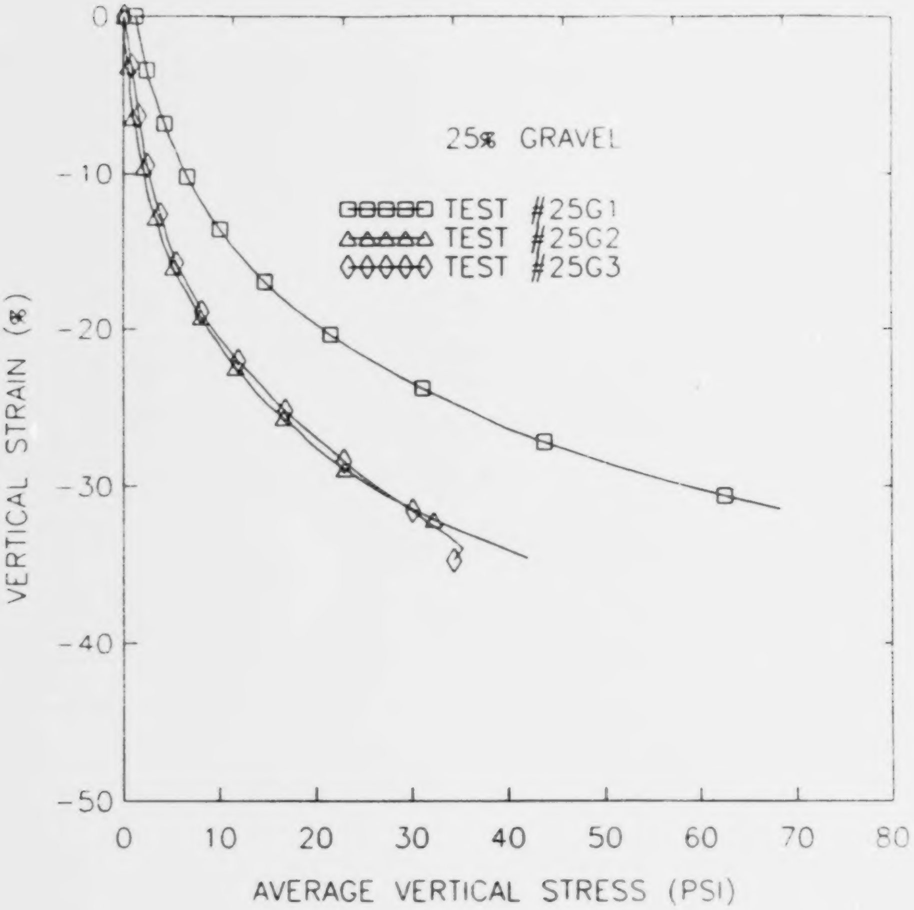

Figure 5.16 Vertical stress - strain initial loading curves for 25% (by weight) 3/4-in. gravel and tire chip mix

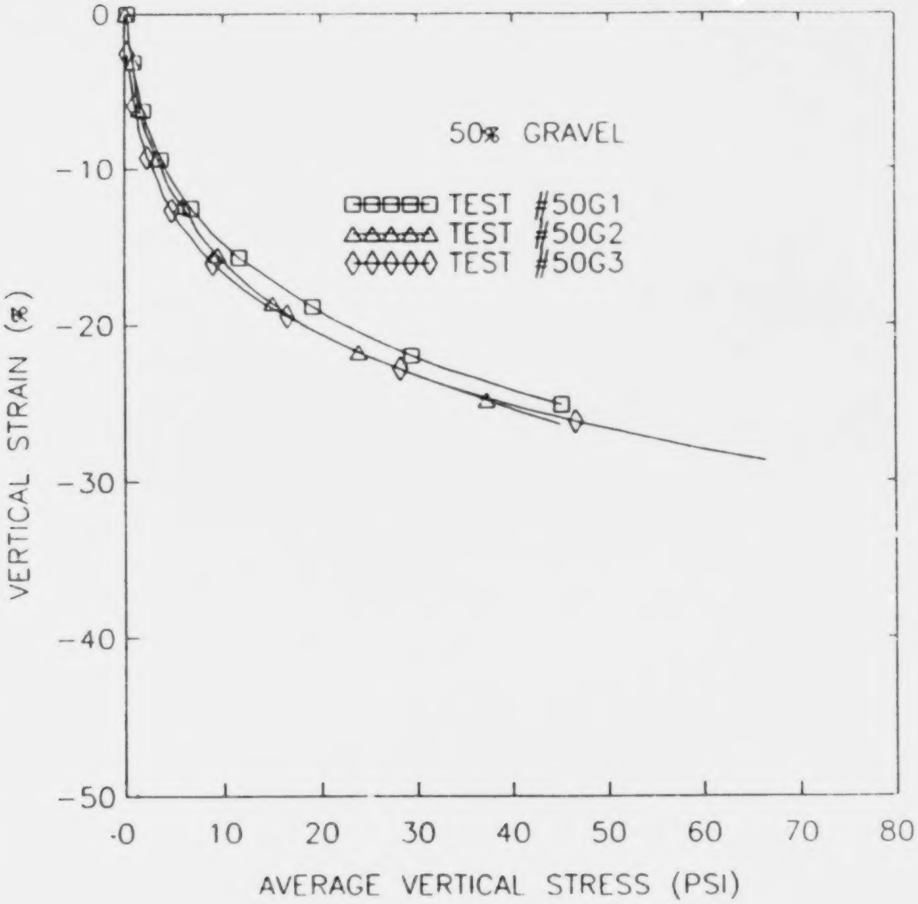

Figure 5.17 Vertical stress - strain initial loading curves for 50% (by weight) 3/4-in. gravel and tire chip mix

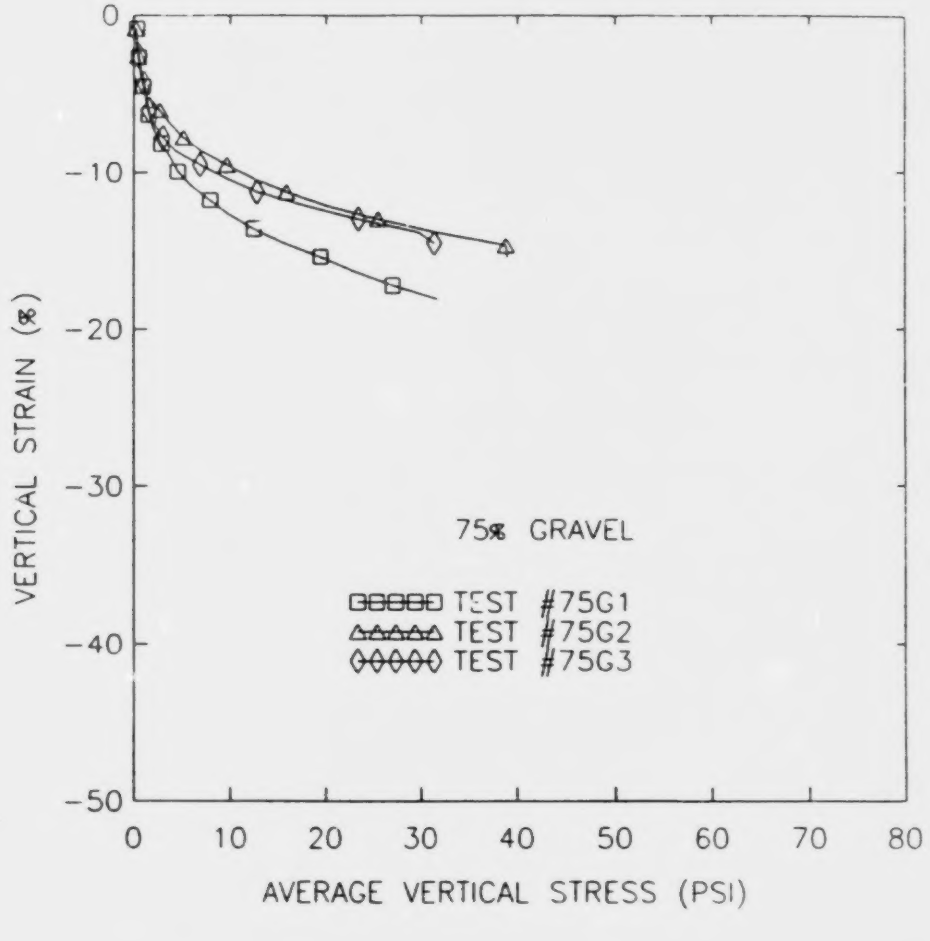

Figure 5.18 Vertical stress - strain initial loading curves for 75% (by weight) 3/4-in. gravel and tire chip mix

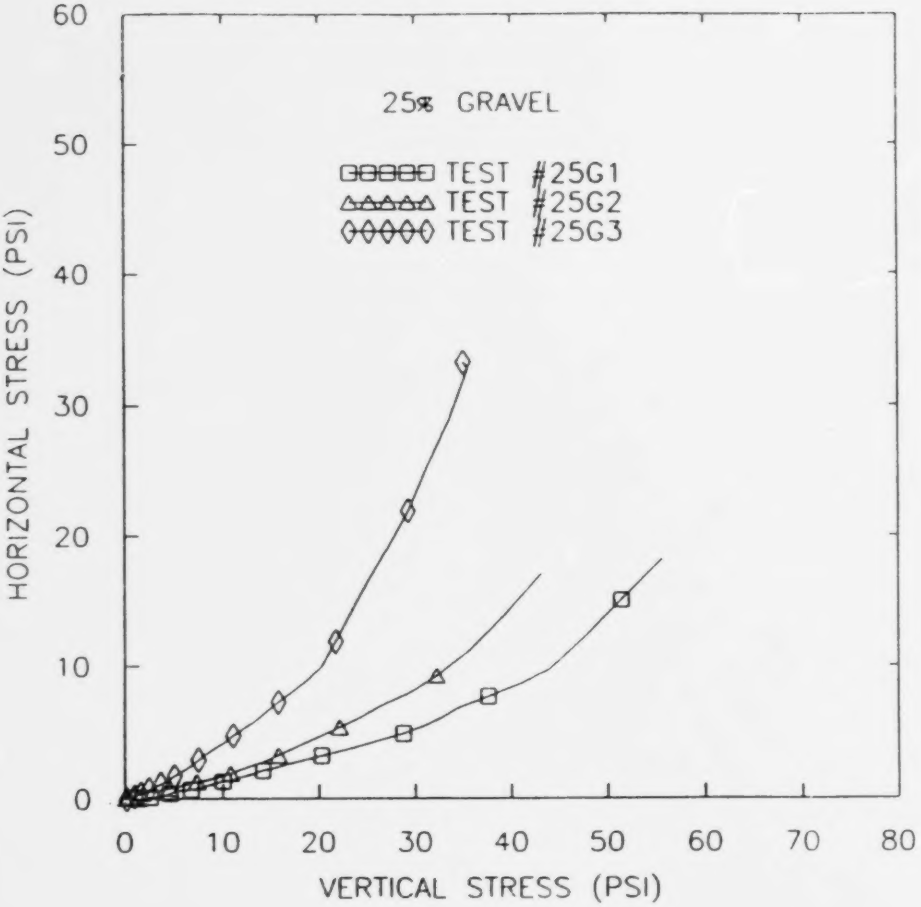

Figure 5.19 Horizontal stress - vertical stress initial loading curves for 25% (by weight) 3/4-in. gravel and tire chip mix

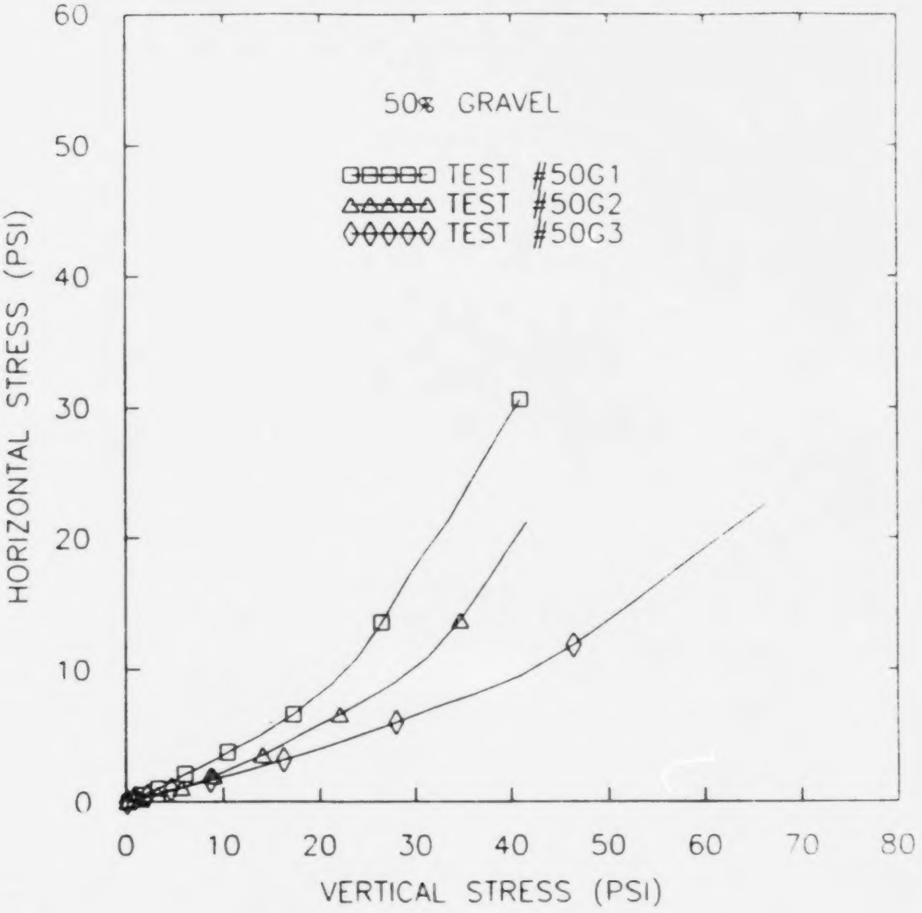

Figure 5.20 Horizontal stress - vertical stress initial loading curves for 50% (by weight) 3/4-in. gravel and tire chip mix

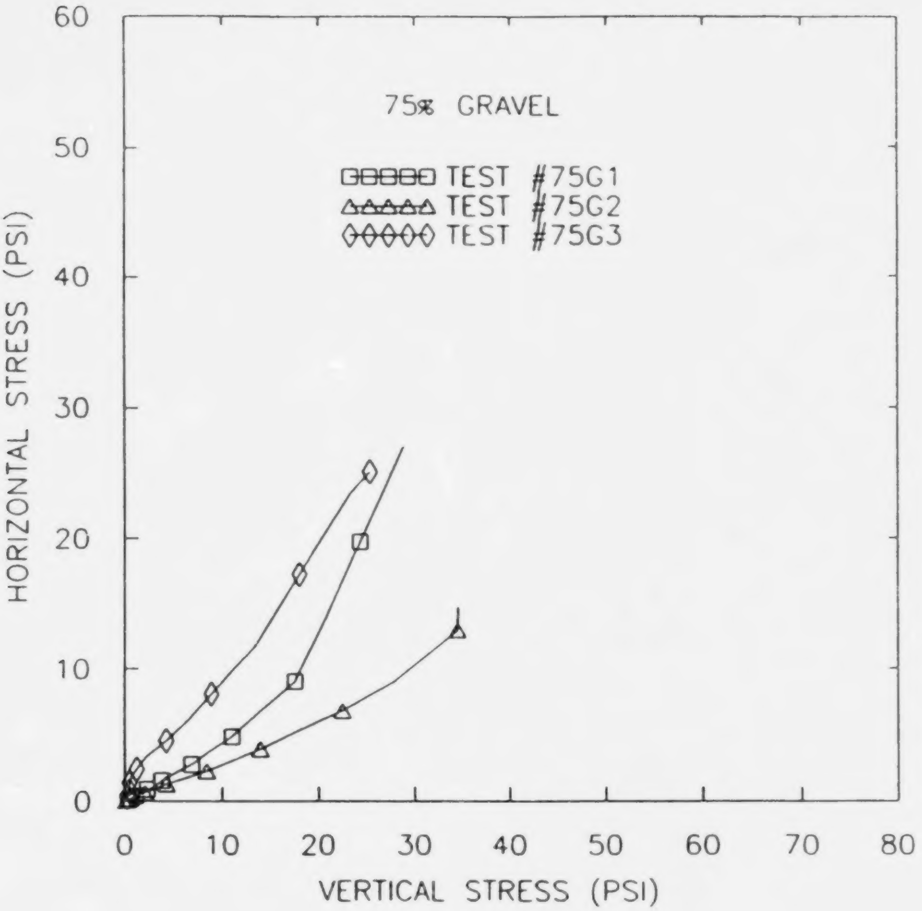

Figure 5.21 Horizontal stress - vertical stress initial loading curves for 75% (by weight) 3/4-in. gravel and tire chip mix

any particular change in Poisson's ratio with gravel content. Therefore, mixing tire chips with gravel should decrease pavement deflections by increasing the elastic modulus, but does not have much effect on Poisson's ratio. There was a significant difference between the horizontal - vertical stress curves for each individual test. This may have been caused by gravel particles pushing against the cylinder at some strain gage locations while there were tire chips or voids at other strain gage locations. Varying degrees of segregation may have also contributed to the scatter as discussed below. Values of K_o, Poisson's ratio and Young's Modulus are summarized in Tables 5.5 and 5.6.

Table 5.5: K_o and Poisson's ratio from compressibility testing of 3/4-in. minus gravel

a. 25% gravel

test	part of curve	K_o	Poisson's ratio
25g1	$\sigma_v > 23$ psi	0.73	0.42
	$\sigma_v < 23$ psi	0.18	0.15
25g2	$\sigma_v > 23$ psi	0.72	0.42
	$\sigma_v < 23$ psi	0.28	0.22
25g3	$\sigma_v > 23$ psi	1.50	0.60
	$\sigma_v < 23$ psi	0.49	0.33
avg	$\sigma_v > 23$ psi	0.98	0.50
	$\sigma_v < 23$ psi	0.32	0.24

b. 50% gravel

test	part of curve	K_o	Poisson's ratio
50g1	$\sigma_v > 23$ psi	1.15	0.54
	$\sigma_v < 23$ psi	0.36	0.27
50g2	$\sigma_v > 23$ psi	1.07	0.52
	$\sigma_v < 23$ psi	0.38	0.28
50g3	$\sigma_v > 23$ psi	0.55	0.36
	$\sigma_v < 23$ psi	0.26	0.21
avg	$\sigma_v > 23$ psi	0.92	0.48
	$\sigma_v < 23$ psi	0.33	0.25

c. 75% gravel

test	part of curve	K_o	Poisson's ratio
75g1	$\sigma_v > 23$ psi	1.63	0.62
	$\sigma_v < 23$ psi	0.49	0.33
75g2	$\sigma_v > 23$ psi	0.58	0.37
	$\sigma_v < 23$ psi	0.27	0.21
75g3	$\sigma_v > 23$ psi	1.18	0.54
	$\sigma_v < 23$ psi	0.86	0.46
avg	$\sigma_v > 23$ psi	1.13	0.53
	$\sigma_v < 23$ psi	0.54	0.35

Table 5.6: Young's modulus from compressibility testing of 3/4-in. minus gravel

a. 25% gravel

test	part of curve	Poisson's ratio	Young's Modulus (psi) initial tangent	secant @ 10%	secant @ 20%
25g1	$\sigma_v < 23$ psi	0.15	29.4	48.3	86.3
25g2	$\sigma_v < 23$ psi	0.22	15.8	22.8	44.7
25g3	$\sigma_v < 23$ psi	0.33	16.3	19.6	31.8
avg	$\sigma_v < 23$ psi	0.23	20.5	30.3	47.0

b. 50% gravel

test	part of curve	Poisson's ratio	Young's Modulus (psi) initial tangent	secant @ 10%	secant @ 20%
50g1	$\sigma_v < 23$ psi	0.27	9.7	34.0	92.2
50g2	$\sigma_v < 23$ psi	0.28	17.4	31.7	74.4
50g3	$\sigma_v < 23$ psi	0.21	21.4	41.1	123.3
avg	$\sigma_v < 23$ psi	0.25	16.2	35.6	96.6

c. 75% gravel

test	part of curve	Poisson's ratio	Young's Modulus (psi) initial tangent	secant @ 10%	secant @ 20%
75g1	$\sigma_v < 23$ psi	0.33	14.9	43.4	NA
75g2	$\sigma_v < 23$ psi	0.21	14.2	131.8	NA
75g3	$\sigma_v < 23$ psi	0.46	5.6	39.9	NA
avg	$\sigma_v < 23$ psi	0.34	11.6	71.7	NA

Segregation of the tire chips and gravel during sample preparation proved to be significant. When the gravel was mixed into the tire chips and the mixture was compacted, the much heavier gravel went to the bottom while the tire chips "floated" to the top. Careful attention to mixing reduced segregation but did not eliminate it. This effect could cause difficulty in field construction using tire chip and gravel mixtures.

Values of K_o were determined to be greater than 1.0 for several of the gravel and tire chip mixtures at high stresses ($\sigma_v > 23$ psi). It is theorized that such abnormally steep sloped horizontal - vertical stress curves were caused by large gravel particles or voids under the strain gage locations, indicating higher horizontal stresses than were actually occurring in the sample.

Overall, adding gravel to tire chips makes the mixture less compressible. Comparing vertical stress strain curves of tire chips alone and tire chip and gravel mixtures generally shows the gravel mixtures straining less for a given stress level. However, at low stress levels (less than 5 psi) the difference is less significant.

5.6 SUMMARY

To predict pavement deflections under load when tire chips are used in an embankment as fill, values of Young's modulus and Poisson's ratio were required. Therefore, a 12-in. diameter by 12-in. high compressibility apparatus made of schedule 40 PVC pipe was fabricated to measure these tire chip properties in the laboratory. An Instron 4204 Universal Testing Machine was used for the load application and measurement of loads and deflections. Electronic resistance strain gages were mounted circumferentially to measure horizontal stress and vertically to measure friction between the sample and the pipe. The horizontal stress calibration of the circumferential strain gages was made by filling the pipe with water, applying increments of pressure and measuring the resultant circumferential strains in the pipe. For calibration of the vertical strain gages used in friction measurements, a load was applied to the top of the pipe and resultant strains were measured. A computer program was written in BASIC to control the Instron machine and record data during testing using an IBM compatible computer.

Three groups of tests were performed: compacted tire chips only, compacted mixtures of 50% (by weight) 2-in. minus MDOT type D gravel and tire chips, and compacted mixtures of 25%, 50% and 75% (by weight) 3/4-in. minus gravel with tire chips.

Compressibility results of compacted tire chips only showed high compressibility at low stresses, decreasing smoothly as stresses increased. Horizontal stress versus vertical stress results showed a flatter slope at lower stresses becoming linear at higher stresses with a slope of about 45 degrees. It is theorized that the flatter initial slope indicates compression of the voids in the sample, and that the steeper slope at higher stresses indicates primarily compression of the rubber. All the tests exhibited this type of behavior. Average values of the coefficient of earth pressure at rest (K_o) and Poisson's ratio (μ) at vertical stresses less than 23 psi were determined to be 0.44 and 0.30 respectively. Values of secant at 10% strain Young's modulus (E) averaged 18.1 psi.

Results of the compressibility testing of mixtures of 50% (by weight) 2-in. minus MDOT type D gravel and tire chips showed slightly less compressibility than without the gravel. Average values of K_o and μ were determined at 0.34 and 0.25 respectively. Young's modulus at secant 10% strain averaged 20.9 psi.

Tests of 25%, 50% and 75% (by weight) 3/4-in. minus gravel and tire chip mixtures showed decreasing compressibility upon increasing gravel content. Table 5.7 summarizes the results of all the compressibility testing.

Table 5.7: Summary of tire chip compressibility results

% gravel	(σ_V < 23 psi) average K_o	average μ	avg. secant @10% modulus (psi)	average V strain @ 50 psi
none	0.44	0.30	18.1	39%
50% 2-in.	0.34	0.25	20.9	25%
25% 3/4-in.	0.32	0.24	30.2	33%
50% 3/4-in.	0.33	0.25	35.6	27%
75% 3/4-in.	0.54	0.35	71.7	17%

A potential problem with tire chip and gravel mixtures is their tendency to segregate. During mixing and compaction in the laboratory, the heavier gravel particles went to the bottom while the tire chips "floated" to the top of the sample. Careful attention to mixing reduced segregation but did not eliminate it.

Comparison of compressibility results between tire chips only and mixtures with gravel generally shows the mixtures straining less at higher stress levels but being comparable to tire chips at low stress levels.

BLANK

CHAPTER 6. PAVEMENT DEFLECTION ANALYSIS

6.1 INTRODUCTION

A finite element analysis was performed to determine the effect of a tire chip layer in the road subgrade soil on pavement deflection. A critical question was to determine the thickness of conventional soil fill that is needed between the bottom of the pavement and the top of the tire chip layer to limit pavement deflections to an acceptable level. Analyses were attempted using several different finite element analysis computer programs, but ultimately SAP86 (Number Cruncher Microsystems, Inc., 1986) was used in the detailed analysis. The linear elastic program SAP86 was chosen because it handles axisymmetric analyses, more accurately modeling pavement deflections under a pressure load from a dual wheel. Other programs had more accurate nonlinear soil models, did not have an axisymmetric element formulation. To approximately model the nonlinear stress-strain behavior of granular soil layers with the SAP86 linear model, an iterative procedure was used as discussed in the next section. The postprocessor software package MTAB POST (Structural Analysis, Inc., 1987) was used to compile and present analysis results.

Preceding page blank

6.2 METHODOLOGY

The finite element analysis modeled an 8.5-ft deep section of roadway. An axisymmetric element formulation was used, rotating the section about the center of an applied wheel load to form a round solid model. The exterior boundary was chosen to be 16 ft from the center of the applied load. Thus, the ratio of the depth to the width of the model was about 2. This is sufficient to minimize the influence of the boundary, following an example in Desai and Christian (1977). To simulate an 11-kip dual wheel load from a 22-kip equivalent single axle load, an 80 psi pressure was applied over a 1.1 ft diameter circular area. Although greater than the legal load limit in Maine, this was similar to load applications found in the literature (Sweere, et al., 1987; Chen, et al., 1986; Gomez-Achecar and Thompson, 1986; Barker, 1972; Duncan, et al., 1968). The axisymmetric element used had two degrees of freedom, vertical and horizontal movement. Boundary conditions consisted of horizontal restriction along the load centerline and the outer vertical boundary while both vertical and horizontal restriction was applied along the bottom.

The embankment was composed of four material types: pavement, subbase, subgrade soil and tire chips. All cases used a 6-in. layer of pavement. The first three cases, A, B and C, modeled a 4-ft layer of tire chips at

1-ft, 2-ft and 4-ft depths below the bottom of the pavement layer. Thicknesses of subgrade soil beneath the tire chips were varied to maintain an 8.5-ft high profile. Cases D and E both had 2 ft of subbase below the pavement layer, and had a 2-ft layer of tire chips at 6 ft and 4 ft beneath the bottom of the pavement, respectively. The remainder of the thickness was made up of subgrade soil. Case F, containing 2 ft of subbase and 6 ft of subgrade soil without tire chips, was included for purposes of comparison. Several stratigraphies were investigated to determine the effect on pavement deflection of changing the thickness of conventional subbase and subgrade soil between the bottom of the pavement and the top of the tire chip layer as shown in Fig. 6.1.

Elastic parameters for the pavement, subbase and subgrade soil were estimated using typical values reported in the literature (Sweere, et al., 1987; Chen, et al., 1986; Gomez-Achecar and Thompson, 1986; Barker, 1972; Duncan, et al., 1968). It was determined from reviewing Duncan, et al. (1968) that finite element analyses of the deflections of paved roads typically use the resilient modulus for Youngs modulus. The resilient modulus, which is much higher than Youngs modulus from a compression test where the load is uniformly increased, is used for short repetitive load durations, much as can be expected for roadway applications.

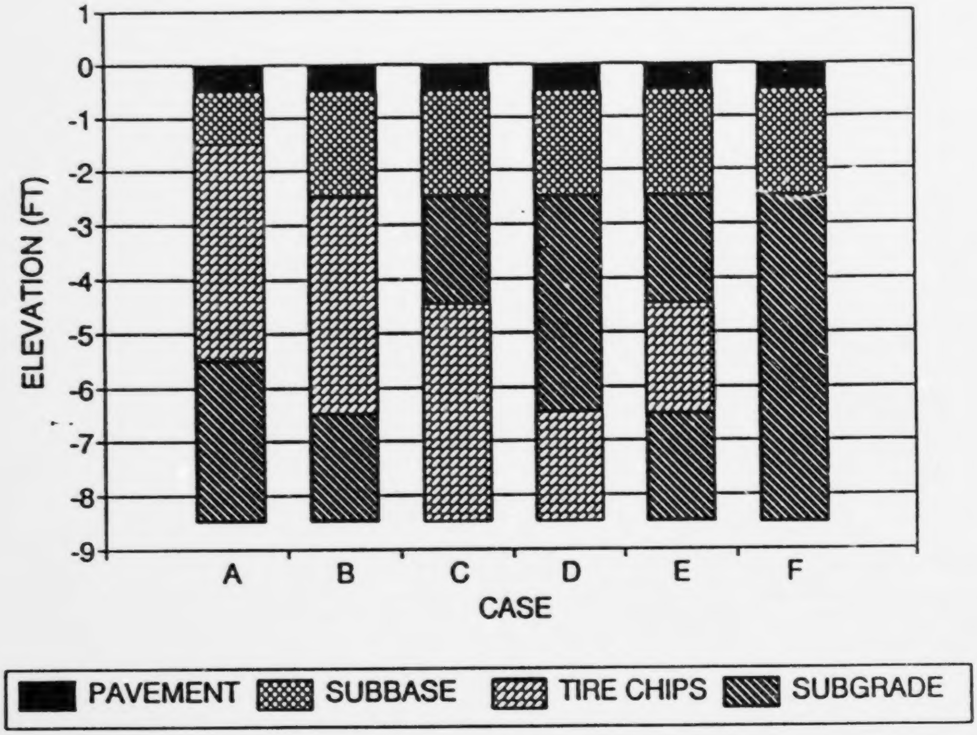

Figure 6.1 Six road embankment stratigraphies used in finite element analysis of pavement deflection

Furthermore, the resilient modulus of granular soils is dependent on the stress level. It was estimated using a relationship between the minor principal stress (σ_3) and the resilient modulus (M_r) found in the literature (Barker, 1972; Duncan, et al., 1968)

$$M_r = K_1 \ (\sigma_3)^{K_2} \quad \text{(in psi)}$$

Values of $K_1 = 10000$ and $K_2 = 0.4$ from were used for both the subbase and subgrade soil (Duncan, et al., 1968). Initial modulus values were determined from values reported in the literature as listed previously.

Since the modulus of granular material is stress level dependent, an iterative method was developed to allow this nonlinearity to be accounted for within the linear elastic material models in SAP86. The results of a computer run were compiled in the postprocessor, and σ_3 contours were printed for the subbase and subgrade soil layers to 5 ft away from the load centerline. It was assumed that beyond 5 ft from the load centerline, the modulus of the subbase and subgrade soil would have only a minor effect on pavement deflection beneath the load. The σ_3 contours were then used to divide the subbase and subgrade soil layers into four or five regions of approximately constant σ_3 as shown for the final iteration of case C in Fig. 6.2. The stresses indicated are from the wheel live load (LL) from finite element analysis plus gravity dead loads (DL). Since stresses

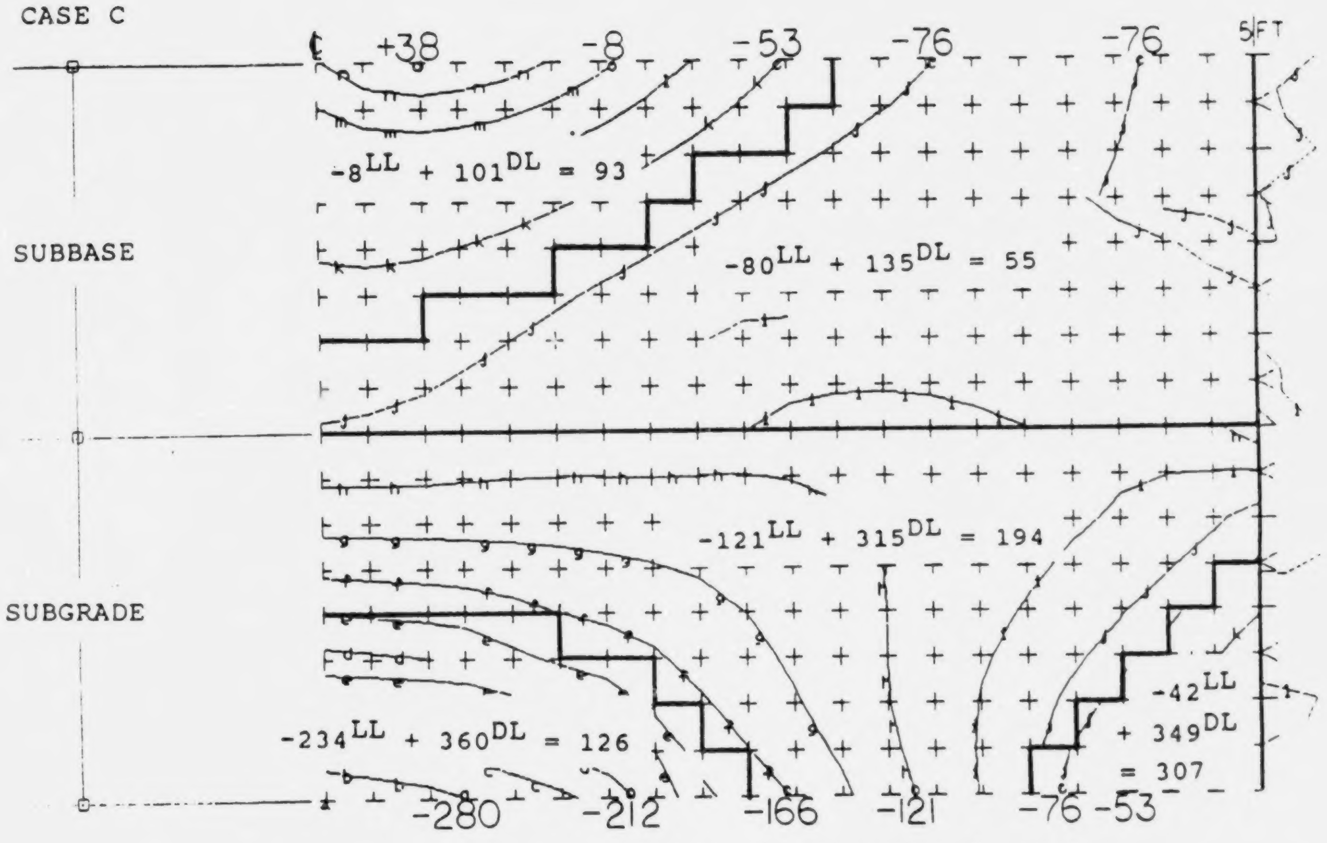

(Note: All stresses in psf)

Figure 6.2 Typical σ_3 contour plot of wheel live load used for iterative modulus method, showing live load (LL), dead load (DL) from overburden, and the net σ_3 stress

due to gravity were not included in the finite element model, horizontal stresses computed using depth of overburden times 120 pcf multiplied by a K_o of 0.75 were added to the live load stresses (LL) from the computer σ_3 contour regions, resulting in the final σ_3 values shown in Fig. 6.2. All stresses are in psf with the positive sign convention being compression. However, this method of adding overburden stress is only approximate since the angle of σ_3 measured with respect to horizontal ranges from 1 to nearly 50 degrees in the region of case C shown in Fig. 6.2. Fig. 6.3 shows the angle of σ_3 (principal angle) versus distance from the centerline of the load application for the top, middle and bottom elevations of the subbase and subgrade soil layers. It is seen that near the top of the subbase (elevation minus 0.75, corresponding to the center of the top subbase elements), the principal angle transitions from 4 degrees under the load to 47 degrees at 5 ft from the load centerline. Principal angles at lower elevations decrease to between 1 and 9 degrees near the bottom of the subgrade soil (elevation minus 4.25).

New resilient modulus values were then calculated for the regions using the equation given above, and input as different materials in the finite element analysis. Repeating this sequence between 5 and 9 times produced convergence to relatively constant stress levels and

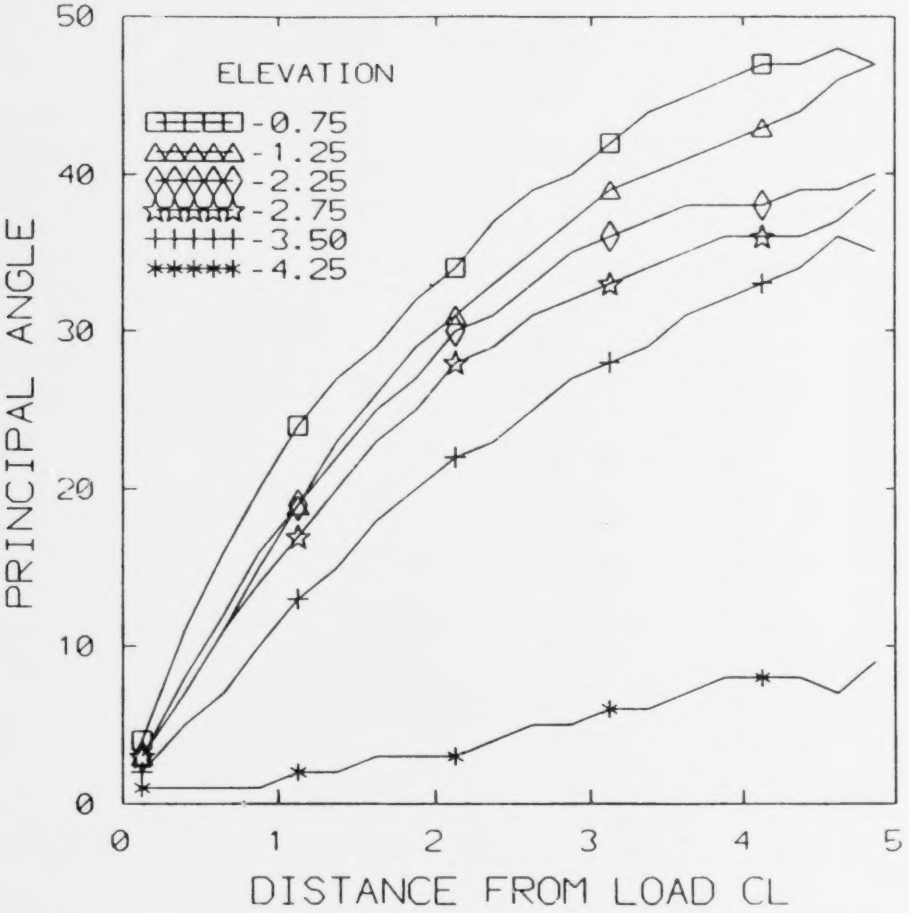

Figure 6.3 Principal stress angle versus distance from the load centerline for six elevations in case C

pavement deflections. Convergence was defined by deflection at the centerline falling within a range of plus or minus 2% of the average deflection determined from the last few iterations, which is probably about the accuracy of the finite element formulation. Plots of the iterative convergence of pavement deflection for case C are shown in Fig. 6.4. The number of iterations required for convergence generally decreased as the thickness of gravel between the tire chips and pavement increases.

As indicated in Fig. 6.2, σ_3 was reduced in the region below the load. For case A, even inclusion of the overburden stress component did not compensate for the tension from the live load. The tire chips were close enough to the pavement that the pavement and relatively shallow depth of subbase was essentially acting as a beam with a load applied at its center supported by a uniform compressible material, creating high tension in the bottom of the beam, i.e., in the subbase. Even after gravity stresses were added, the minor principal stress was still tensile for case A. This clearly shows that greater than 1 ft of subbase is needed between the bottom of the pavement and the top of the tire chip layer.

Values of Young's modulus and Poisson's ratio for the pavement, and initially for the subbase and subgrade soil were obtained from the literature (Sweere, et al., 1987; Chen, et al., 1986; Gomez-Achecar and Thompson,

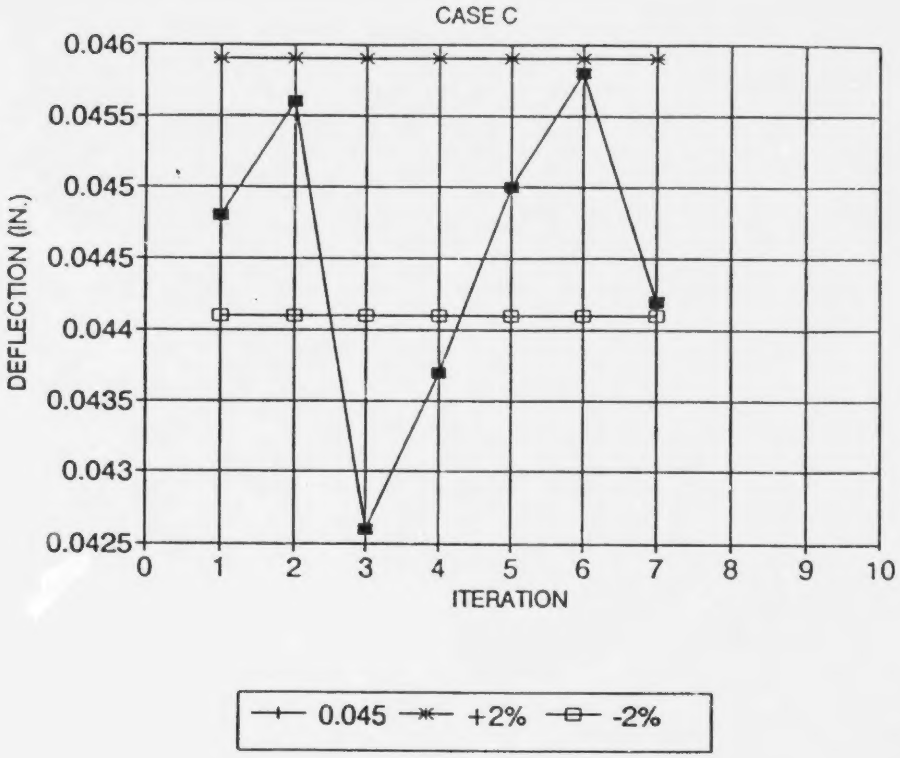

Figure 6.4 Plot of iterative convergence of pavement deflection for case C

1986; Barker, 1972; Duncan, et al., 1968). Values of Young's modulus and Poisson's ratio for the tire chips were determined from the compressibility results presented in Chapter 5. To estimate the modulus of the tire chips for use in the analysis, the applied vertical stress due to overburden was estimated and used with the corresponding unloading and reloading portion of vertical stress-strain testing results. Table 6.1 lists the material properties used in the analysis.

Table 6.1: Material properties used in finite element analysis

Material	Young's Modulus (psi)	Poisson's Ratio
Pavement	1.0×10^6	0.35
Subbase	1.2×10^4 *	0.25
Subgrade soil	6.0×10^3 *	0.25
Tire Chips	2.0×10^2	0.32

* modulus used for first iteration; modified in subsequent iterations for stress level as described above

Three levels of finite element mesh were developed to determine if the mesh geometry itself was affecting the results. The only difference between the three meshes, shown in Fig. 6.5, is the number of elements in the region from 5 ft away from the load centerline and 4.5 ft below the top of pavement. This region was chosen because preliminary meshes and analyses showed that most

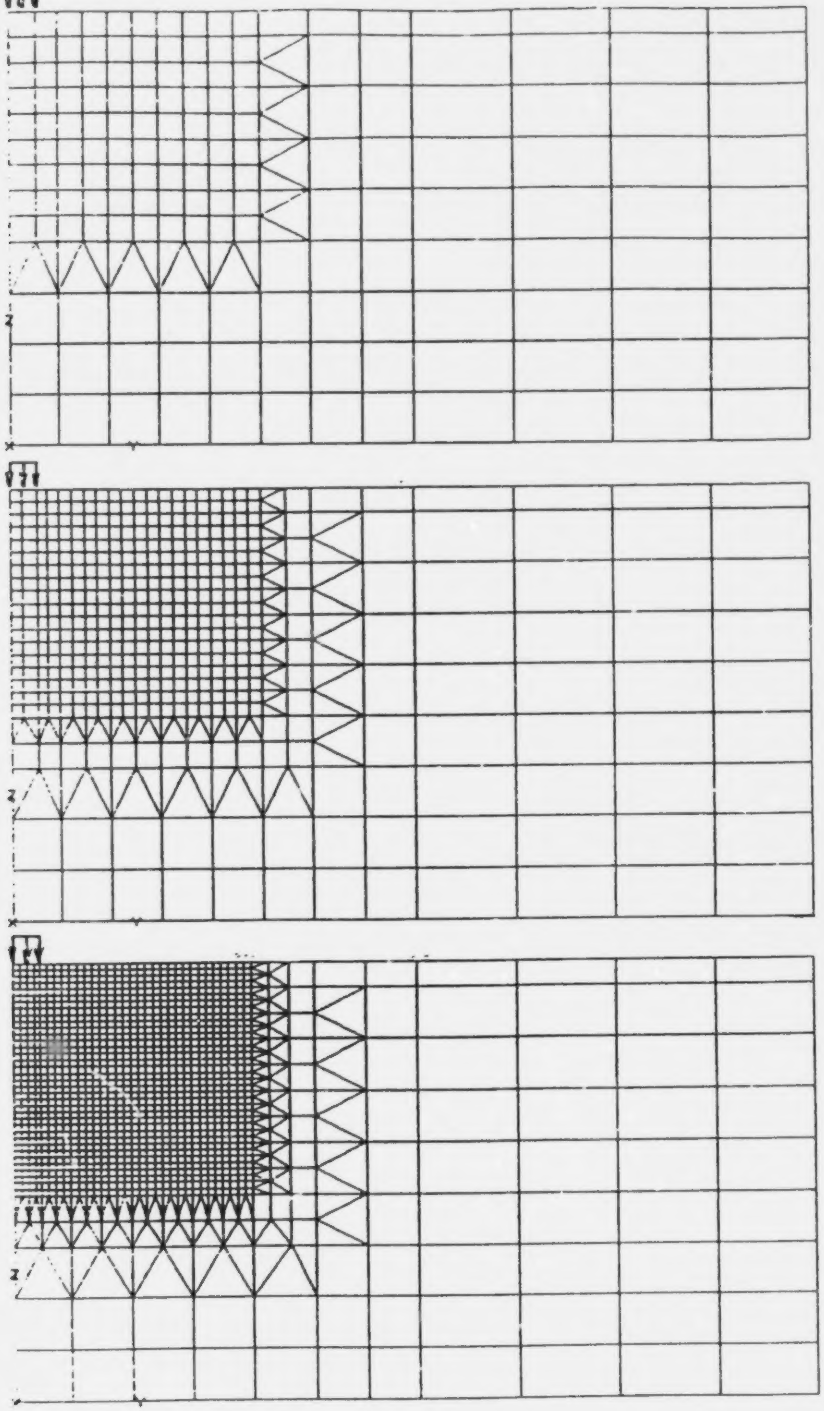

Figure 6.5 Three different meshes used to check influence of model geometry

of the stress and deflection activity occurred there. The uniformity of elements in this region provided smooth stress and deflection transfers, improving the accuracy of the model. Results from the three meshes, shown in Table 6.2, were inconclusive, so the 534 element medium mesh was utilized for subsequent analyses.

Table 6.2: Results of 3 different meshes

Mesh level	Pavement Deflection (ft) at centerline
Coarse	7.808×10^{-5}
Medium	8.251×10^{-5}
Fine	7.400×10^{-5}

6.3 RESULTS

A summary of the pavement deflections at the load centerline superimposed on the embankment profiles is shown in Fig. 6.6 and a plot of pavement deflection as a function of thickness of soil cover is shown in Fig. 6.7. As could be predicted intuitively, pavement deflection decreases as thickness of gravel between the tire chips and pavement increases from 1 ft in case A to 4 ft in case C, while maintaining a 4-ft thick tire chip layer. Reducing the thickness of the tire chip layer from 4 ft to 2 ft also decreases pavement deflection in cases D and E. Comparing cases D and E, E exhibits more

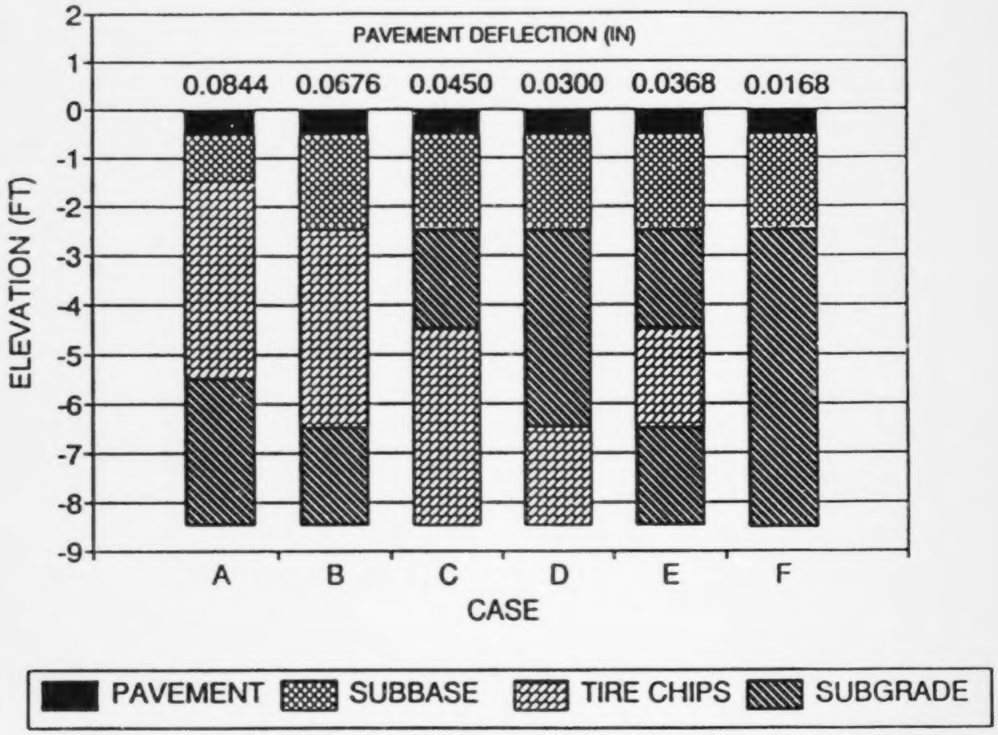

Figure 6.6 Pavement deflections shown with the six road embankment stratigraphies

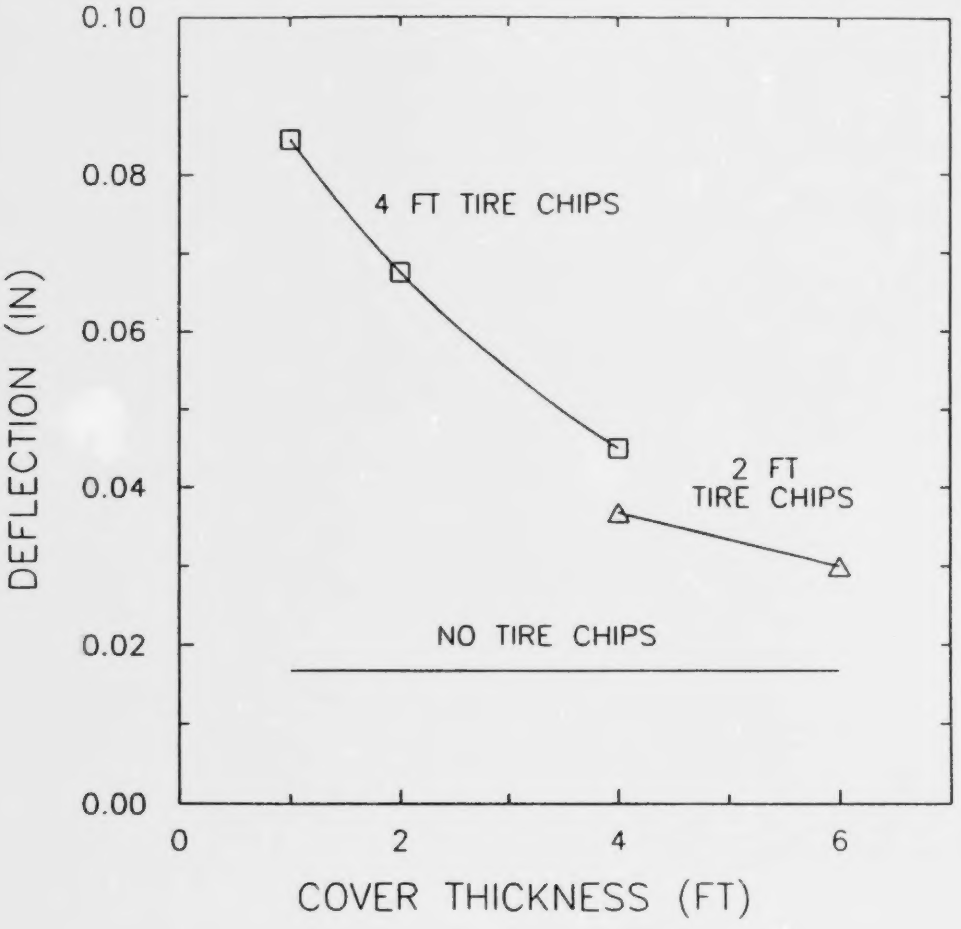

Figure 6.7 Plot of pavement deflection versus soil cover thickness

deflection since it has 4 ft of soil cover compared to 6 ft for case D. The pavement deflection in cases D and E are twice the deflection of case F, with no tire chips at all.

It was rather difficult to determine an acceptable maximum pavement deflection for a typical roadway. MDOT indicated that based on typical Benkleman beam data, "good" roads will show a maximum deflection of 0.03 in. A Pavement Design Manual, presumably by Tomasetti (1962) indicated that "a deflection level of 0.03 in. can be tolerated." A design rebound deflection chart, based on Benkleman beam results, from AASHTO (1986b), was used to determine the equivalent axle load (EAL) corresponding to the centerline deflections determined in finite element analysis shown in Table 6.3

Table 6.3: Equivalent axle load from deflection using AASHTO (1986b) method

Case	Finite element centerline Deflection (in)	EAL
A	0.0844	25,000
B	0.0676	70,000
C	0.0450	380,000
D	0.0300	2,000,000
E	0.0368	900,000
F	0.0168	26,000,000

It is seen that less deflection allows for a larger number of equivalent axle loads, which would translate into a longer estimated roadway life.

Profiles of the increase in vertical stress due to the applied wheel load for the six cases are presented in Fig. 6.8. The profiles extend only to 5 ft from the axis of rotation and are divided into the layers of different materials for clarity. Stresses are reported in psf using the geotechnical sign convention of positive for compression. It is seen that the increase in vertical stress in the tire chip layers is generally less than 75 psf (0.52 psi). Table 6.4 lists the average increase in vertical stress (σ_V avg) and maximum increase in vertical stress (σ_V max) in the tire chip layer over the 5-ft radius shown in each case. The maximum vertical stress always occurred at the highest elevation of the tire chip layer directly under the load centerline.

Table 6.4: Vertical stress in the tire chip layer for each case

Case	z (ft)	$\delta\sigma_V$ avg (psf)	$\delta\sigma_V$ max (psf)
A	3.5	45	73
B	4.5	35	52
C	6.5	22	27
D	7.5	22	26
E	5.5	32	37

z = depth to center of tire chip layer

It is seen that the increase in vertical stress due to the wheel load decreases with increasing depth. From compressibility testing results, a change in stress of 72 psf (0.5 psi) would cause about 0.3% strain and 29 psf (0.2 psi) about 0.1% strain, using the slope of the

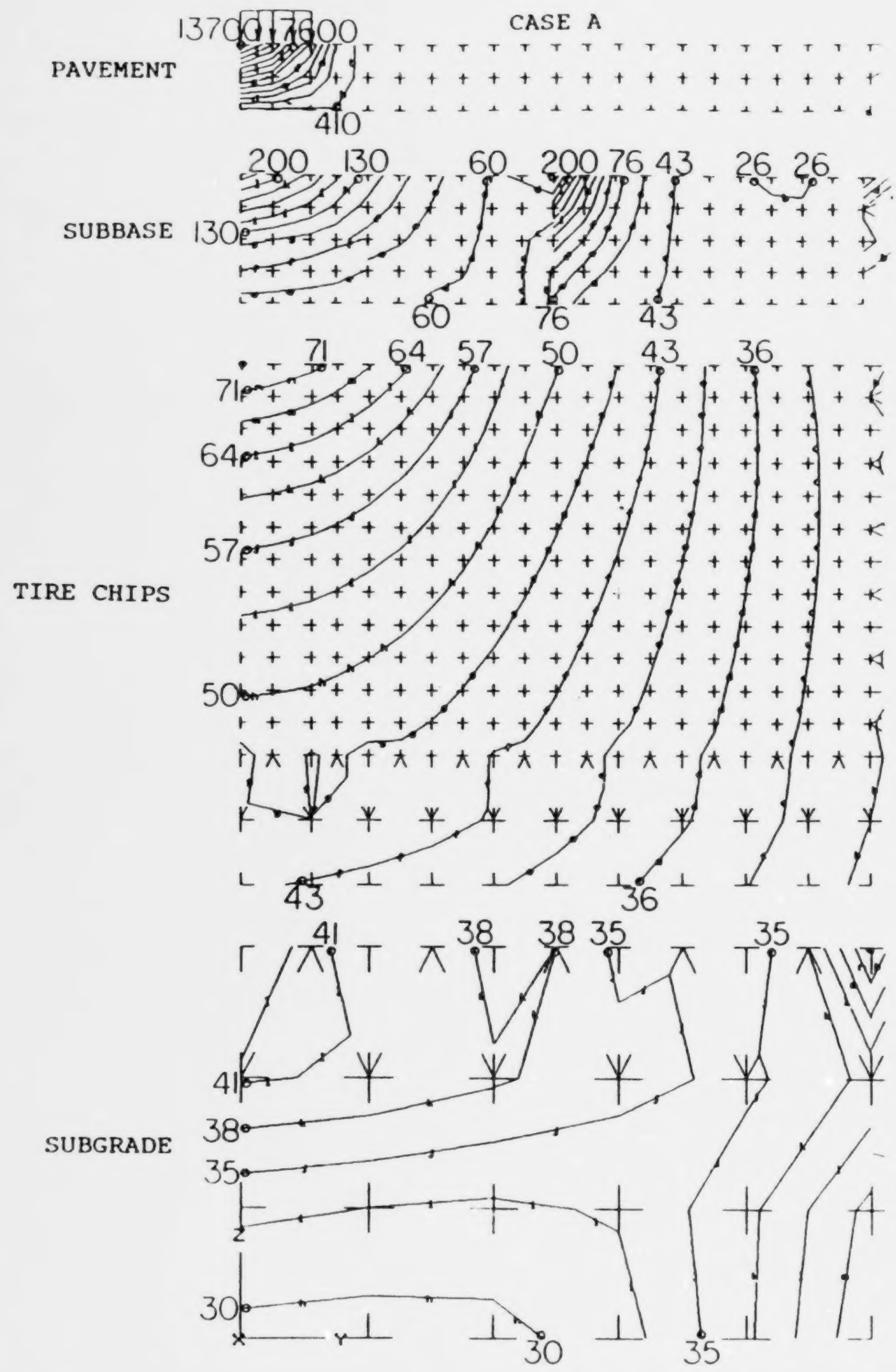

Figure 6.8(a) Increase in vertical stress contours for Case A

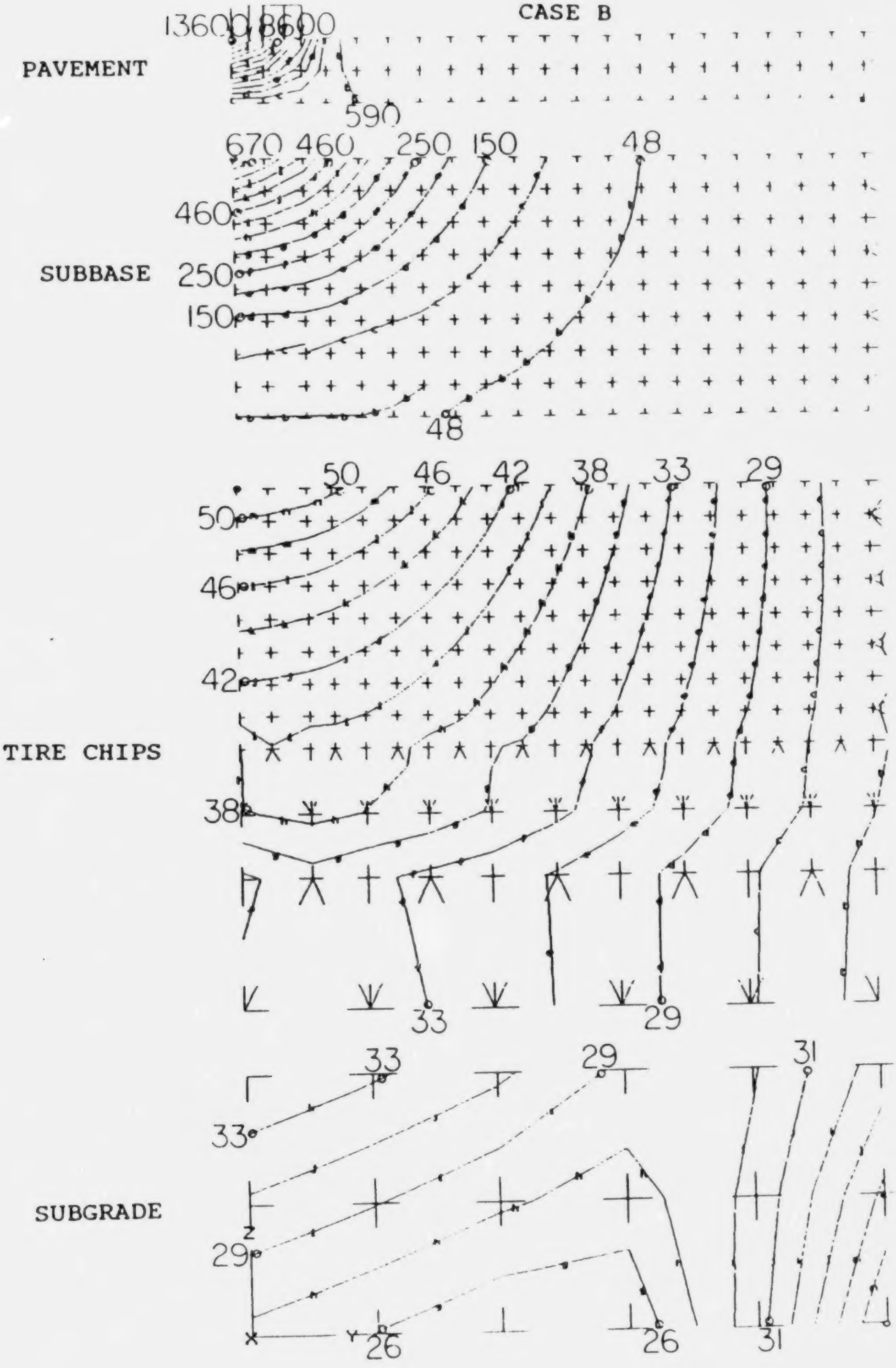

Figure 6.8(b) Increase in vertical stress contours for Case B

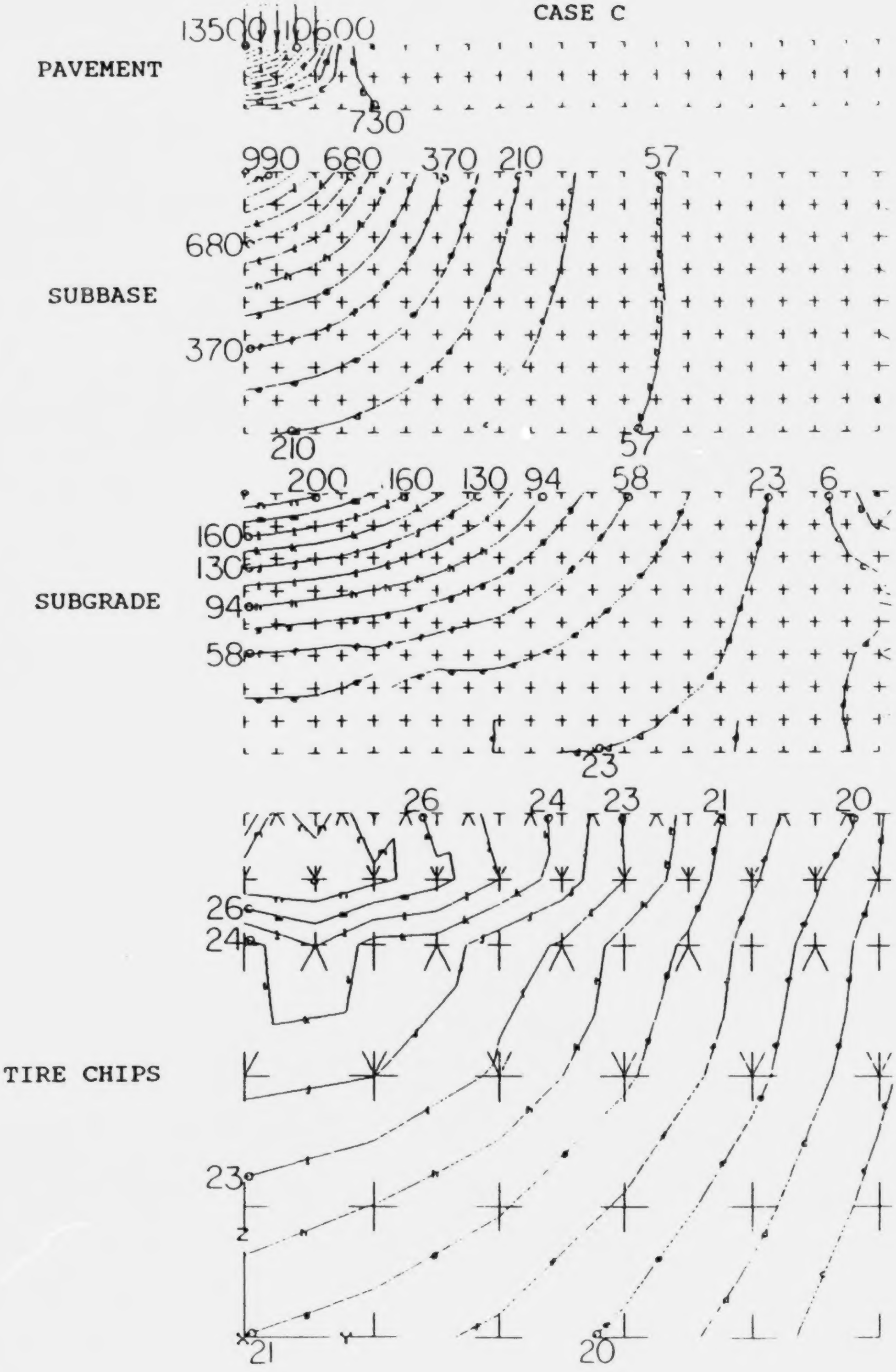

Figure 6.8(c) Increase in vertical stress contours for Case C

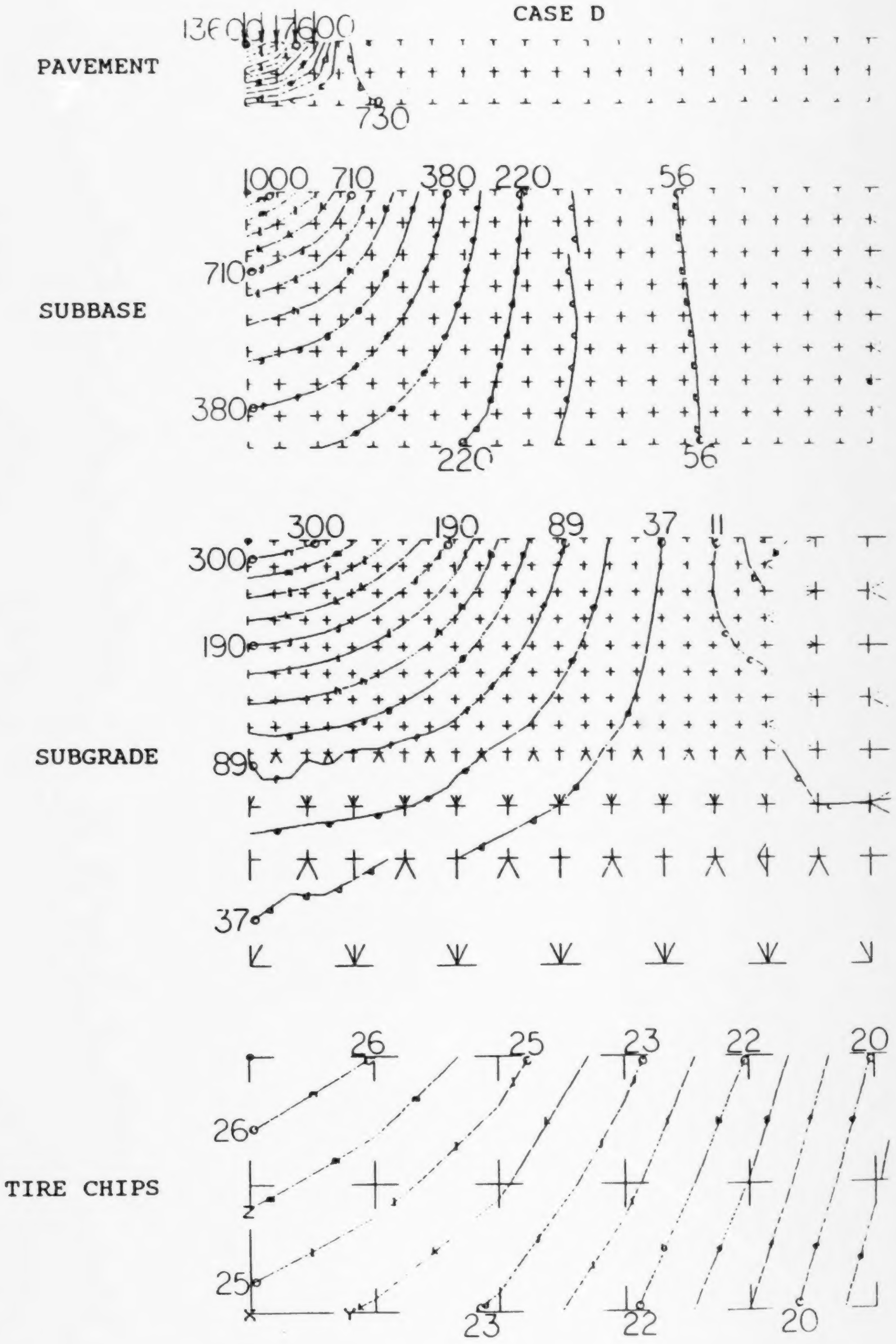

Figure 6.8(d) Increase in vertical stress contours for Case D

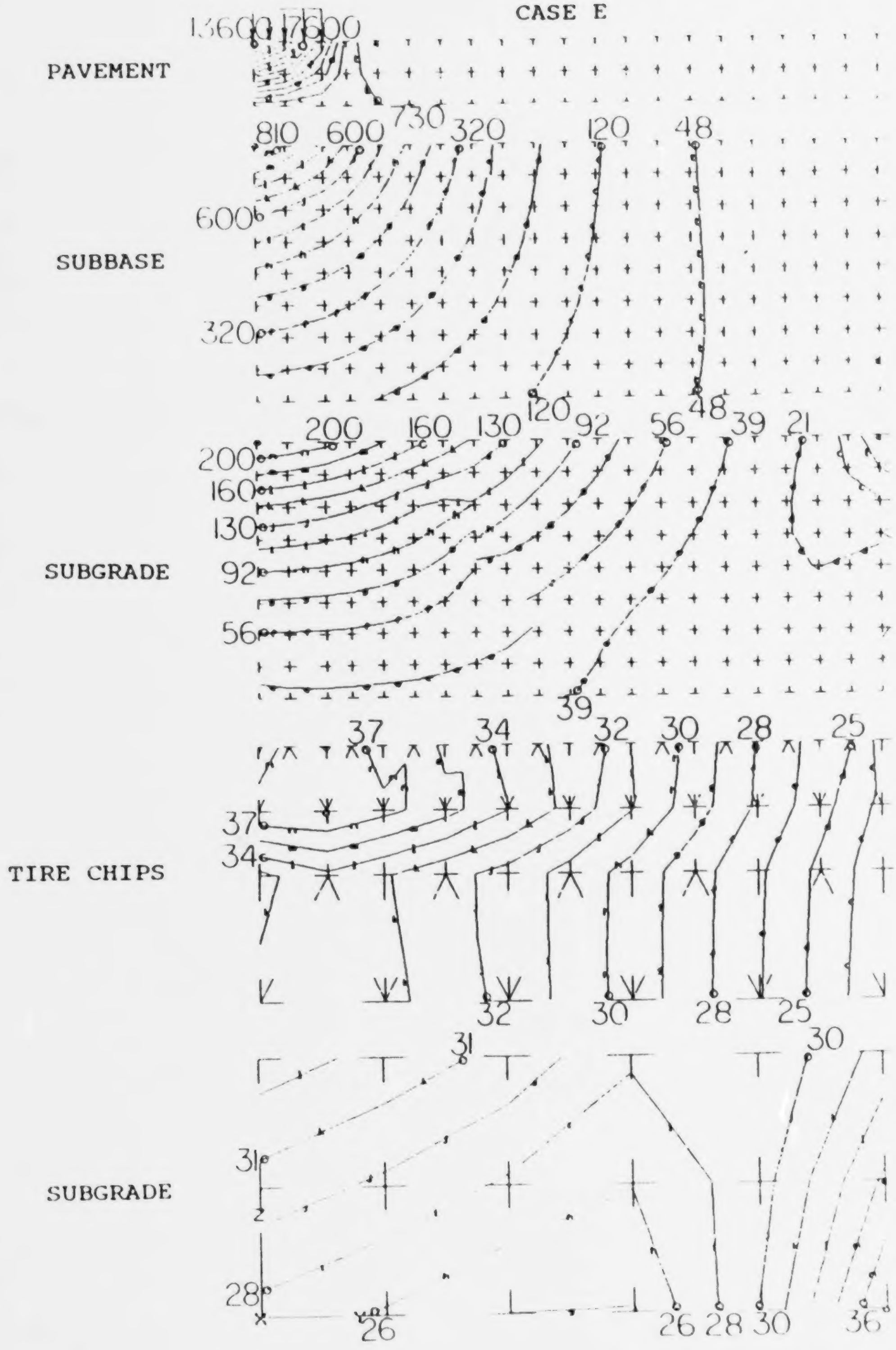

Figure 6.8(e) Increase in vertical stress contours for Case E

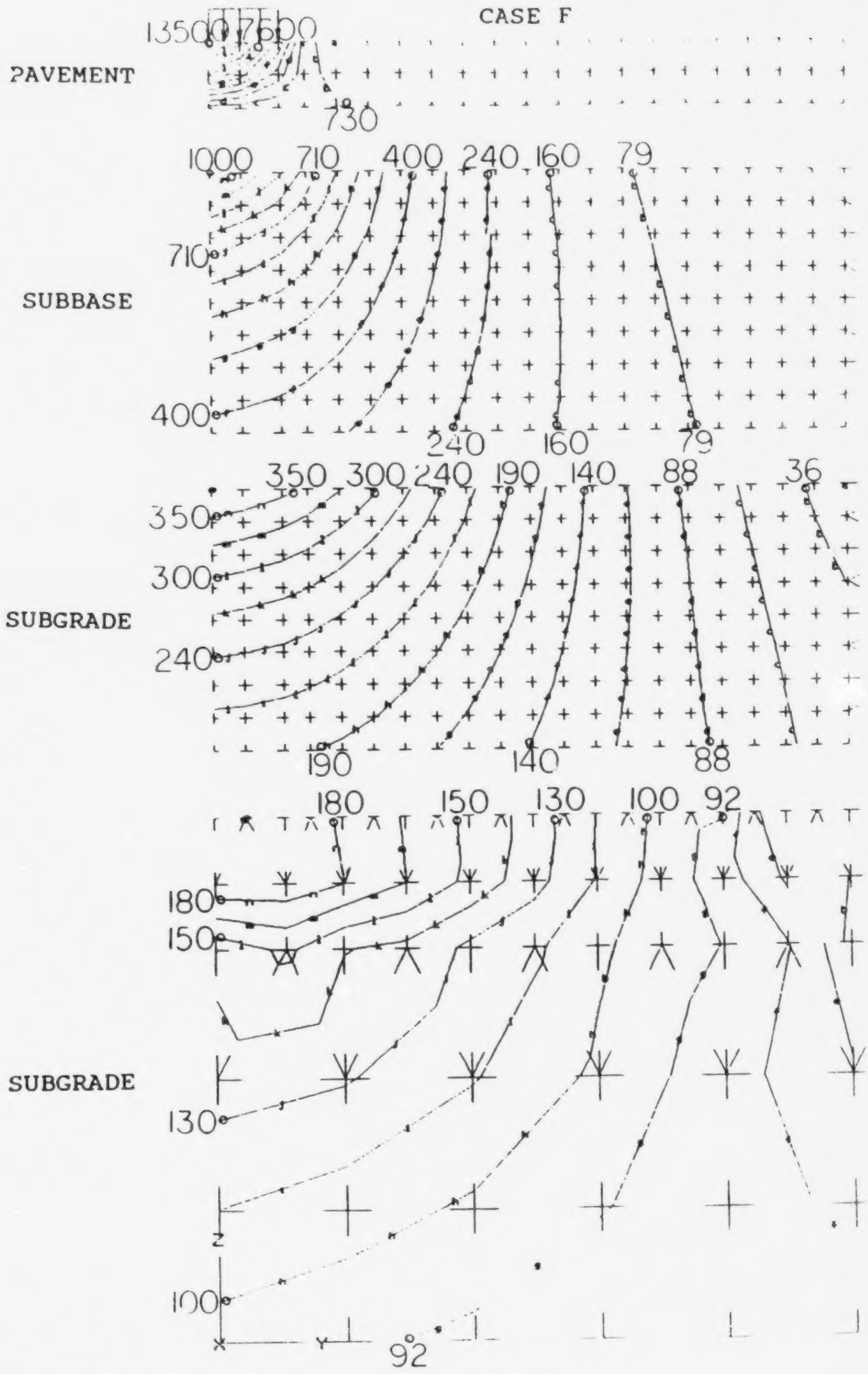

Figure 6.8(f) Increase in vertical stress contours for Case F

vertical stress-strain rebound curve.

Plots of the deformed mesh for each case are shown in Fig. 6.9. The maximum deflection for each case is automatically scaled to 20% of the embankment height, so all the plots will show the same relative deflection at the load centerline. Most of the deflection occurs in the tire chip layer, but the deformed mesh plots also show some deflection in the granular layers close to the load application in areas of high stress. For comparison between the cases, Fig. 6.10 shows plots of pavement deflection with distance from the axis of rotation for the two different thicknesses of tire chip layer considered. It is seen that for the cases with tire chips, the zone of vertical deflection extends over a wider area than for the case with no tire chips. This would tend to offset some of the pavement damage caused by the larger vertical deflections associated with the tire chip cases.

One of the potential variables considered for analysis was the effect of tire chip modulus on pavement deflection. To investigate this effect, multiple computer runs of case C were performed with different tire chip moduli, ranging from 18 to 200 psi. It is recalled that the 200 psi value was estimated from the unload and reload portions of vertical stress strain

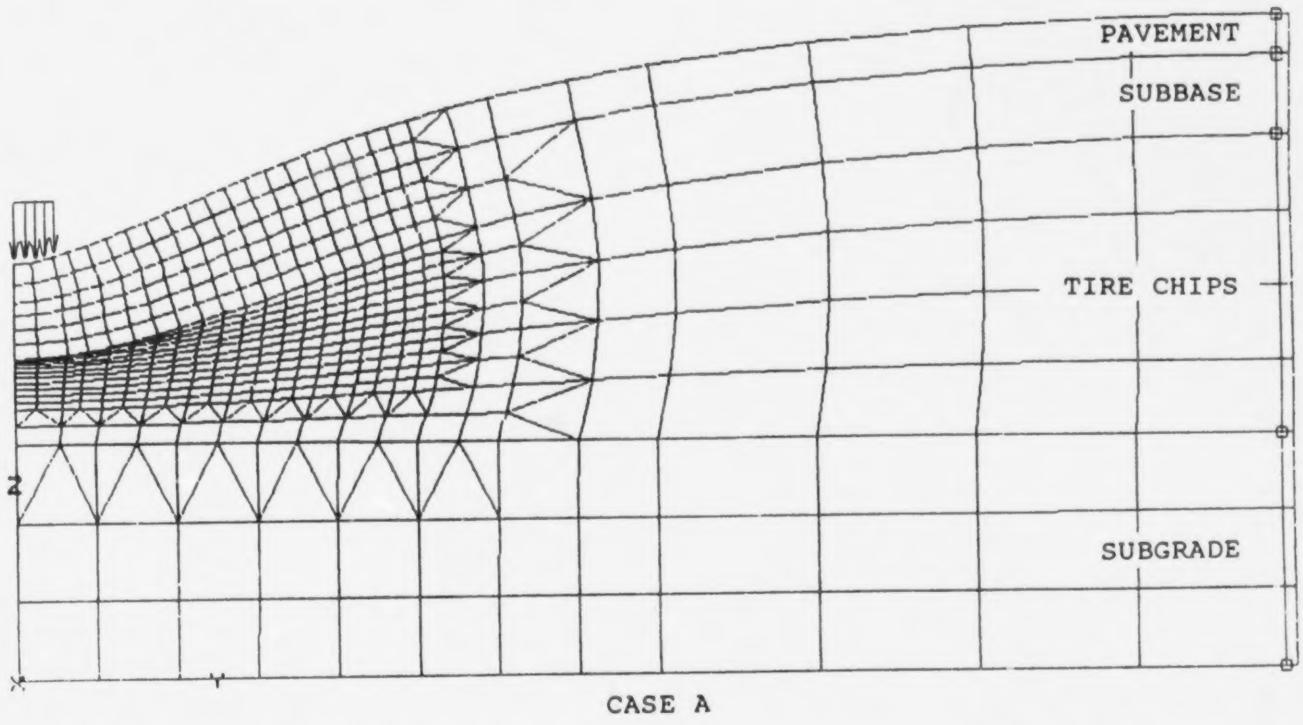
PAVEMENT
SUBBASE
TIRE CHIPS
SUBGRADE
Z
X
Y
CASE A

Figure 6.9(a) Deformed mesh plot for case A

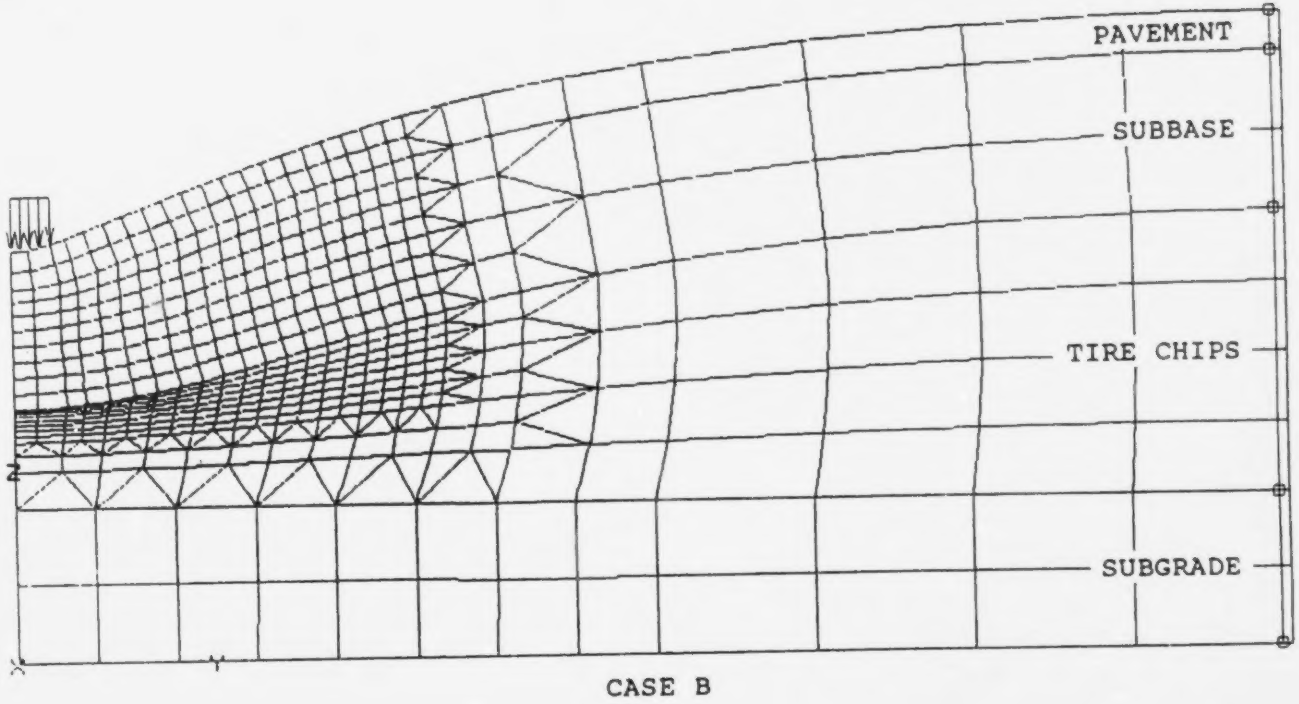
PAVEMENT
SUBBASE
TIRE CHIPS
SUBGRADE
Z
X
Y
CASE B

Figure 6.9(b) Deformed mesh plot for case B

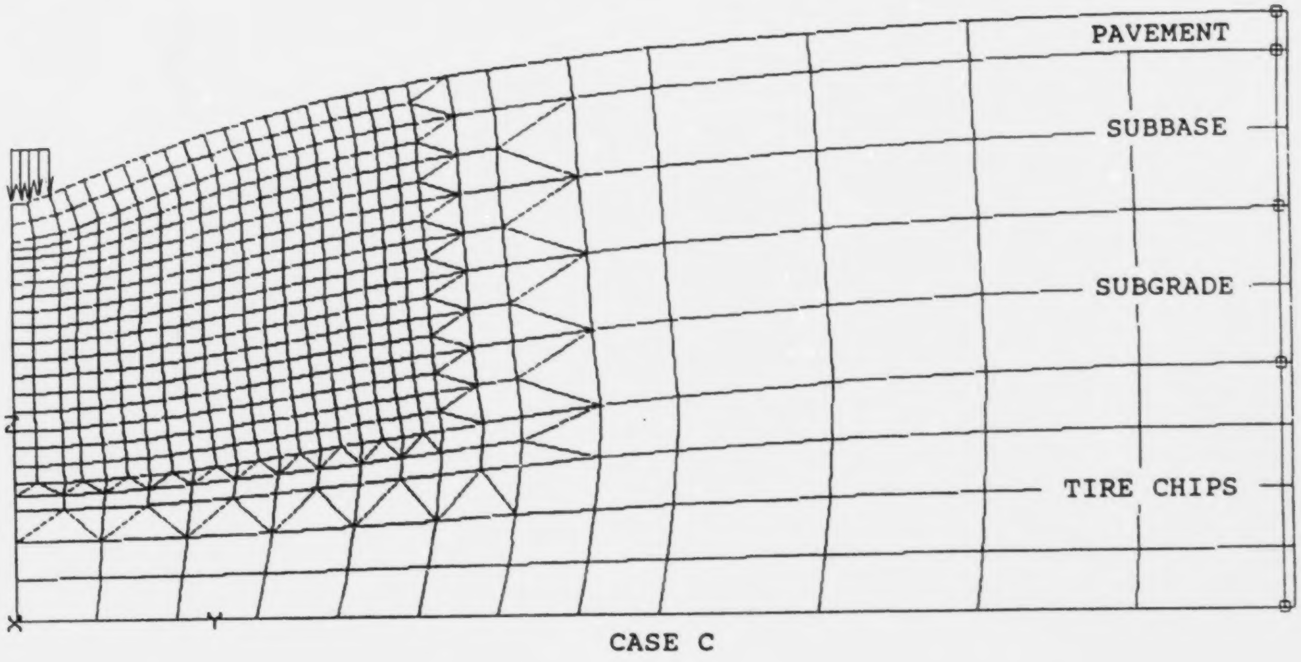
PAVEMENT
SUBBASE
SUBGRADE
TIRE CHIPS
X
Y
Z
CASE C

Figure 6.9(c) Deformed mesh plot for case C

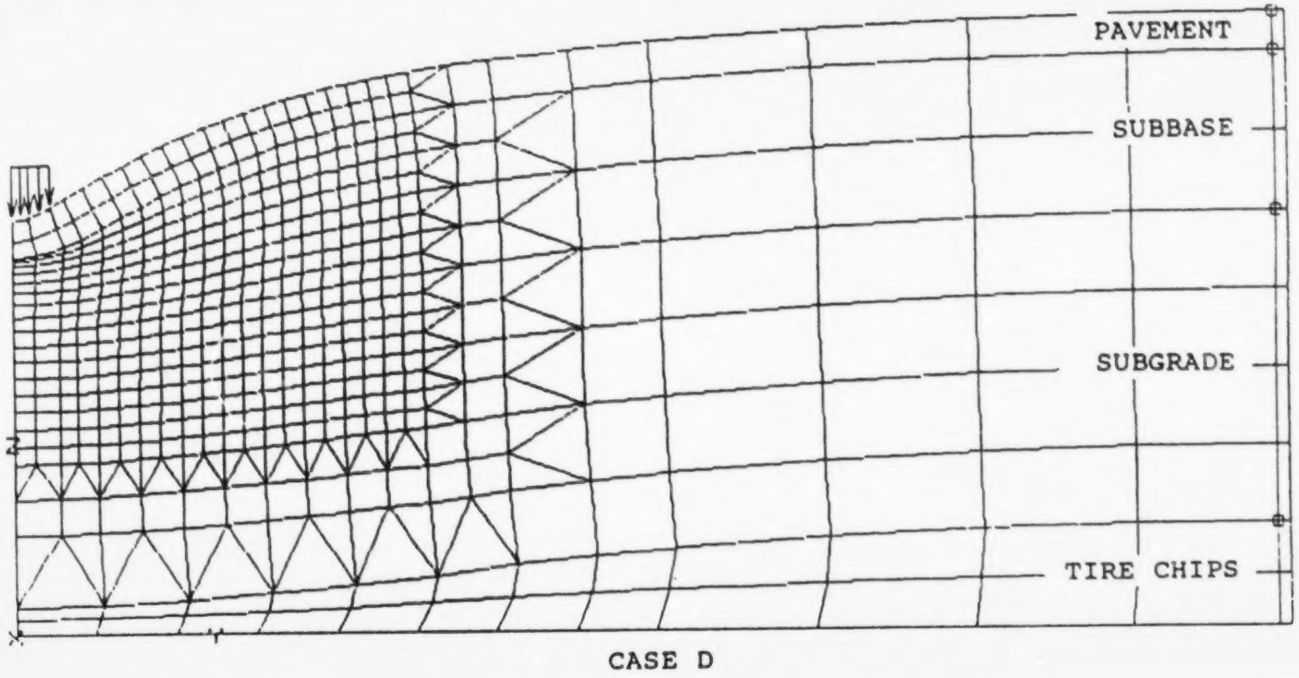
PAVEMENT
SUBBASE
SUBGRADE
TIRE CHIPS
Z
Y
X
CASE D

Figure 6.9(d) Deformed mesh plot for case D

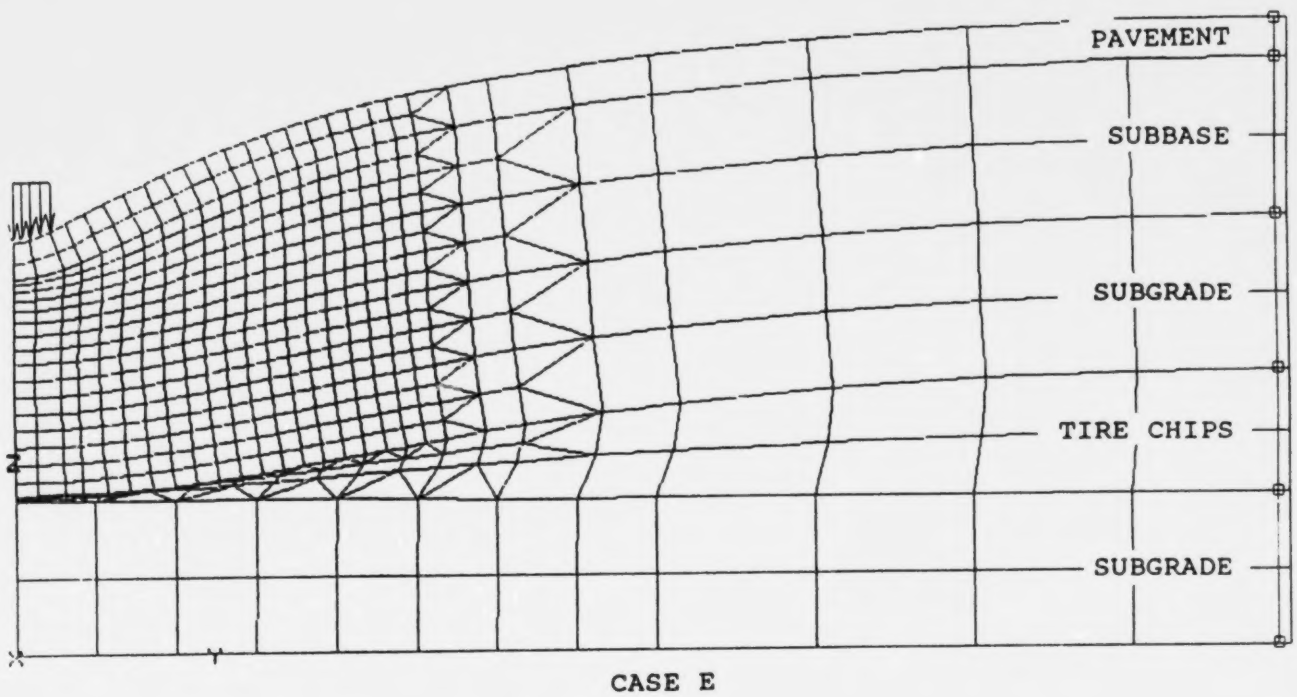
PAVEMENT
SUBBASE
SUBGRADE
TIRE CHIPS
SUBGRADE
Z
X
Y
CASE E

Figure 6.9(e) Deformed mesh plot for case E

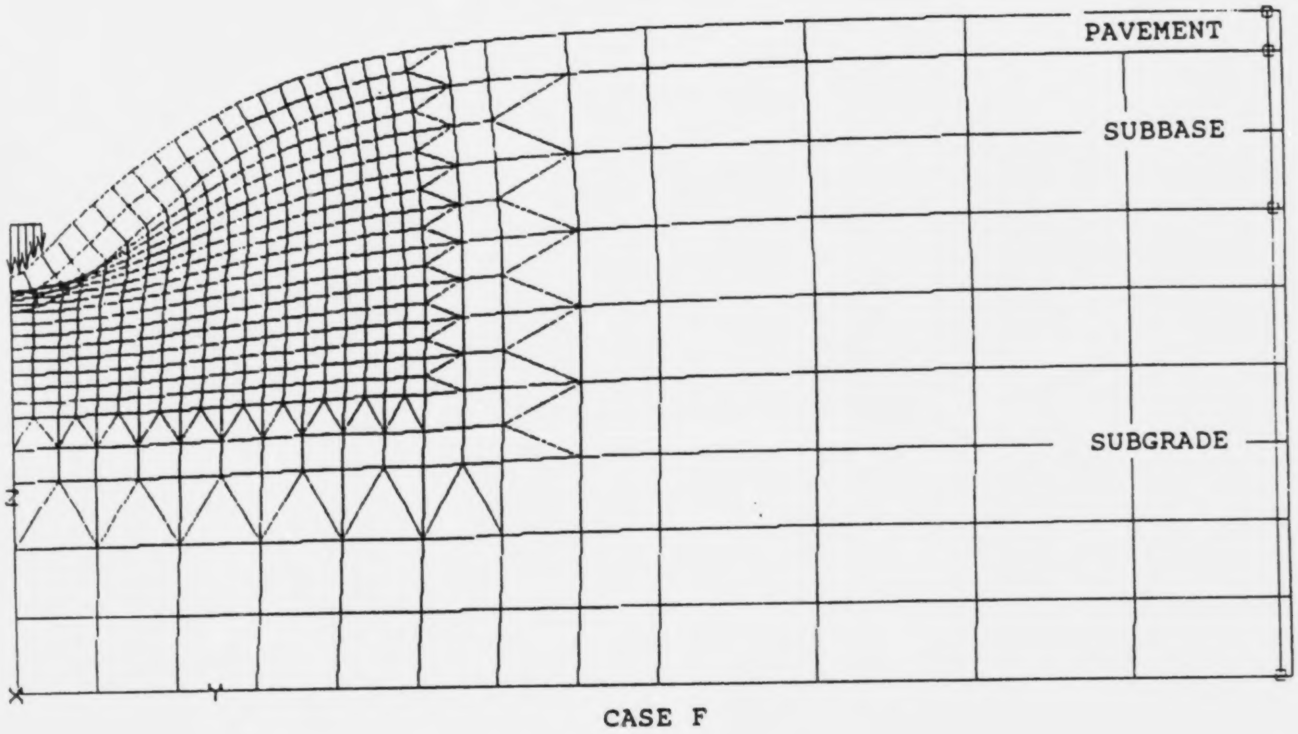
PAVEMENT
SUBBASE
SUBGRADE
Z
X
Y
CASE F

Figure 6.9(f) Deformed mesh plot for case F

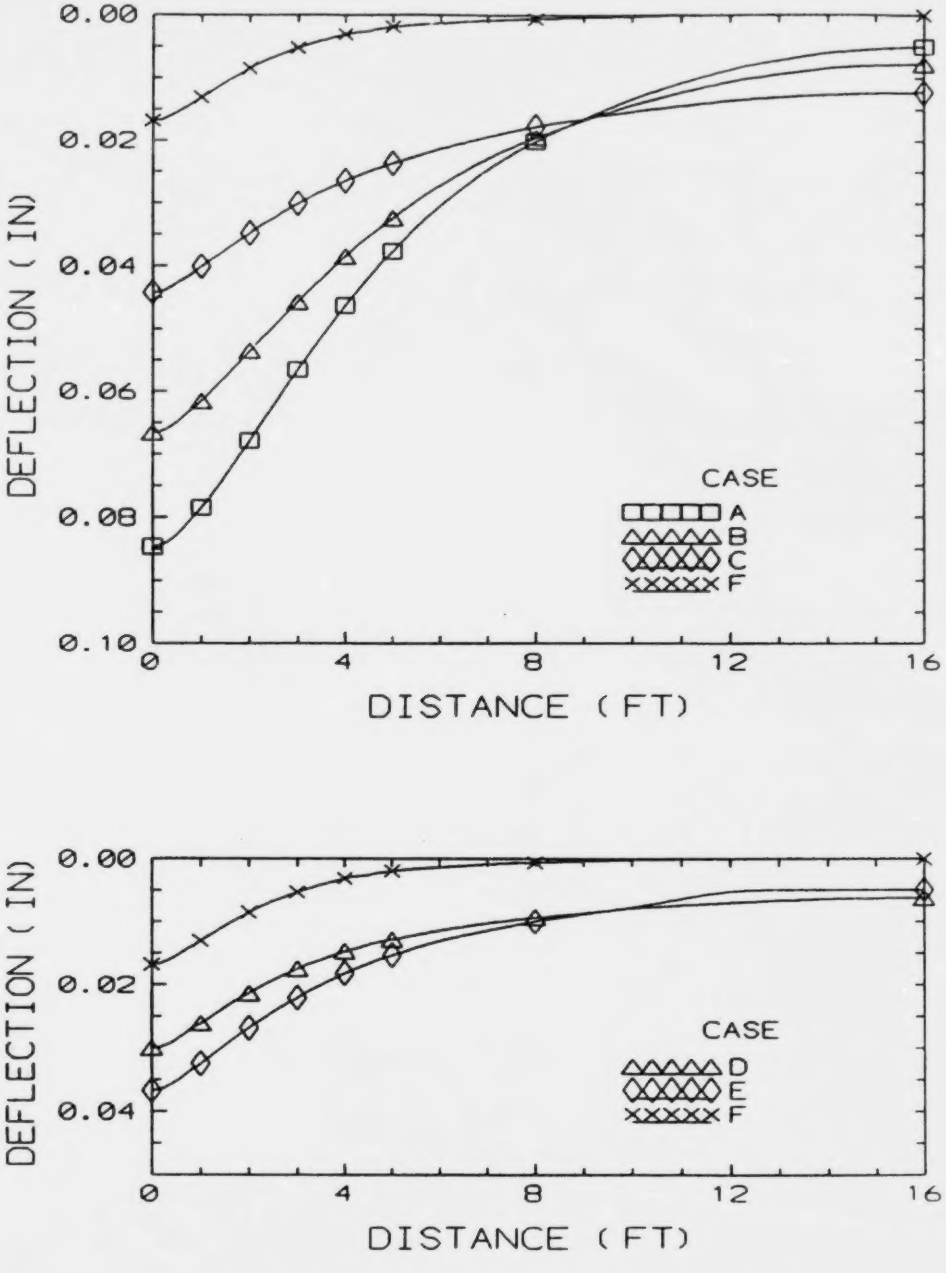

Figure 6.10 Pavement deflection versus distance from axis of rotation for three 4-ft tire chip thicknesses and two 2-ft tire chip thicknesses with case without tire chips

curves. A plot of centerline pavement deflection versus tire chip modulus is shown in Fig. 6.11. It can be seen that deflection increases significantly for moduli below 80 psi. However, for the range of soil cover thicknesses examined in this analysis, it is unlikely that the tire chip modulus would be that low.

6.4 CONCLUSIONS

Overall, there are four major variables in the pavement deflection analysis presented above: tire chip layer thickness, thickness of soil cover, tire chip modulus and soil moduli. Consequently, performance of roads with tire chip layers can only be roughly estimated without further testing and verification under actual field conditions. However, several general conclusions can be made.

Increasing the thickness of soil between the tire chip layer and pavement or decreasing the thickness of the tire chip layer decreases pavement deflection, thereby increasing pavement design life.

Using a finite element analysis it was estimated that for a 2-ft tire chip layer, 6 ft of soil cover is needed to reduce pavement deflections to 0.03 in., which is considered to be the maximum allowable for good pavement life. Increasing the tire chip modulus

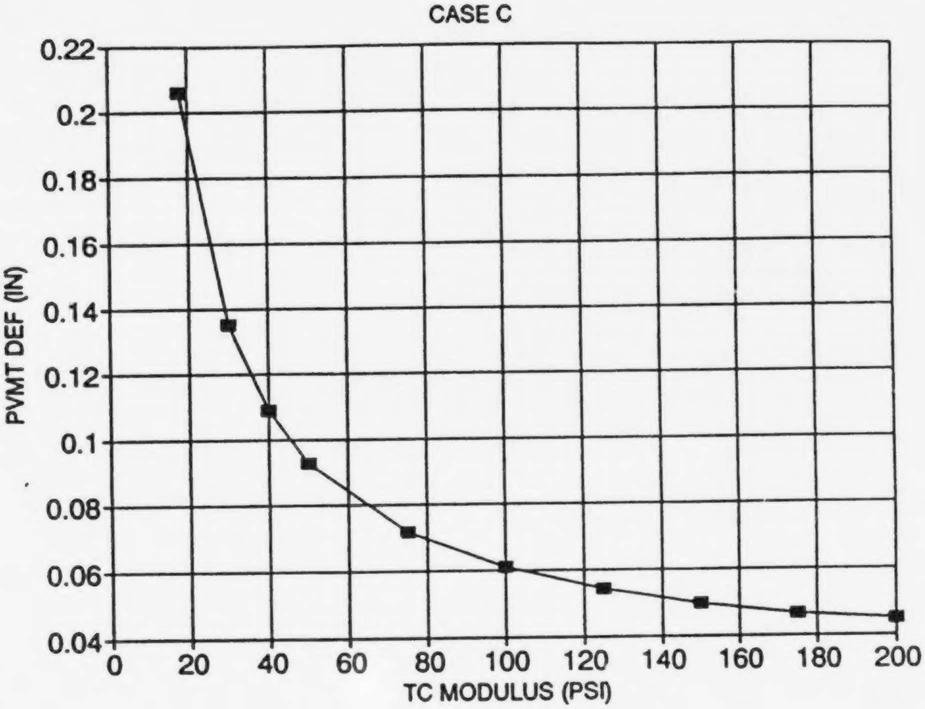

Figure 6.11 Effect of changing tire chip modulus on pavement deflection

decreases pavement deflection, again increasing pavement design life. For tire chip moduli below 80 psi, pavement deflections increase dramatically. Increasing the moduli of soil strata between the tire chip layer and pavement also decreases pavement deflection, increasing pavement design life. The results of this study can be used for preliminary estimates of allowable tire chip layer thickness and required thickness of soil between the pavement and tire chips.

CHAPTER 7. COST ANALYSIS

7.1 MATERIAL COST

To estimate the potential costs of using tire chips for road embankment fill, several tire chip manufacturers in Maine were contacted for prices of the raw tire chip material. In addition, one price was found in the literature. Table 7.1 shows the sources and prices of tire chips.

Table 7.1: Purchase prices of tire chips

Source	Cost
Sawyer Environmental Hampden, ME	$21/cy delivered
CP Tek Auburn, ME	$22/cy delivered
Massachusetts supplier to Sawyer Environmental	$15/cy delivered
Pine State	$7.50/cy delivered
Vermont Project (Winters, 1991)	$0.40/cy from Vermont $1.50/cy New Hampshire

The costs from Sawyer Environmental and CP Tek reflect the cost of buying refined tire chips at 1-in. maximum size for use as fuel in paper mill boilers. Since the current demand for tire chips to burn is higher than the present suppliers can handle, they want to sell all their chips at the higher refined rate, driving the price of 2-in. chips to the same level as smaller fuel grade chips. In Vermont, Winters (1991) reports the very low purchase and delivery costs were due to the manufacturer's interest in the project. In the near future, when more facilities like Pine State's tire chipping facilities are on line, the supply may better balance the demand for tire chips as fuel, decreasing the cost for the larger size chips used in highway applications. Additionally, increasing the number of chipping facilities in Maine may lead to more competitive pricing and incentive to sell the larger sized chips which have lower processing costs.

7.2 PLACEMENT AND COMPACTION COSTS

It was estimated that two Caterpillar D6 sized dozers, operating at cost of $110 per hour each including the operator, could spread and compact about 225 cy/hr, equivalent to about three 30 ton truckloads per hour. It was assumed that compaction could be achieved with 5 complete coverages with the track of the D6 dozer. The cost to place and compact the tire chips was roughly estimated at about $1/cy using the above construction scheme. The geotextile to enclose the tire chip layer was estimated to add about $2 per square yard, thus the cost per cubic yard of tire chips is dependent on tire chip layer thickness. Assuming a tire chip thickness of 4 ft, the total cost to place the tire chip layer enclosed by geotextile would be \$4/cy. For comparison, Winters (1991) reported a cost of \$1.65/cy, including geotextile work, for a project in Vermont. Actual costs will have to be determined in a future field trial.

Thus, the total cost to furnish and place tire chip fill could range from \$11.50/cy to \$26/cy. As discussed in Chapter 1, the cost for lightweight expanded shale fill is about \$44/cy, so tire chips have the potential to be economically competitive for use as lightweight fill. However, the cost of granular borrow is typically in the range of \$5 to \$10/cy so with current pricing, tire chips would not be an economical substitute for granular borrow.

BLANK

CHAPTER 8. SUMMARY, CONCLUSIONS, AND RECOMMENDATIONS

8.1 SUMMARY

An estimated 240 million used tires are discarded in the United States every year. In the state of Maine, about 1.2 million used tires are discarded annually. Since it is difficult to dispose of tires in a conventional landfill, they are generally just left in open piles, creating fire hazards and breeding grounds for disease carrying mosquitoes, as well as degrading the landscape. To recycle these tires, a number of uses have been developed in recent years including: highway uses of whole tires, recycled tire rubber in asphalt pavements and maintenance, tire derived fuel, and recycling tire materials into other petroleum derived products.

The research documented herein investigated the use of waste tires chipped to a maximum 2-in. size for use as conventional and lightweight embankment fill. The low unit weight (40 pcf) of these tire chips would provide Maine with a local source of lightweight fill, while also helping to fulfill the mandate by the Maine State Legislature to the Maine Department of Transportation regarding use of recyclable materials in construction (Maine State Legislature, M.R.S.A., Ch. 26, Section 18, Department of Transportation Recycling Program). In addition, use of tire chips for lightweight fill may prove to be more economical than other lightweight fills

Preceding page blank

such as expanded shale. To predict how tire chips would behave as fill in an embankment, an extensive laboratory research program was implemented including: a review of available literature, determination of basic engineering properties, laboratory measurement of compressibility, estimation of reduction in settlement due to use of tire chips as lightweight fill, pavement deflection analysis, and cost analysis. Laboratory measurement of compressibility of tire chips and prediction of the minimum thickness of soil required between the pavement and tire chip layers to limit pavement deflection to acceptable levels comprised the major research goals.

Limited information found in the literature indicated that tire chips have been used successfully as fill in several road projects, but reported values of actual engineering properties were sketchy or nonexistent. Some information on particle sizes, unit weights, compaction, and compressibility were found, in addition to eight case histories. Based on the literature reviewed, environmental concern for using tire chips as embankment fill seems minimal. Even though they leach very small amounts of hazardous substances, using tire chips below the ground water table is of greater concern than above the ground water table.

The gradation, specific gravity, and compacted unit weight of tire chips was determined using slightly modified conventional testing techniques. Gradation testing was accomplished using a large mechanical aggregate sieve machine. The tire chips used in this study were found to be uniformly graded with 90% of the particles larger than 0.5 in., and 50% between 1 and 1.5 in. Specific gravity of the tire chips was determined to be about 1.05. Compacted unit weight, determined in the laboratory using a 10-in. diameter by 10-in. high mold and compaction energy equivalent to modified proctor, standard proctor and 60% of standard proctor energy was determined to be about 40 pcf. The different energy levels did not create significant differences in compacted unit weight and neither did compacting samples in the saturated surface dry condition rather than air dried.

Settlements of embankments built over deposits of Presumpscot formation and peat were predicted to be reduced up to 40% when tire chips are used as a major part of the embankment fill.

A specially designed apparatus was constructed to determine the compressibility of tire chips in the laboratory. This apparatus could accommodate the large tire chip size and allowed measurement of horizontal stress and the portion of the vertical stress transferred to the walls of the apparatus by friction. The final design consisted of a 12-in. diameter by 12.5-in. high piece of schedule 40 PVC pipe, instrumented with strain gages mounted in the horizontal and vertical directions. The vertical load was applied using an Instron 4204 Universal Testing Machine. An IBM compatible computer was used to control the test and record the data. Vertical stress - strain data revealed high compression at low stresses, with compressibility decreasing at higher stresses. At 10 psi vertical stress, vertical strain was about 20% and at 50 psi, vertical strains approached 40%. Plots of horizontal stress versus vertical stress in tire chip samples showed values of Poisson's ratio at about 0.30 at low stress levels and 0.50 at higher stress levels. Young's modulus determined at a the secant of 10% strain ranged between 9 and 25 psi. Mixtures of tire chips and gravels had lower compressibility and higher Young's modulus values, but Poisson's ratio was unaffected by addition of gravel. Vertical strains at 10 psi vertical stress were reduced 3 to 7% and at 50 psi were reduced 9 to 22% with the addition of gravel.

A finite element analysis of a road embankment containing a layer of tire chips was performed to predict pavement deflection under a 5.5 ton wheel load. Four major variables were found to affect pavement deflection: tire chip layer thickness, thickness of soil cover between the tire chip layer and pavement, tire chip modulus, and soil moduli. Decreasing the tire chip layer thickness or increasing the thickness of soil cover, tire chip modulus or soil moduli all decreased the resulting pavement deflection. Estimated pavement deflections were as low as 0.03 in. with 2 ft of tire chips and 6 ft of soil between the tire chips and pavement, and as high as 0.084 in. with 1 ft. of gravel overlying 4 ft of tire chips. Pavement deflections were correlated with roadway design life using a figure from AASHTO (1986b). Design equivalent axle loads ranged from 25,000 for 1 ft of soil between the pavement and a 4-ft tire chip layer to 2,000,000 for 6 ft of soil between the pavement and a 2-ft tire chip layer.

The current cost of 2-in. tire chips ranged from \$7.50/cy from smaller chipping facilities to \$22/cy from facilities selling fuel grade chips to paper mills. Since other tire chip manufacturers are in the process of developing their businesses in Maine, it is hoped that this will create the competition necessary to reduce the cost of purchasing the larger size chips for use in highway applications. In general, larger tire chips are less expensive, since they require less effort to produce. Placement and compaction costs were roughly estimated at \$4/cy for a 4-ft layer of tire chips placed and compacted by two Caterpillar D6 sized dozers, and enclosed by a geotextile at the top, bottom, and sides.

8.2 CONCLUSIONS

Based on the research contained in this report, the following conclusions were made:

1. Using tire chips for embankment fill in highway applications is a feasible method of reuse for waste tires. Furthermore, the low unit weight of tire chips makes them suitable for use as lightweight fill.

2. The tire chips studied in this research, from Sawyer Environmental Recovery Inc. of Hampden, Maine, were uniformly graded with 90% of particle sizes greater than 0.5-in., 50% between 1 and 1.5-in. size and all less than the 2-in. maximum size allowed in the manufacturing process.

3. The specific gravity of a mixture of glass and steel belted tires was 1.05 and absorption was about 4%.

4. The compacted unit weight of tire chips was about 40 pcf. Compaction efforts ranging from modified proctor to 60% of standard proctor had only a small effect on compacted unit weight.

5. Settlements of road embankments over Presumpscot formation and peat could be reduced up to 40% using tire chips as a major portion of the embankment fill.

6. Compressibility testing in a specially designed apparatus showed tire chips to be very compressible with

secant Young's modulus at 10% strain between 9 and 25 psi. At 10 psi vertical stress, vertical strain was about 20% and at 50 psi, vertical strains approached 40%. The Poisson's ratio was determined to be about 0.30 at low stress levels and 0.50 at high stress levels. Compressibility testing of mixtures of tire chips and gravel revealed that increasing gravel content increased Young's modulus and decreased maximum strains. Poisson's ratio was not significantly affected by addition of gravel.

7. Finite element analysis of pavement deflection showed values ranging from as low as 0.03 in. with 2 ft of tire chips and 6 ft of gravel between the tire chips and pavement, and as high as 0.084 in. with 1 ft. of gravel overlying 4 ft of tire chips. This range of deflection corresponds to a range of 25,000 equivalent axle loads for 0.084 in. of deflection to 2,000,000 equivalent axle loads for the 0.03-in. deflection (AASHTO, 1986b). Based on these results, it seems reasonable to investigate a range of cover thickness between 2 and 6 ft over a 2-ft layer of tire chips.

8.3 RECOMMENDATIONS FOR FUTURE RESEARCH

1. The gradations, specific gravities, unit weights and compressibilities of tire chips from other sources should

be determined to evaluate the feasibility of using different size chips.

2. A field trial should be performed to validate and improve the finite element modeling of pavement deflections caused by the use of a tire chip layer in the road embankment.

3. Further finite element modeling of pavement deflections should be performed using material models which better represent the nonlinear, stress dependent behavior of the subbase and subgrade soil soils and the tire chips.

REFERENCES

AASHTO (1986a), Standard Specifications for Transportation Materials and Methods of Sampling and Testing, Part II: Methods of Sampling and Testing, Fourteenth edition, American Association of State Highway and Transportation Officials, Washington, D.C., 1275 pp.

AASHTO (1986b), AASHTO Guide for Design of Pavement Structures, American Association of State Highway and Transportation Officials, Washington, D.C., 404 pp.

ASTM (1988a), Annual Book of ASTM Standards, Construction Section 4, Soil and Rock, Building Stones; Geotextiles Volume 04.08, American Society for Testing and Materials, Philadelphia, Pennsylvania, 951 pp.

ASTM (1988b), Annual Book of ASTM Standards, Construction Section 4, Road and Paving Materials; Traveled Surface Characteristics Volume 04.03, American Society for Testing and Materials, Philadelphia, Pennsylvania, 673 pp.

Barker, W.R. (1972), "Nonlinear Finite Element Analysis of Heavily Loaded Pavement Systems," Proceedings of the Symposium on Applications of the Finite Element Method in Geotechnical Engineering, U.S. Army Waterways Experiment Station, Vicksburg, Miss., Vol II, pp. 657-693.

Batchelder Adams, G.P. (1984), "Analysis and Prediction of the Compression of Peats and Organic Soils," a thesis submitted to the University of New Hampshire in partial fulfillment of the requirements for the degree of Master of Science in Civil Engineering, 107 pp.

Beatty, J.R. (1981), "Physical Properties of Rubber Compounds," Mechanics of Pneumatic Tires, Clark, S.K., ed., United States Department of Transportation, National Highway Traffic Administration, Washington, D.C., 931 pp.

Beniwal, R.K., Eaton, G. and Morgan, M.W. (1971), "Subsurface Investigation for the Proposed Reconstruction of a Portion of Route 77 in the Town of Cape Elizabeth, Cumberland County," Soils Report No. 71-20, Maine State Highway Commission, Materials and Research Division, 18 pp. and 97 sheets.

Bressette, T. (1984), "Used Tire Material As an Alternate Permeable Aggregate," California Department of Transportation, Office of Transportation Laboratory, Sacramento, California, 23 pp.

Chen, H.H., Marshek, K.M., and Saraf, C.L. (1986), "Effects of Truck Tire Contact Pressure Distribution on the Design of Flexible Pavements: A Three-Dimensional Finite Element Approach," Transportation Research Record No. 1095, Highway Research Board, Washington D.C., pp. 72-78.

Clark, P.S. (1991), "Tire Chips Provide Fuel for Boiler at Champion," The Ellsworth American, Thursday, March 7.

Colorado Department of Highways (1991), Research Newsletter, February 1991, 4 pp.

Das, B.M. (1990), Principles of Foundation Engineering, Second Edition, PWS-Kent, Boston, 731 pp.

Desai, C.S., and Christian, J.T. (1977), Numerical Methods in Geotechnical Engineering, McGraw-Hill, New York, 783 pp.

Dodson, T. (1990), "Camas Valley-Muns Creek, Highway 35 Landslide: Plans, Construction Sequencing and Staging," Oregon State Highway Division, Geotechnical Group, 6 pp.

Duncan, J.M., Monismith, C.L., and Wilson E.L. (1968), "Finite Element Analyses of Pavements," Highway Research Record No. 228, Highway Research Board, Washington D.C., pp. 18-33.

Eaton, R.A., Roberts, R.J. and Blackburn, R.R. (1991), "Use of Scrap Rubber in Asphalt Pavement Surfaces," prepared for presentation at the ARA International Tire Recycling Conference, San Jose, California, January, 1991, 37 pp.

Edil, T.B., Bosscher, P.J., and Eldin, N.N. (1990), "Development of Engineering Criteria for Shredded or Whole Tires in Highway Applications," Interim report to the Wisconsin Department of Transportation, University of Wisconsin - Madison, 99 pp.

El Puente newsletter (1990), "New Use for Old Tires," Transportation Technology Transfer Center, University of Puerto Rico, Volume 4, Number 4, Fall 1990, p. 3.

Forsyth, R.A., and Egan, J.P. (1976), "Use of Waste Materials in Embankment Construction," Transportation Research Record 593, Use of Waste Materials and Soil Stabilization, Transportation Research Board, Washington, D.C., pp. 3-8.

Frascoia, R.I. (1991) "Use of Tire Chips in a Georgia Vermont Town Highway Base," Research Update Number U91-6, Vermont Agency of Transportation Materials and Research Division, April 17, 5 pp.

Geisler, E., Cody, W.K., and Niemi, M.K. (1989), "Tires for Subgrade Support," Annual Conference on Forest Engineering Meeting, Coeur D'Alene, ID, 5 pp.

Gomez-Achecar, M., and Thompson, M.R. (1986), "ILLI-PAVE-Based Response Algorithms for Full-Depth Asphalt Concrete Flexible Pavements," Transportation Research Record No. 1095, Highway Research Board, Washington, D.C., pp. 11-18.

Hannon, J.B., and Forsyth, R.A. (1973), "Fill Stabilization Using Non-biodegradable Waste Products - Phase I," California Department of Transportation, Office of Transportation Laboratory, Sacramento, California, 46 pp.

Harvey, G. (1989), "Discarded Tires Shredded for Useful Life as Roadbed in Swampy Areas," Community newspaper article, Minnesota, April 13, pp. 1Y and 10Y.

King, A.R. (1970), Soils report prepared for the Construction of the Route 1 Connector, City of South Portland, Maine, Soils Project No. 1-295-3(52) 11-01-1(31), Maine Department of Transportation, Technical Services Division, Geotechnical Section.

King, A.R., Waldo, G.A. and Morgan, M.W. (1988), "A Subsurface Investigation for the Proposed Replacement of the Maine Turnpike-Falmouth Spur (I-95) Bridges over the Canadian National Railroad in Falmouth," Soils Report No. 88-10, Maine Department of Transportation, Technical Services Division, Geotechnical Section, 11 pp. and 18 sheets.

Lambe, T.W., and Whitman, R.V. (1969), Soil Mechanics, John Wiley & Sons, New York, 553 pp.

Maine Department of Environmental Protection (DEP) (1989), Bureau of Solid Waste Management, report to Maine State Legislature on Tires, White Goods and Demolition Debris, May.

Minnesota Pollution Control Agency (1990), "Environmental Study of the Use of Shredded Waste Tires for Roadway Sub-grade Support", by Twin City Testing Corp., St. Paul MN, for Andy Ronchak, Waste Tire Management Unit, Site Response Section, Groundwater and Solid Waste Division, Minnesota Pollution Control Agency, St. Paul, MN, 34 pp.

Nguyen, M.X., and Williams, J.A. (1989), "Implementaion Package for Using Discarded Tires in Highway Maintenance," California Department of Transportation, Office of Transportation Laboratory, Sacramento, California, 58 pp.

Number Cruncher Microsystems (1986), SAP86: A Finite Element Program for Static and Dynamic Analysis of Linear Structural Systems, Release 3.0, Number Cruncher Microsystems, Inc., San Francisco, California.

Palmer, A., and Verdegan, C.T. (1989), "Soils Investigation Embankment Failure CSAH 21: One Mile North of the City of Rice, MN," report from Braun Engineering Testing Inc., Minnesota, to Dennis Carlson, Benton County Highway Dept., Foley, Minnesota, 8 pp.

Recycled Products Guide (1991), "Old Tires Recycled Into Soil Conditioner," June 1991, p. 6.

Richman, R.L., and Jackura, K.A. (1984), "Field Performance of Experimental Tire Anchor Timber Wall," California Department of Transportation, Office of Transportation Laboratory, Sacramento, California, 74 pp.

Sikora, M.B. (1988), "Tire Recovery and Disposal: A National Problem with New Solutions," Resource Recovery Report, Washington, D.C., June 1986, pp. 65-75.

Smith, M. (1991), "Getting Rid of Old Tires," Truck and Van Show, October 3, p. 10.

Stark, J.F. III, and Korte R.A. (1988), "The Tirecycle Solution: Minnesota's Answer to the Scrap Tire Problem," *Emerging Solutions to the Disposal Crisis*, Seventh Annual New England Resource Recovery Conference and Exposition, Portland, Maine, June 9, 1988, 8 pp.

Structural Analysis (1987), *MTAB * POST; General Purpose Finite Element Solution Postprocessor for the IBM-PC and Compatible Micro Computers*, Version 1.0 Structural Analysis, Inc., Austin, Texas.

Sweere, H., Penning, A., and Vos, E. (1987), "Development of a Structural Design Procedure for Asphalt Pavements With Crushed Rubble Base Courses," *Proceedings of the Sixth International Conference on Structural Design of Asphalt Pavements,* Vol.I, University of Michigan, Ann Arbor, Michigan, pp. 34-49.

Williams, J., and Weaver, D. (1987) "Guidelines for Using Recycled Tire Carcasses in Highway Maintenance," California Department of Transportation, Office of Transportation Laboratory, Sacramento, California, 127 pp.

Winters, P. (1991) "Use of Tire Chips in a Highway Embankment," *Research Update Number U91-5*, Vermont Agency of Transportation, Materials and Research Division, 7 pp.

Yee, W.S. (1979), "Fill Stabilization Using Non-biodegradable Waste Products-Phase II," California Department of Transportation, Office of Transportation Laboratory, Sacramento, California, 100 pp.

BLANK

APPENDIX OF COMPRESSIBILITY TESTING RESULTS

Legend

Test Number	Material
301	All tire chips
1001	All tire chips
1002	All tire chips
2001	All tire chips
2002	All tire chips
G2003	50% MDOT type D gravel
G2004	50% MDOT type D gravel
G2005	50% MDOT type D gravel
25G1	25% 3/4-in. gravel
25G2	25% 3/4-in. gravel
25G3	25% 3/4-in. gravel
50G1	50% 3/4-in. gravel
50G2	50% 3/4-in. gravel
50G3	50% 3/4-in. gravel
75G1	75% 3/4-in. gravel
75G2	75% 3/4-in. gravel
75G3	75% 3/4-in. gravel

Preceding page blank

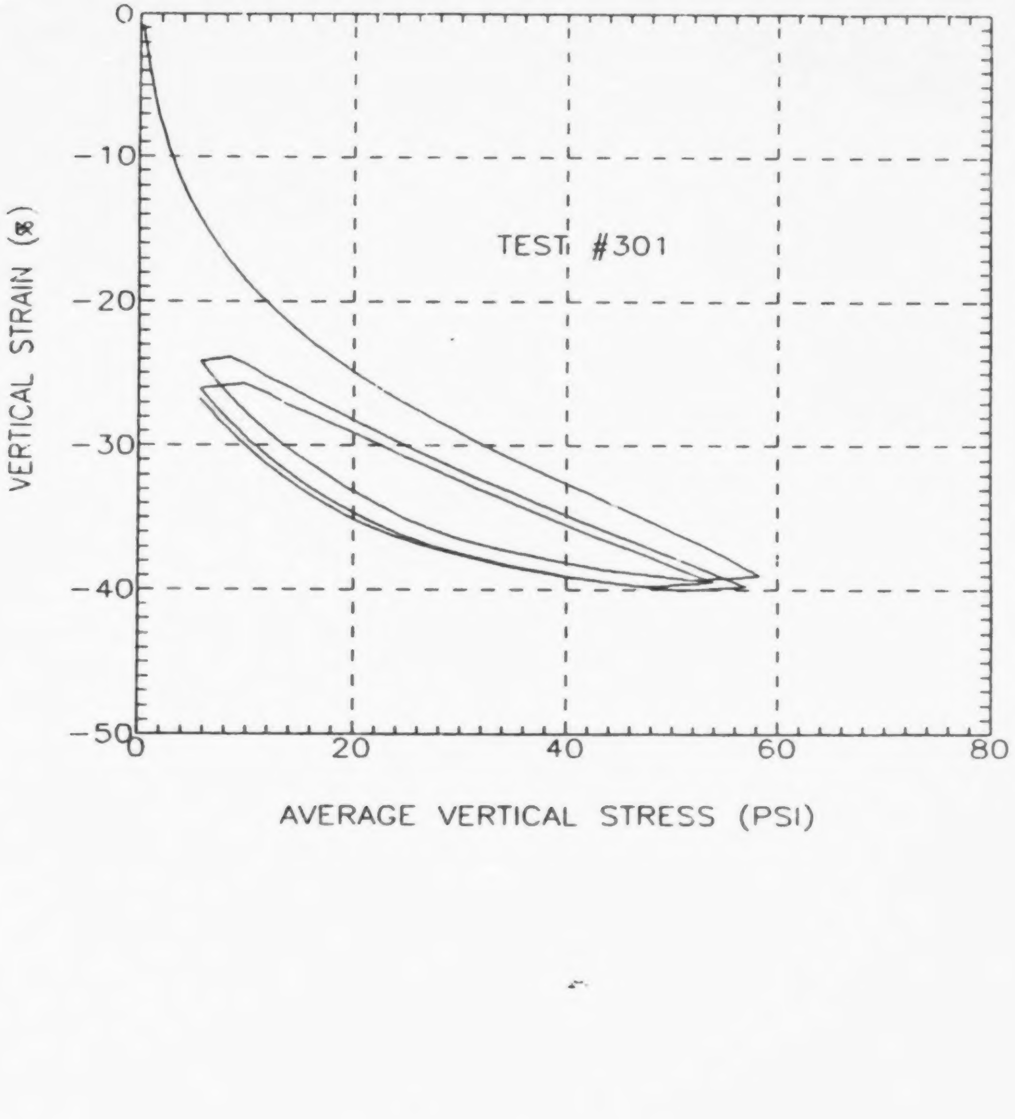
0
-10
-20
-30
-40
-50
0
20
40
60
80
VERTICAL STRAIN (%)
AVERAGE VERTICAL STRESS (PSI)
TEST #301

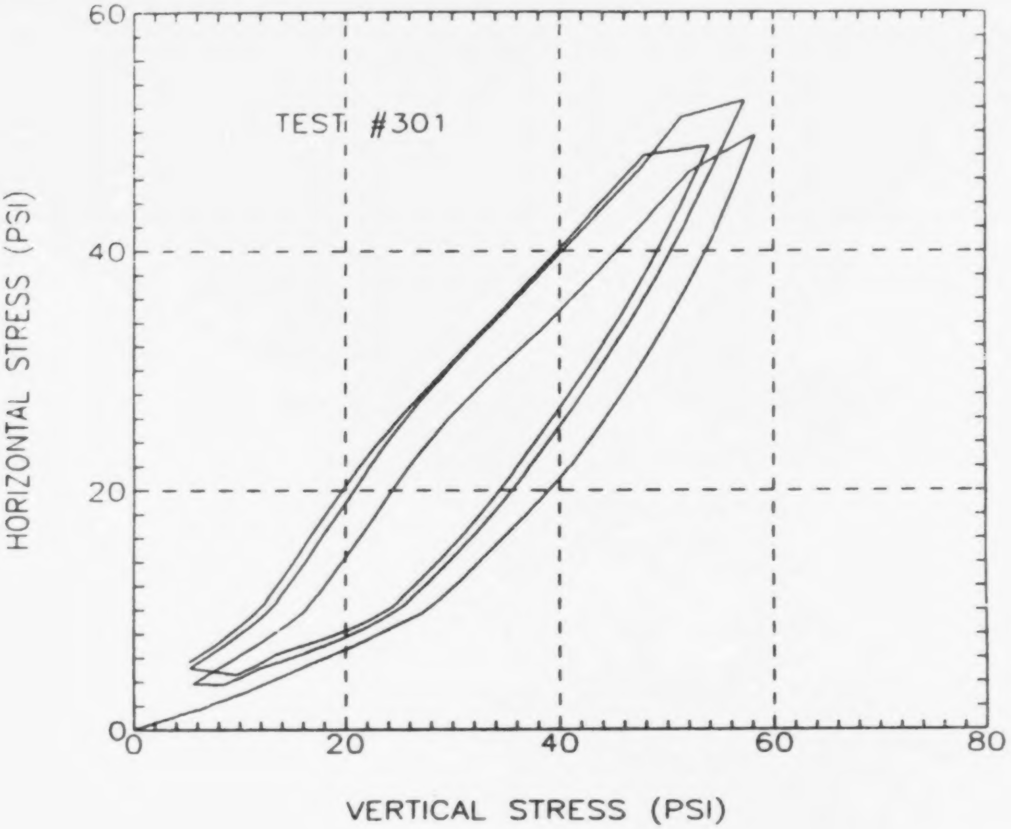

TEST #301
HORIZONTAL STRESS (PSI)
VERTICAL STRESS (PSI)
0
20
40
60
0
20
40
60
80

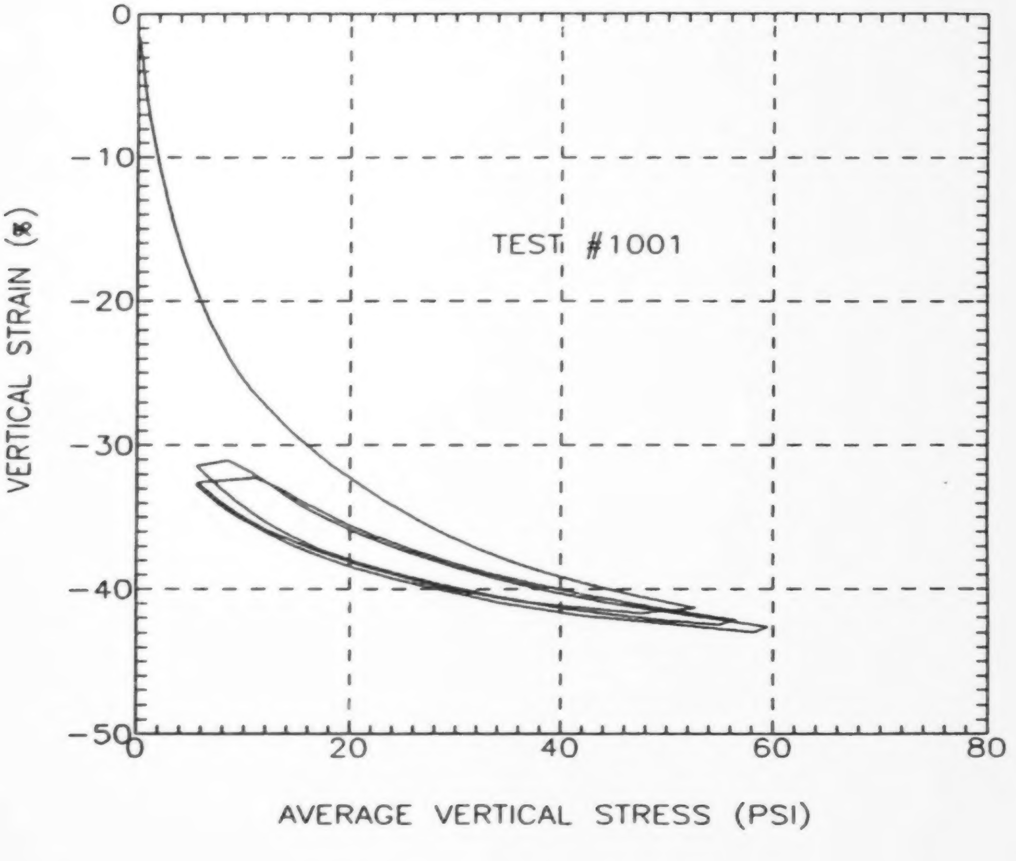
0
−10
−20
−30
−40
−50
0
20
40
60
80
VERTICAL STRAIN (%)
TEST #1001
AVERAGE VERTICAL STRESS (PSI)

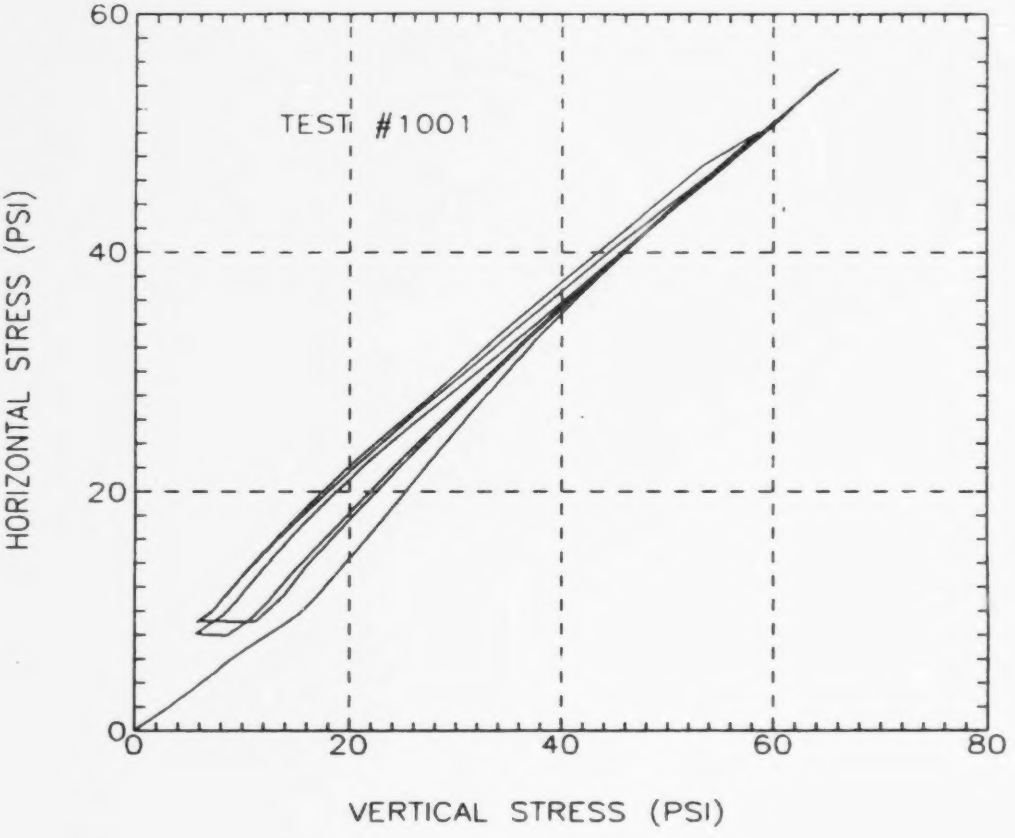
TEST #1001
HORIZONTAL STRESS (PSI)
VERTICAL STRESS (PSI)
0
20
40
60
0
20
40
60
80

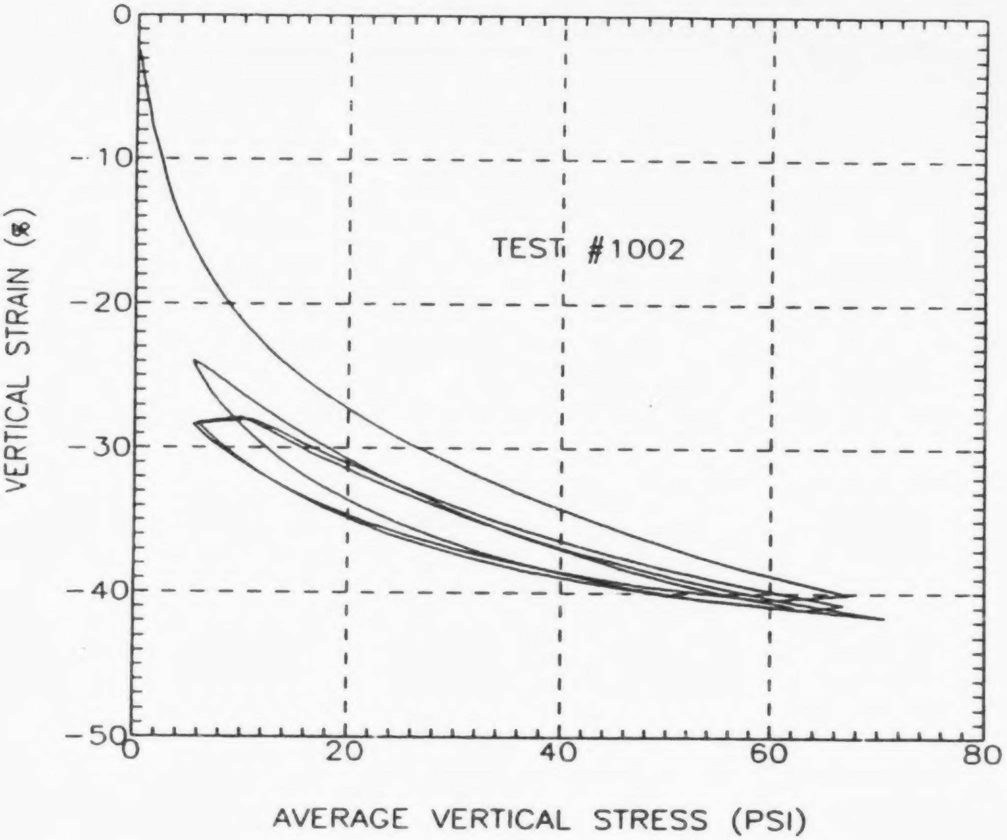
TEST #1002
VERTICAL STRAIN (%)
AVERAGE VERTICAL STRESS (PSI)
0
-10
-20
-30
-40
-50
0
20
40
60
80

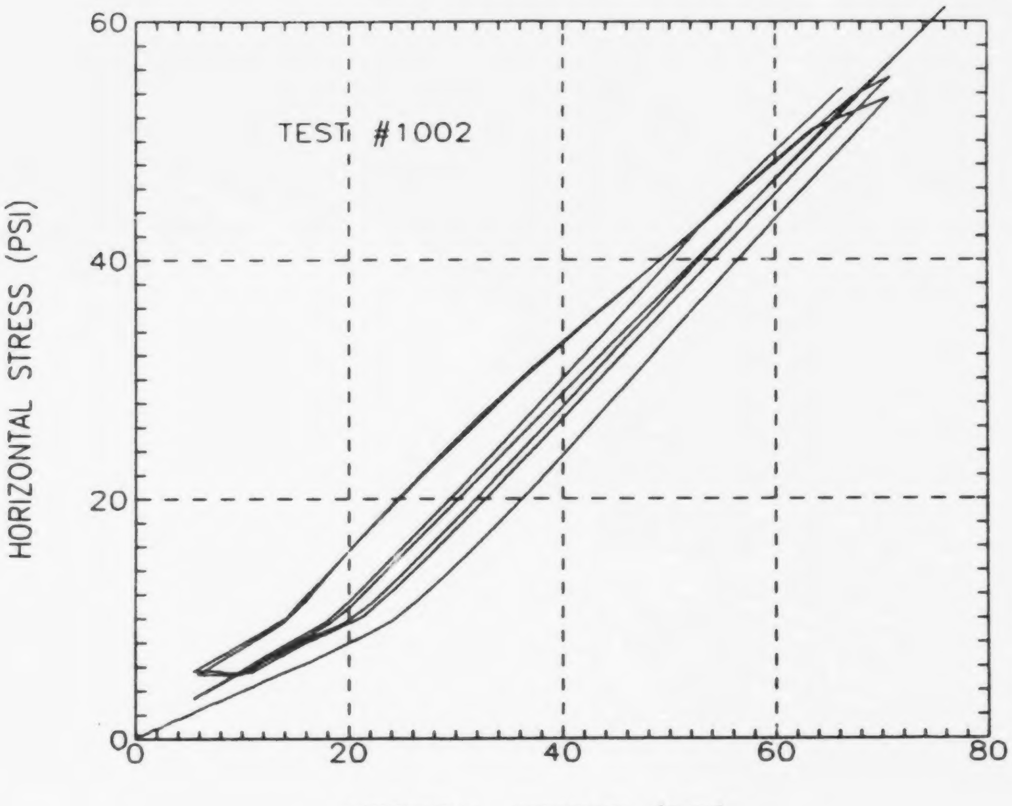
TEST #1002
HORIZONTAL STRESS (PSI)
VERTICAL STRESS (PSI)
0
20
40
60
0
20
40
60
80

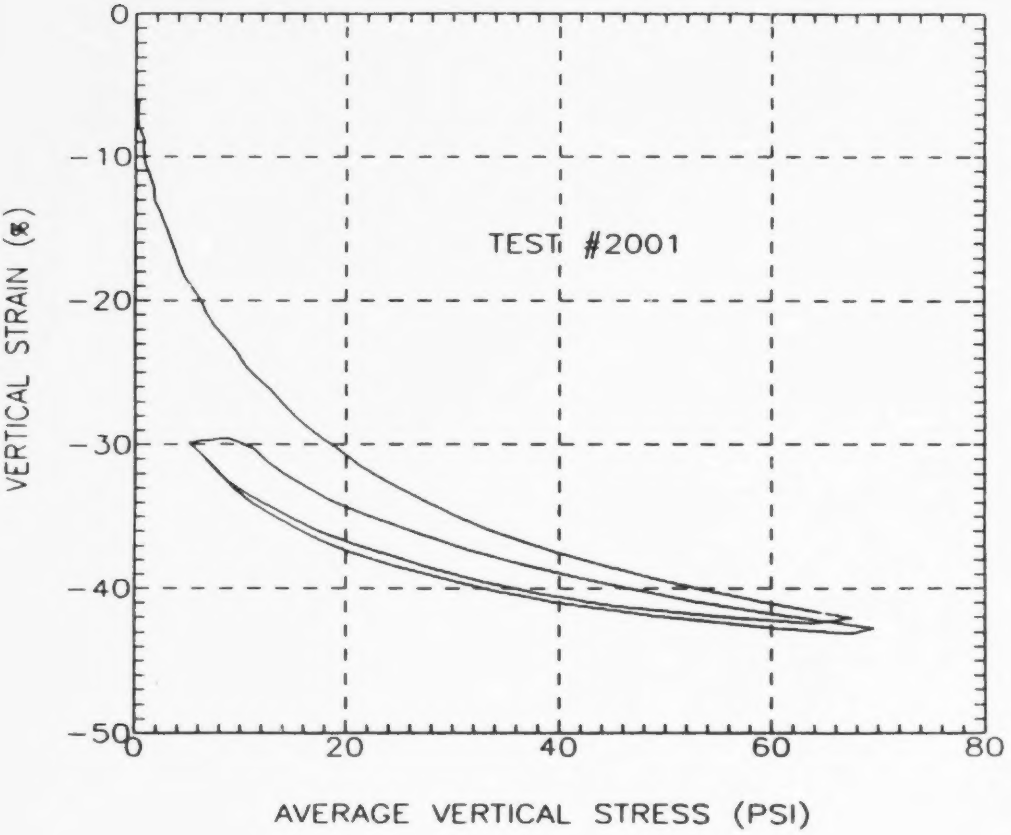
0
-10
-20
-30
-40
-50
0
20
40
60
80
VERTICAL STRAIN (%)
AVERAGE VERTICAL STRESS (PSI)
TEST #2001

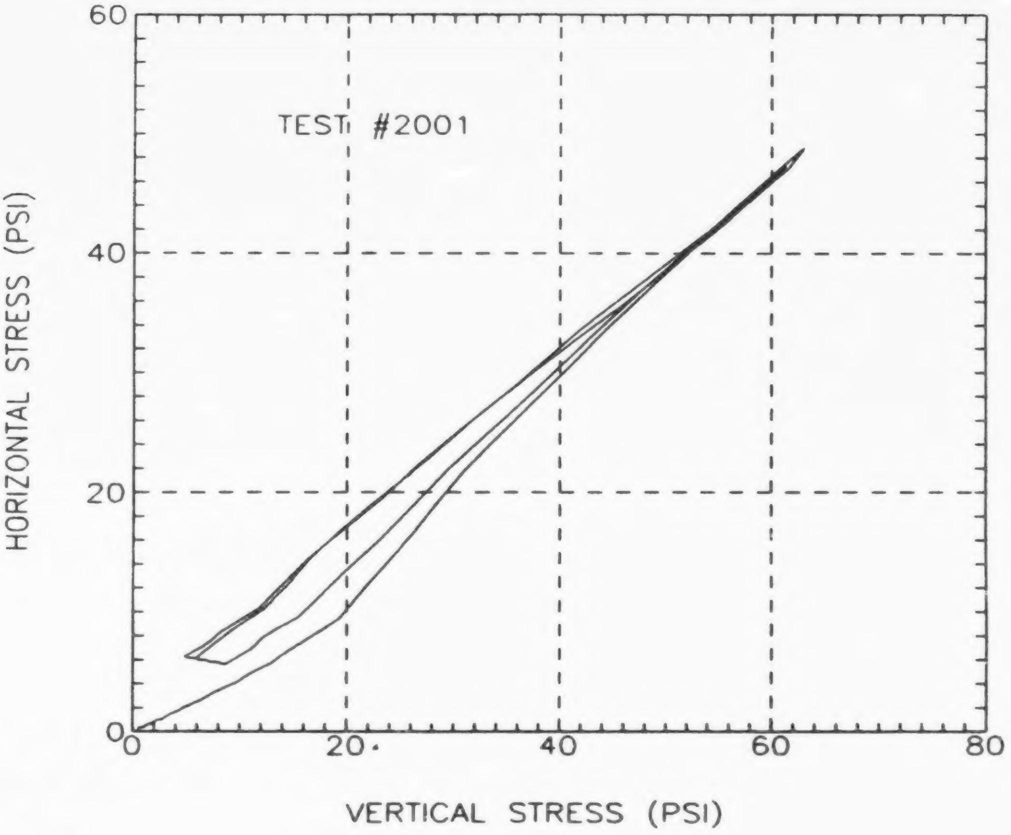
TEST #2001
HORIZONTAL STRESS (PSI)
VERTICAL STRESS (PSI)
0
20
40
60
0
20
40
60
80

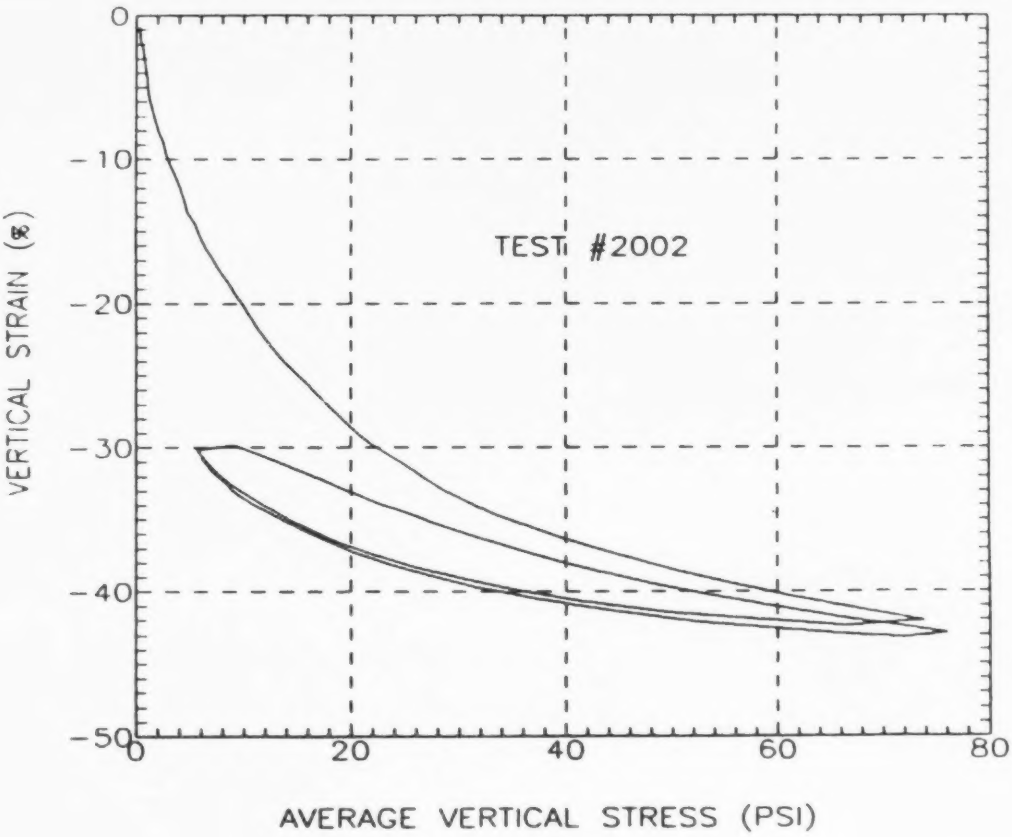
TEST #2002
VERTICAL STRAIN (%)
AVERAGE VERTICAL STRESS (PSI)
0
-10
-20
-30
-40
-50
0
20
40
60
80

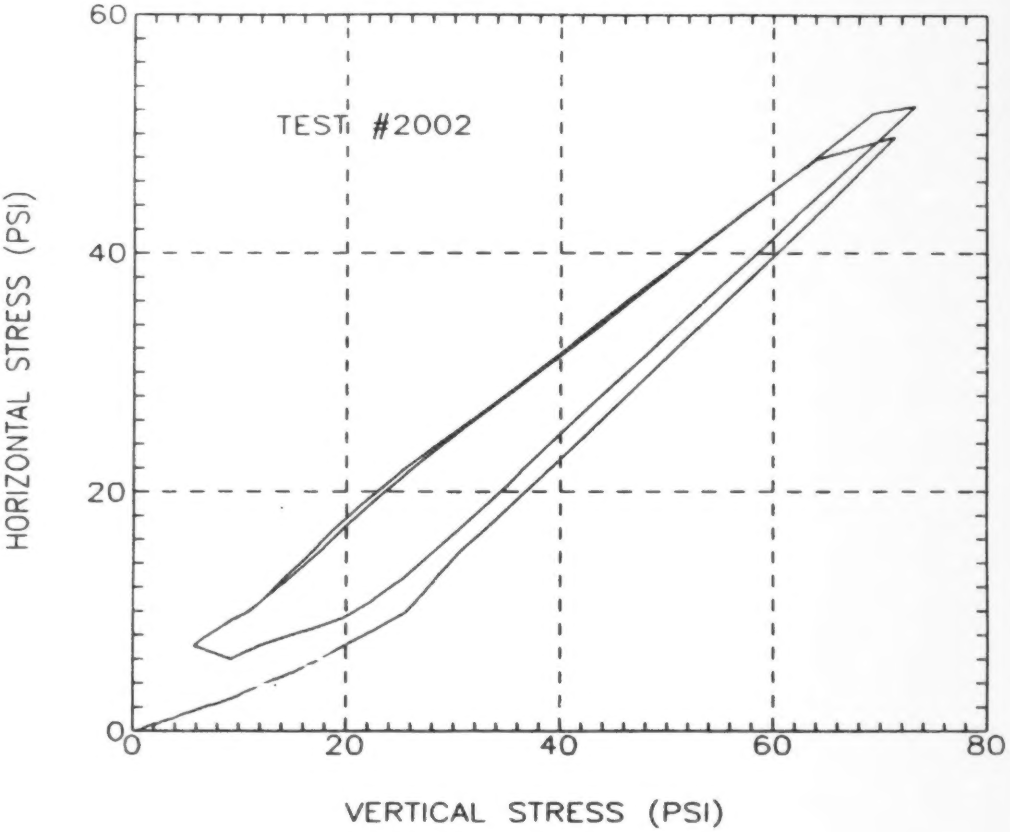
TEST #2002
HORIZONTAL STRESS (PSI)
VERTICAL STRESS (PSI)
0
20
40
60
0
20
40
60
80

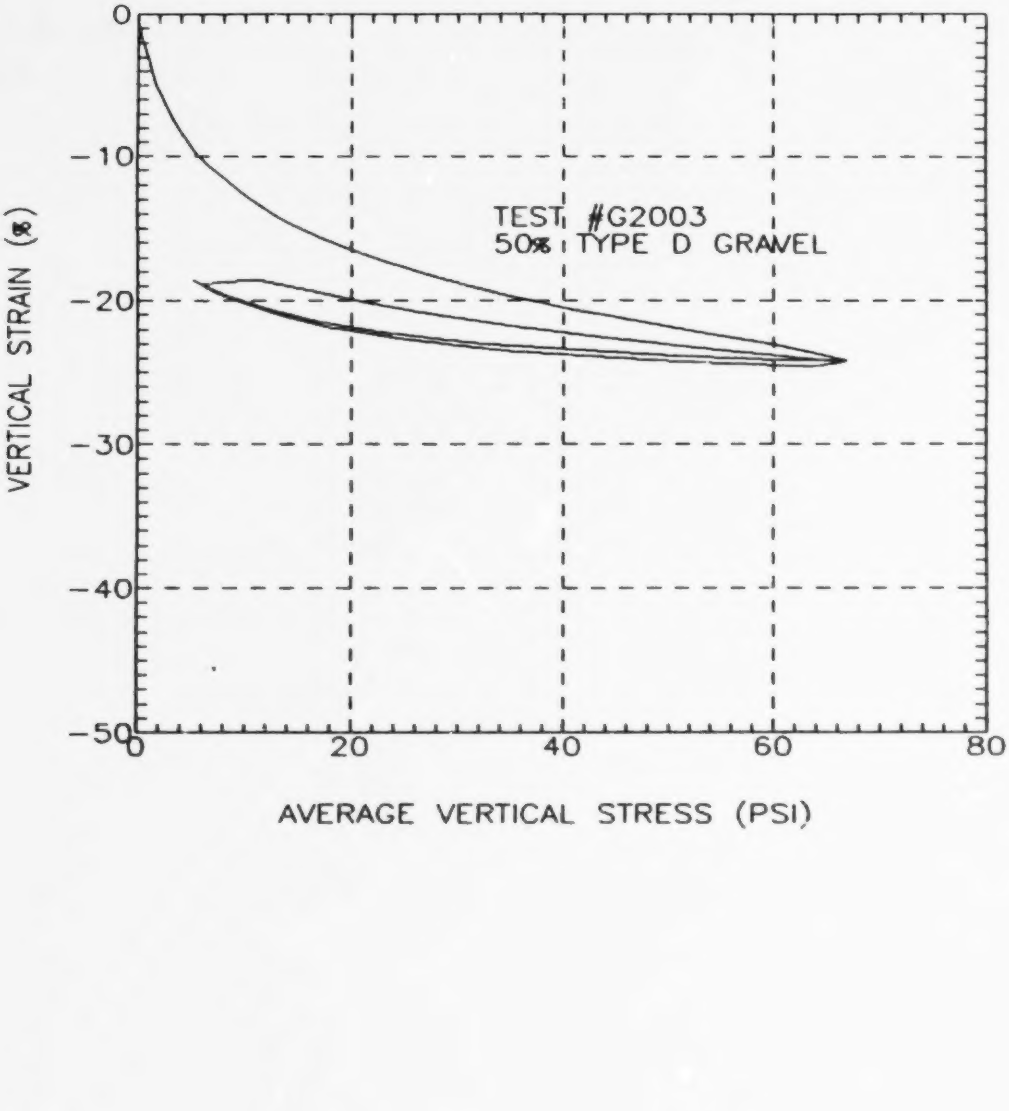
TEST #G2003
50% TYPE D GRAVEL
VERTICAL STRAIN (%)
AVERAGE VERTICAL STRESS (PSI)
0
-10
-20
-30
-40
-50
0
20
40
60
80

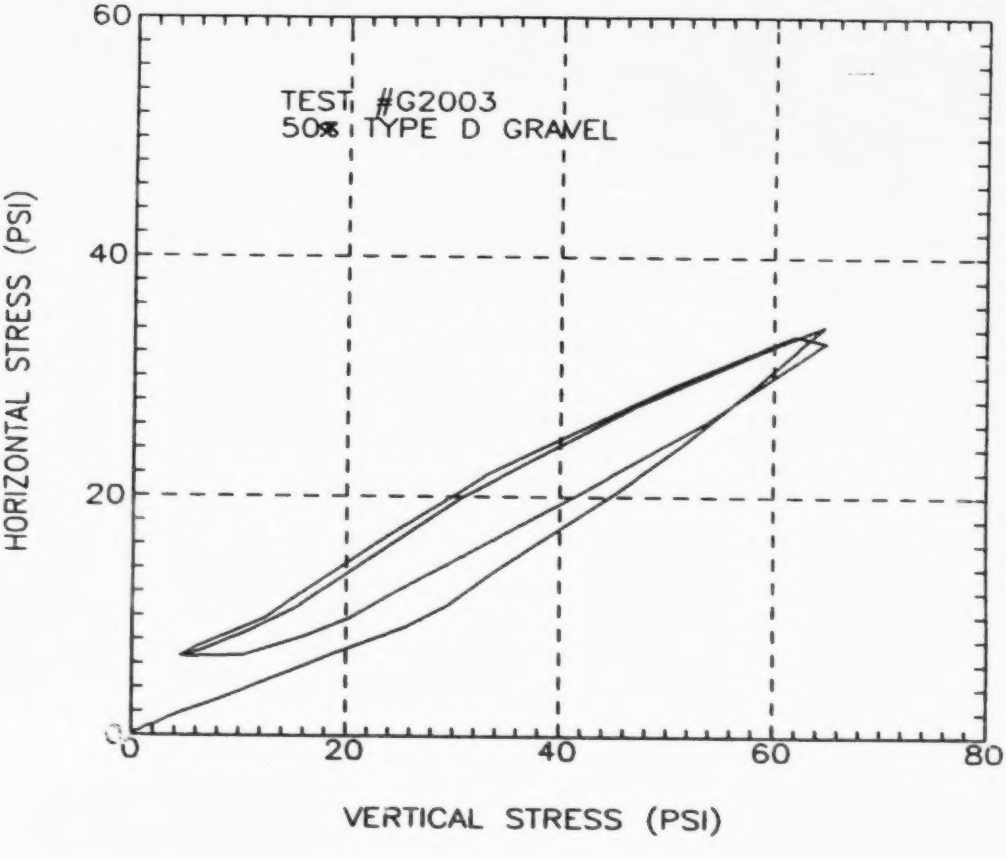
TEST #G2003
50% TYPE D GRAVEL
HORIZONTAL STRESS (PSI)
VERTICAL STRESS (PSI)
0
20
40
60
0
20
40
60
80

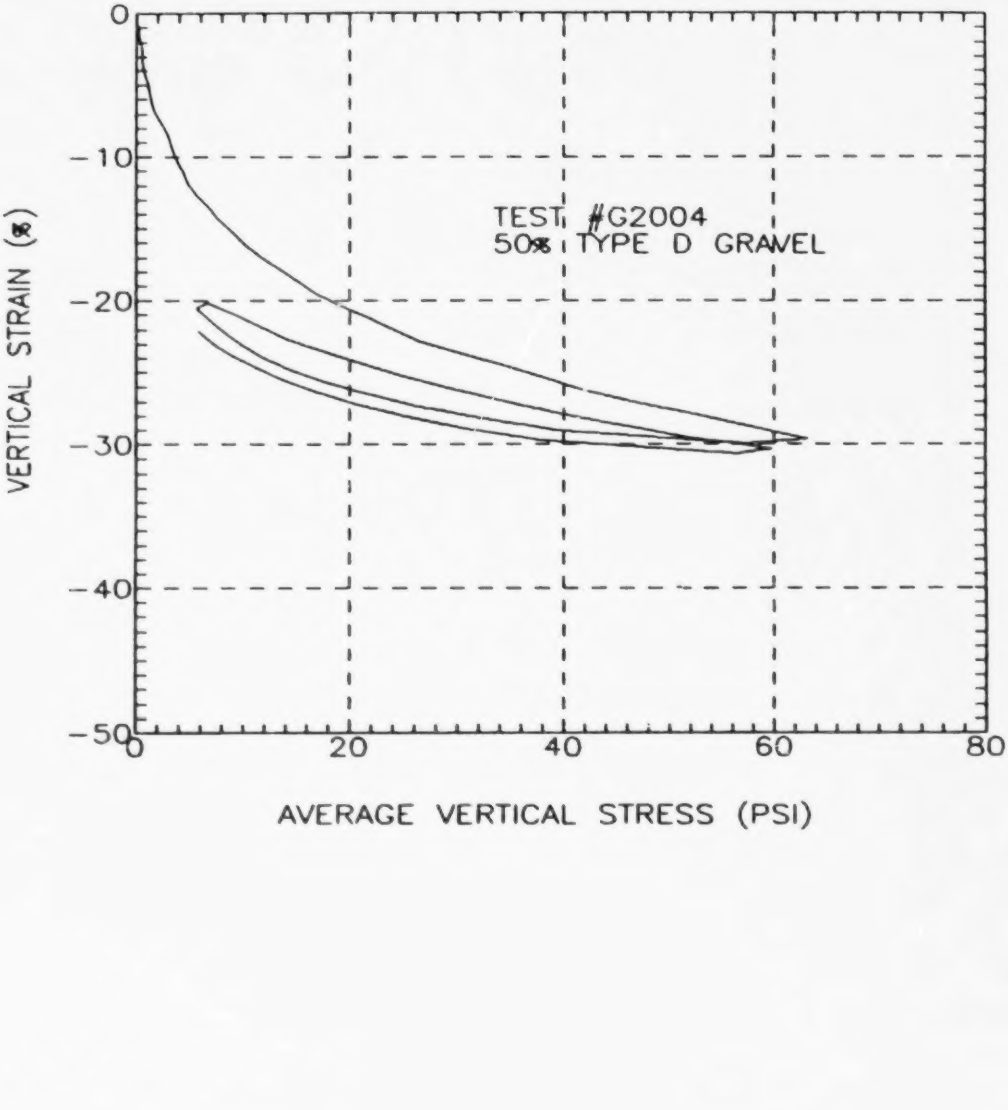
0
-10
-20
-30
-40
-50
0
20
40
60
80
VERTICAL STRAIN (%)
AVERAGE VERTICAL STRESS (PSI)
TEST #G2004
50% TYPE D GRAVEL

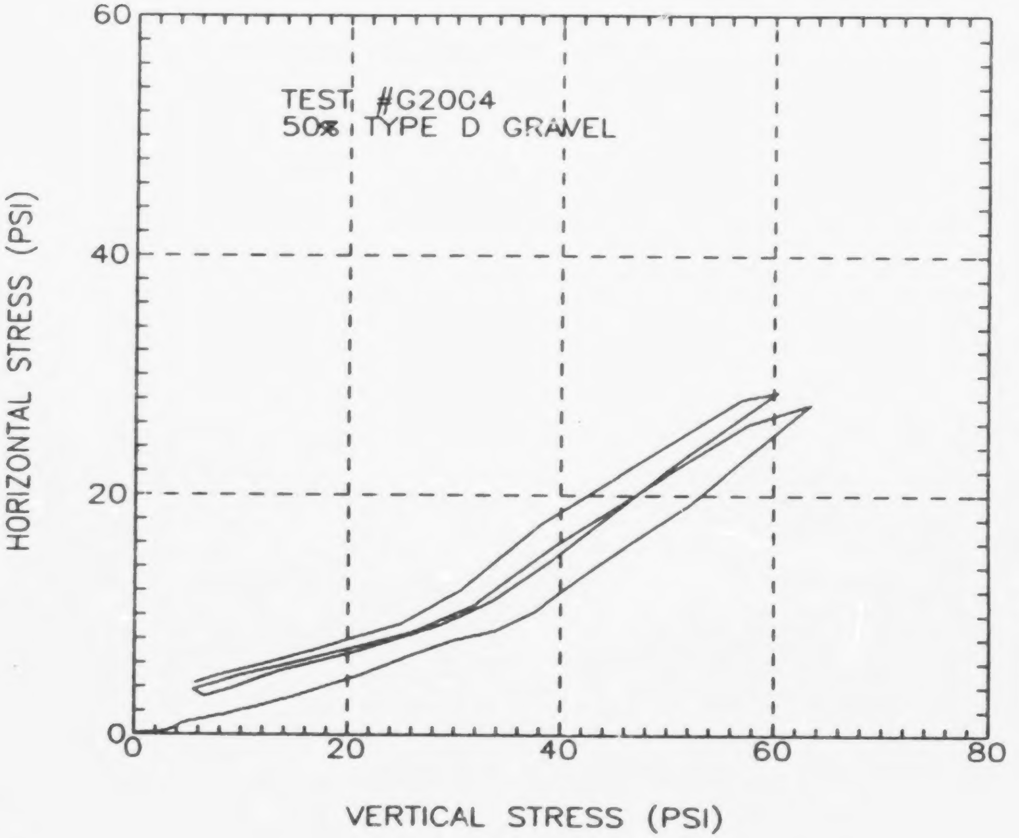
TEST #G2004
50% TYPE D GRAVEL
HORIZONTAL STRESS (PSI)
VERTICAL STRESS (PSI)
0
20
40
60
0
20
40
60
80

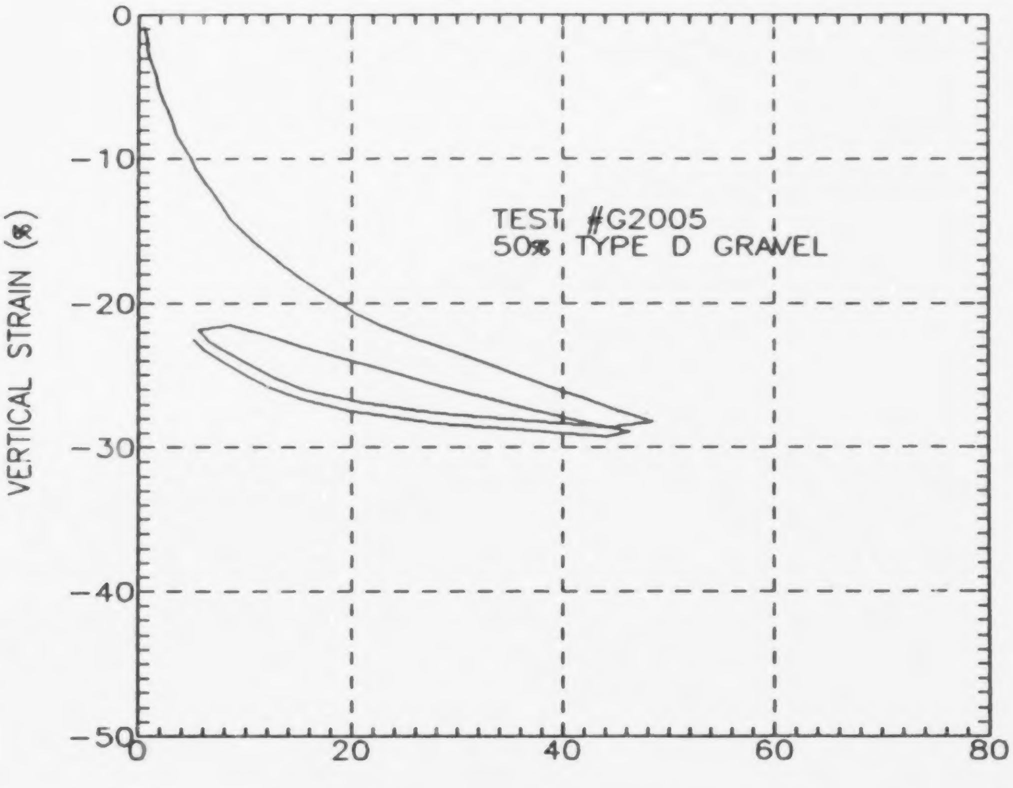
0
-10
-20
-30
-40
-50
0
20
40
60
80
VERTICAL STRAIN (%)
AVERAGE VERTICAL STRESS (PSI)
TEST #G2005
50% TYPE D GRAVEL

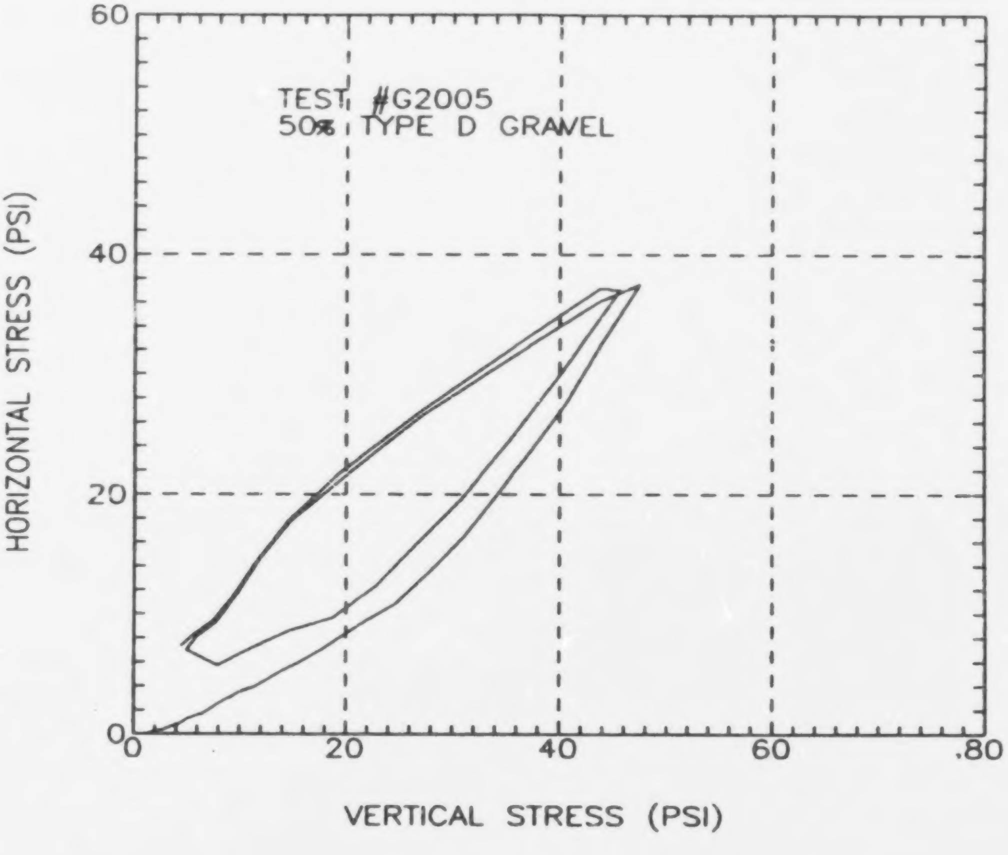

TEST #G2005
50% TYPE D GRAVEL
HORIZONTAL STRESS (PSI)
VERTICAL STRESS (PSI)
0
20
40
60
0
20
40
60
80

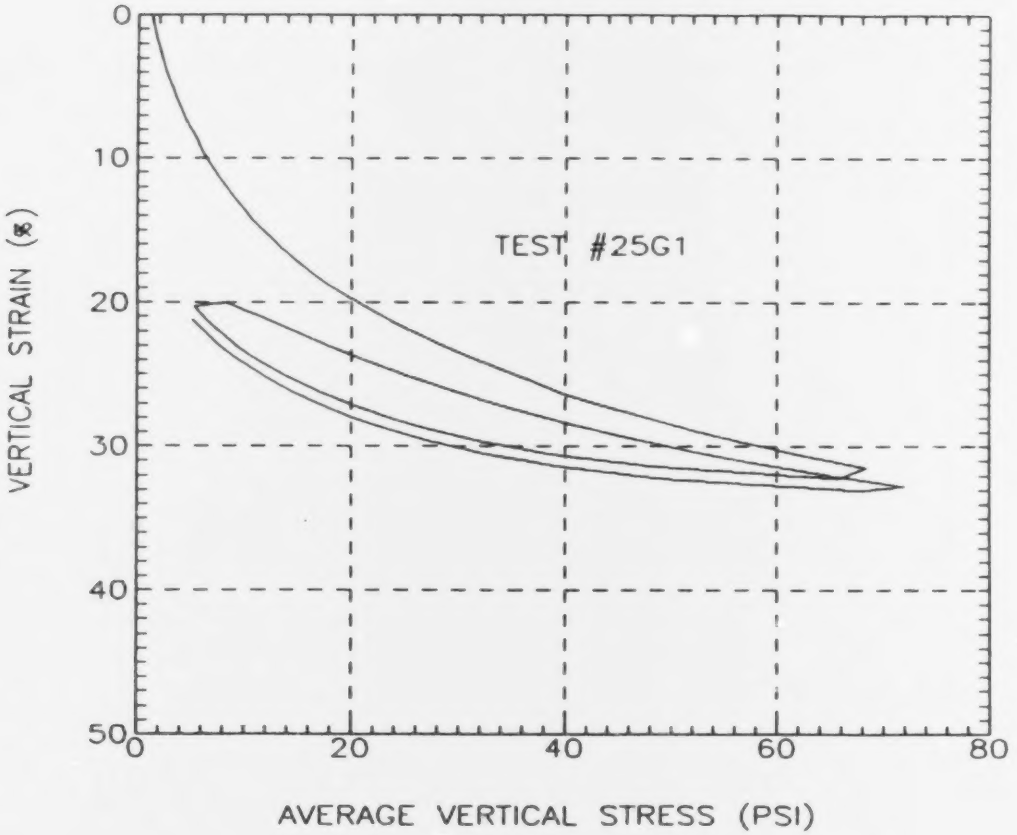

TEST #25G1
VERTICAL STRAIN (%)
0
10
20
30
40
50
0
20
40
60
80
AVERAGE VERTICAL STRESS (PSI)

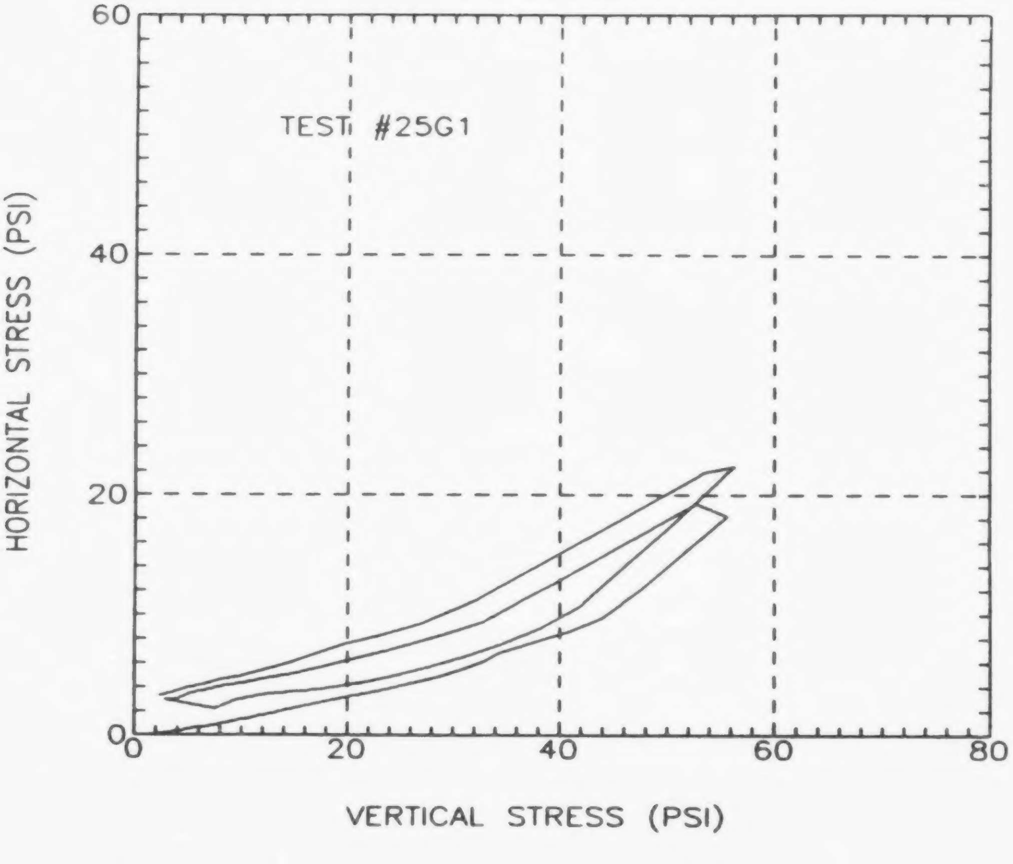
TEST #25G1
HORIZONTAL STRESS (PSI)
VERTICAL STRESS (PSI)
0
20
40
60
0
20
40
60
80

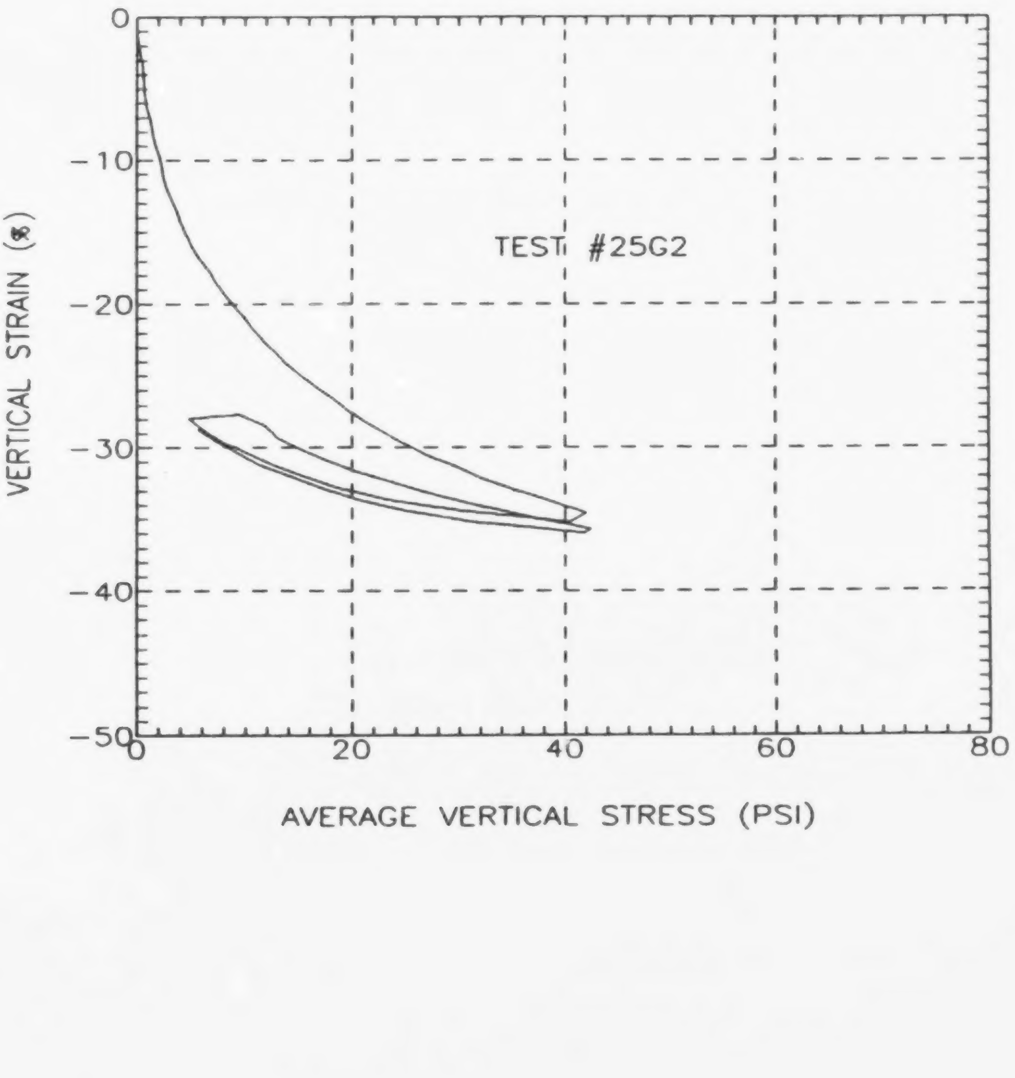
0
-10
-20
-30
-40
-50
0
20
40
60
80
VERTICAL STRAIN (%)
AVERAGE VERTICAL STRESS (PSI)
TEST #25G2

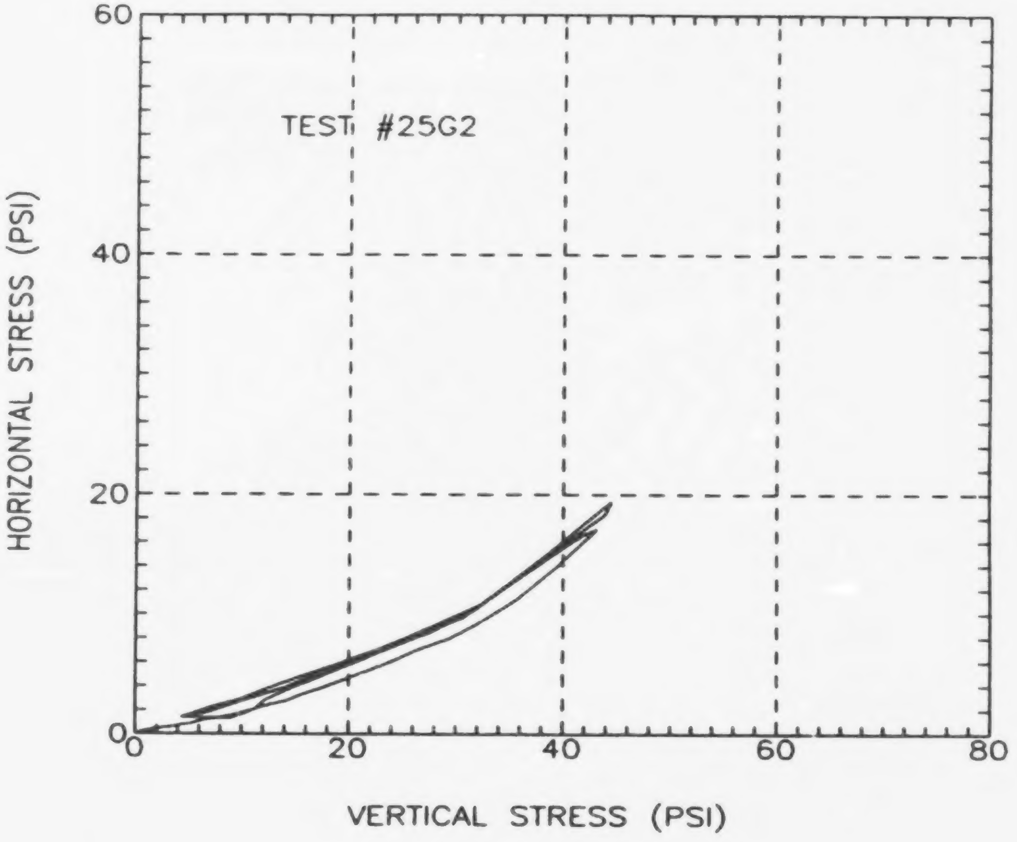
TEST #25G2
HORIZONTAL STRESS (PSI)
VERTICAL STRESS (PSI)
0
20
40
60
0
20
40
60
80

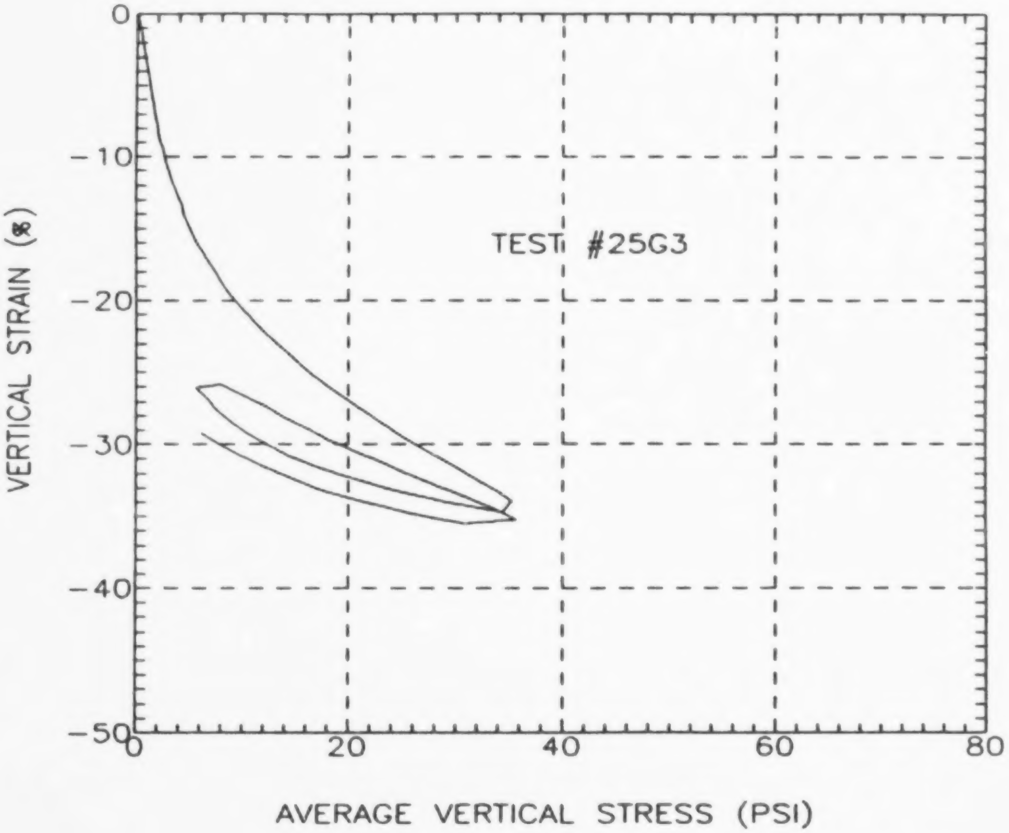

TEST #25G3
VERTICAL STRAIN (%)
AVERAGE VERTICAL STRESS (PSI)
0
-10
-20
-30
-40
-50
0
20
40
60
80

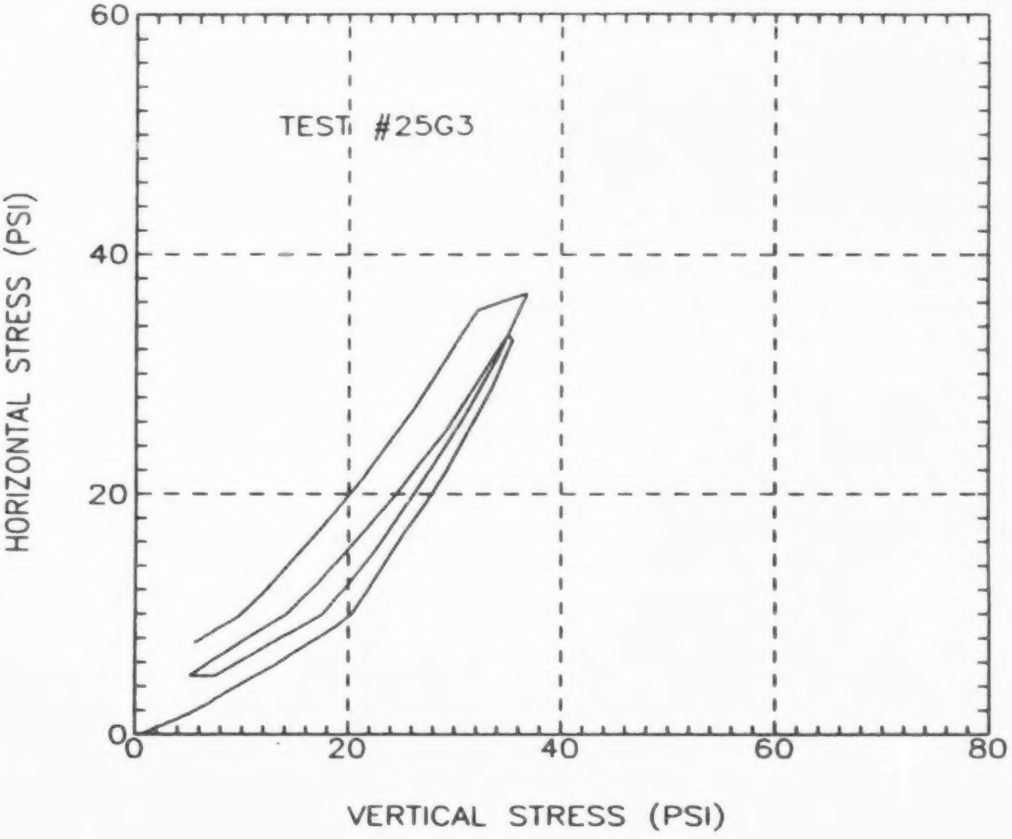
TEST #25G3
HORIZONTAL STRESS (PSI)
VERTICAL STRESS (PSI)
0
20
40
60
0
20
40
60
80

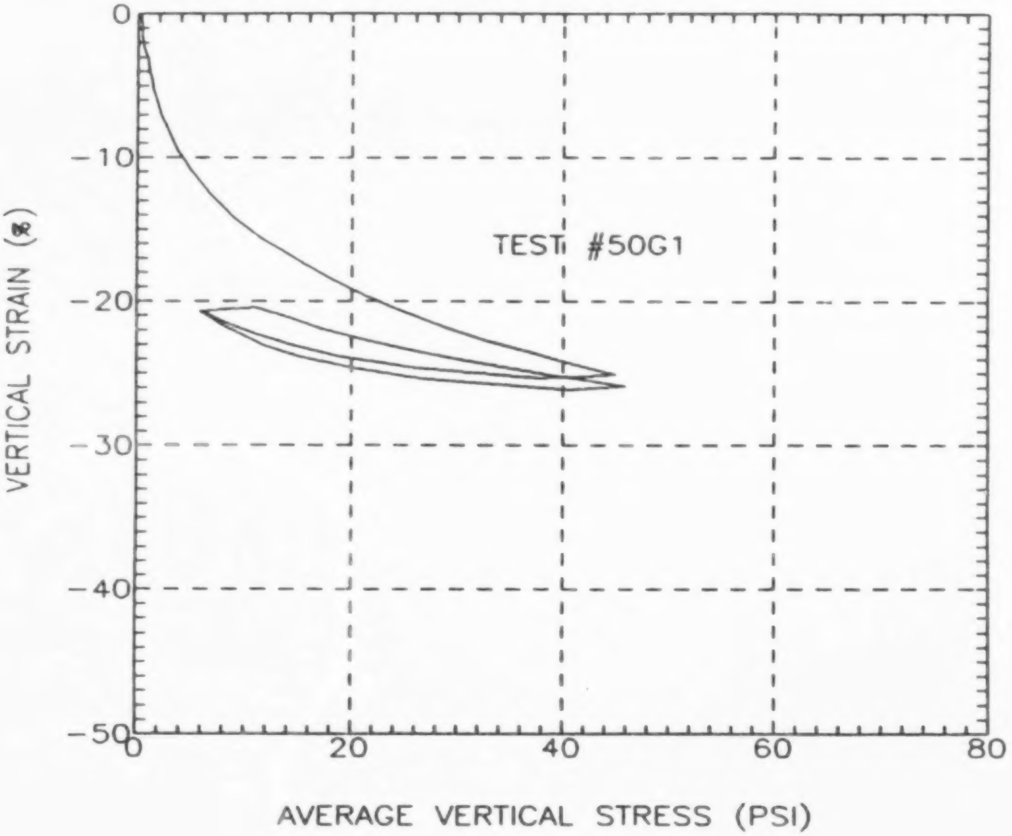
0
-10
-20
-30
-40
-50
VERTICAL STRAIN (%)
TEST #50G1
0
20
40
60
80
AVERAGE VERTICAL STRESS (PSI)

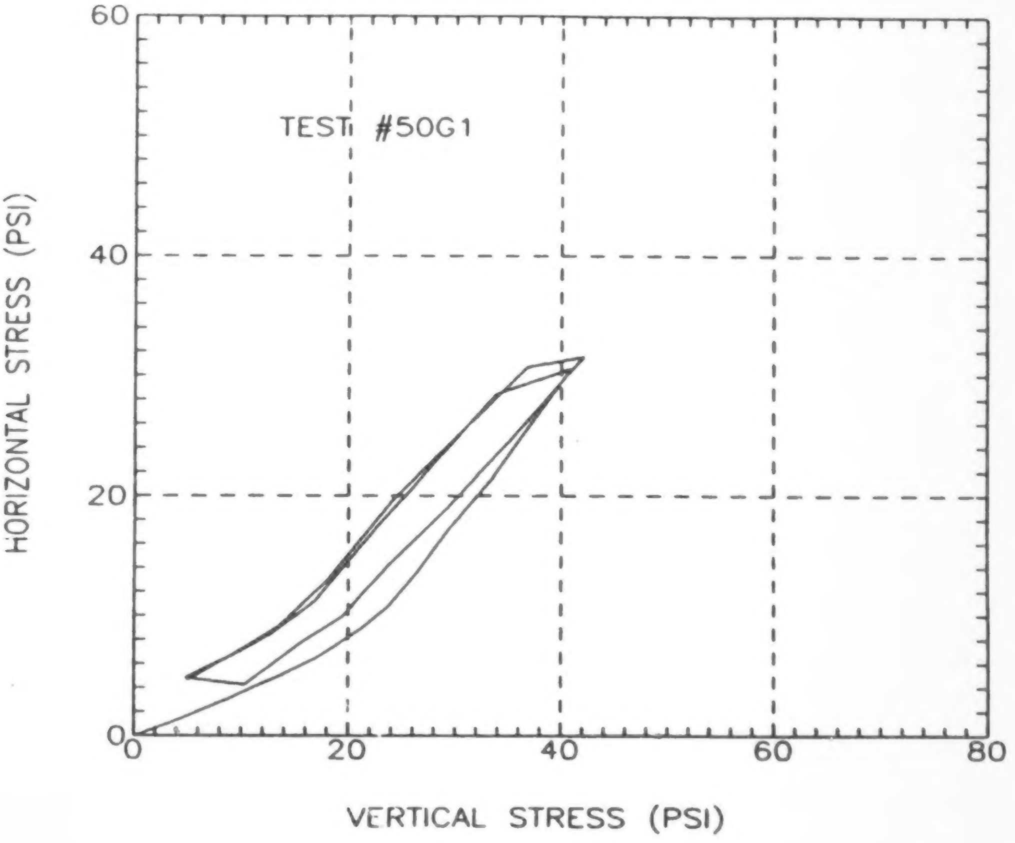
TEST #50G1
HORIZONTAL STRESS (PSI)
VERTICAL STRESS (PSI)
0
20
40
60
0
20
40
60
80

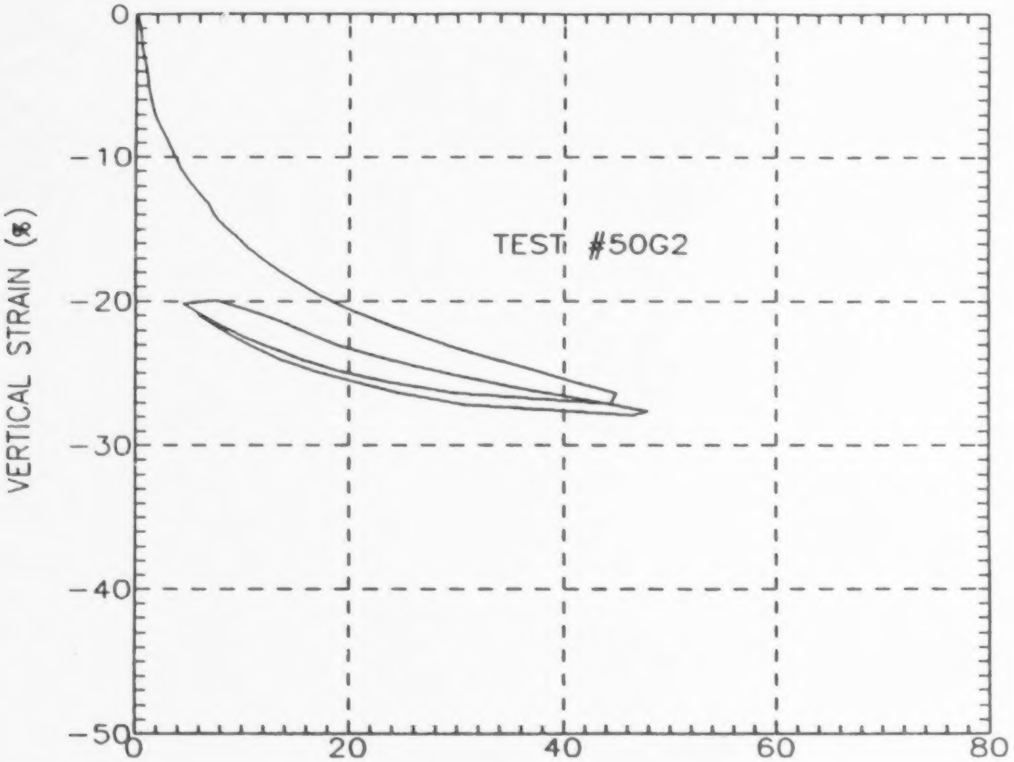

0
-10
-20
-30
-40
-50
0
20
40
60
80
VERTICAL STRAIN (%)
AVERAGE VERTICAL STRESS (PSI)
TEST #50G2

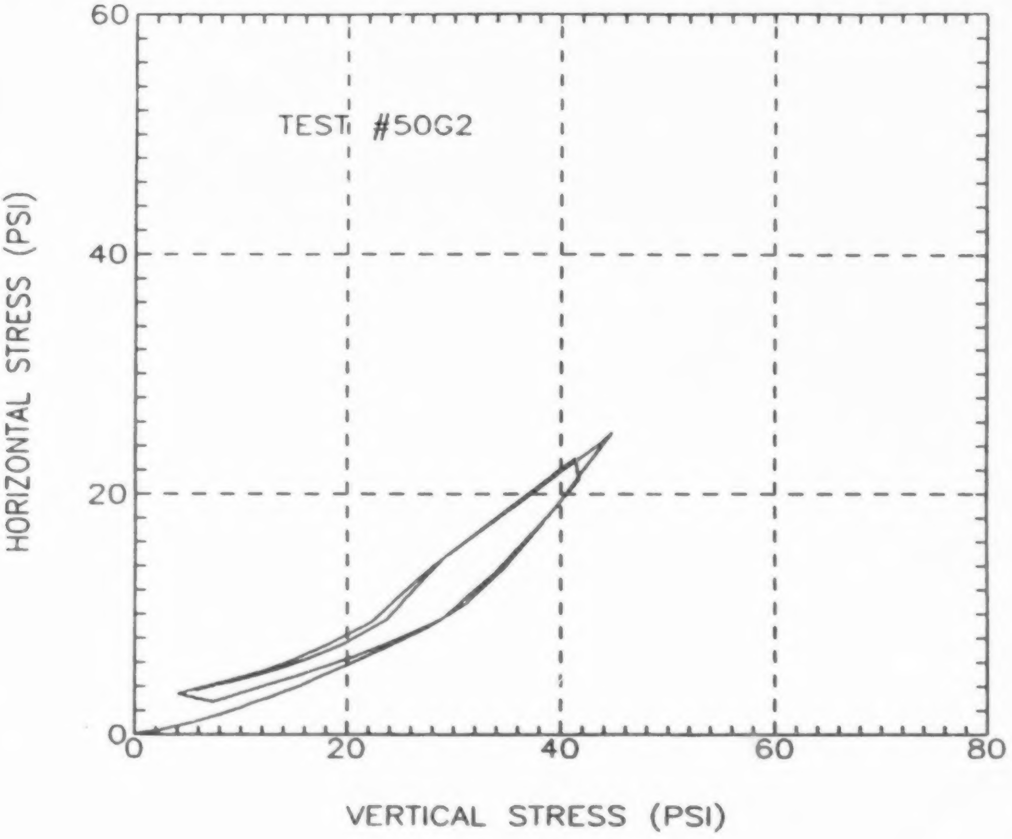
TEST #50G2
HORIZONTAL STRESS (PSI)
0
20
40
60
VERTICAL STRESS (PSI)
0
20
40
60
80

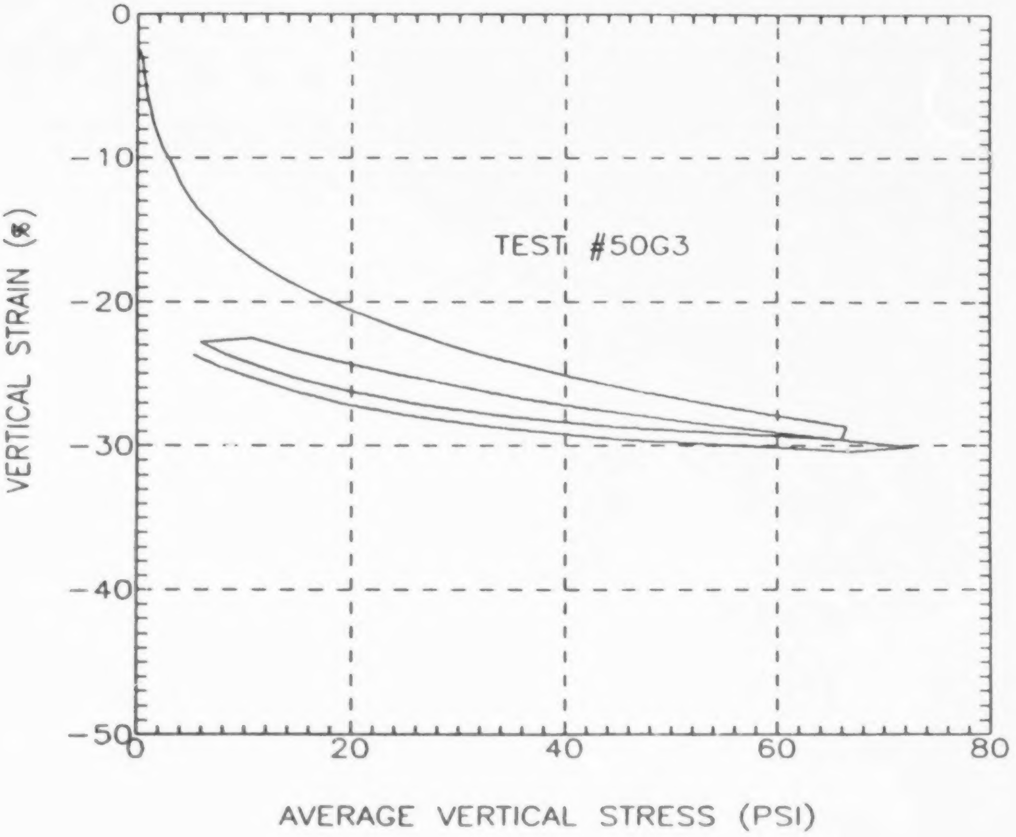
TEST #50G3
VERTICAL STRAIN (%)
0
-10
-20
-30
-40
-50
0
20
40
60
80
AVERAGE VERTICAL STRESS (PSI)

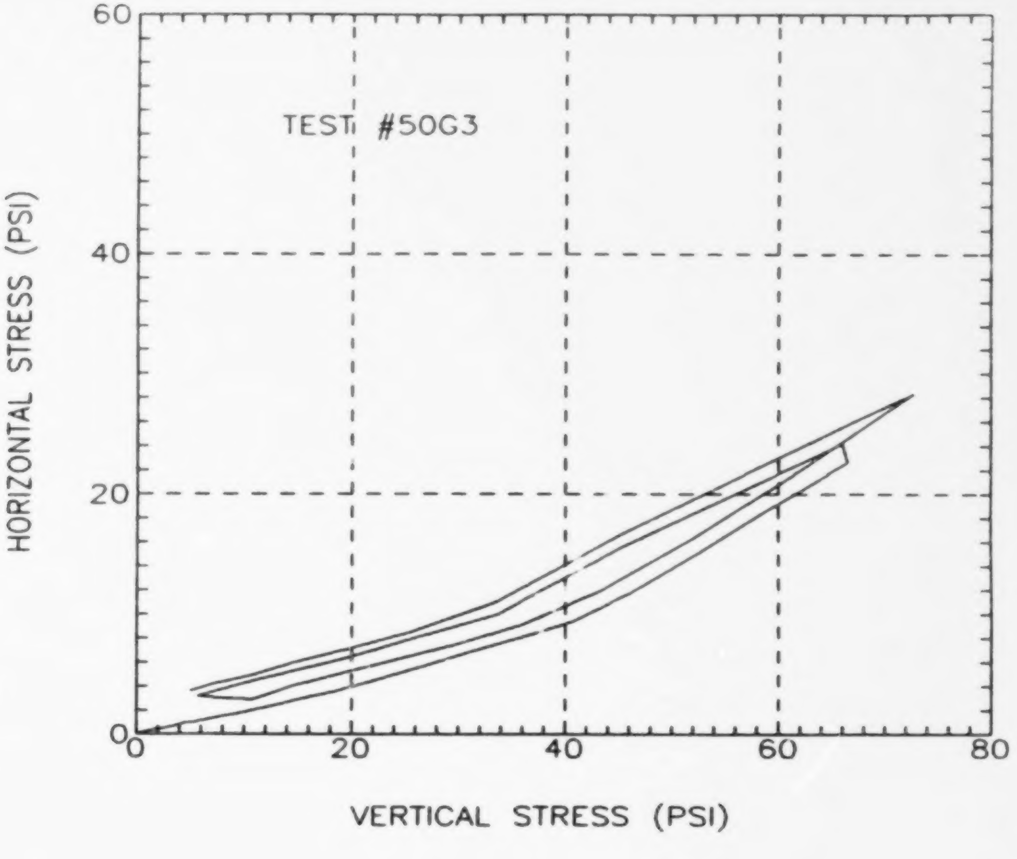
TEST #50G3
HORIZONTAL STRESS (PSI)
VERTICAL STRESS (PSI)
0
20
40
60
0
20
40
60
80

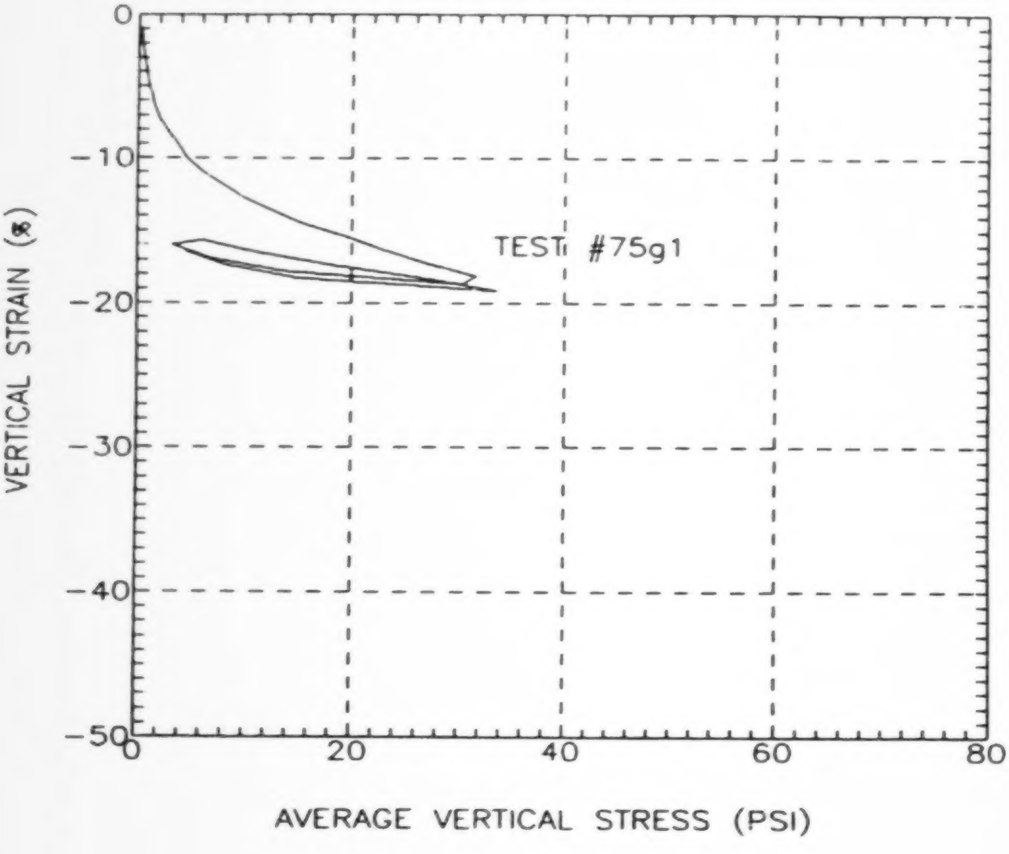
0
-10
-20
-30
-40
-50
VERTICAL STRAIN (%)
0
20
40
60
80
AVERAGE VERTICAL STRESS (PSI)
TEST #75g1

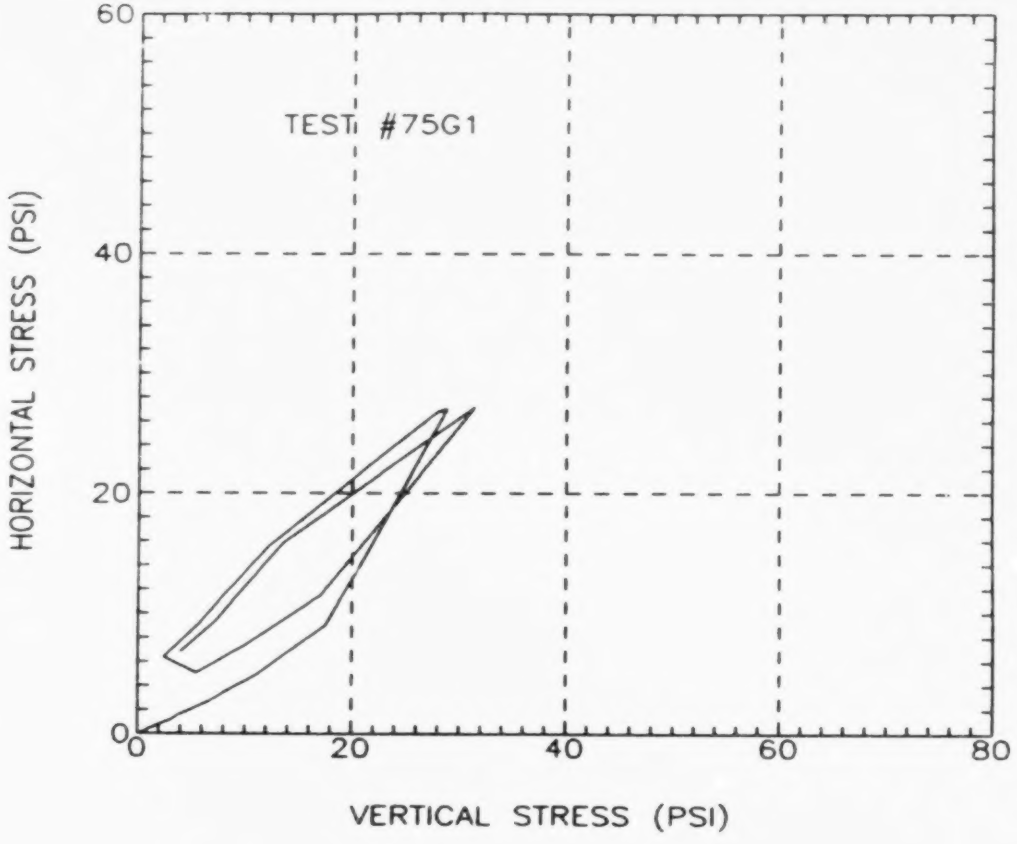
60
40
20
0
HORIZONTAL STRESS (PSI)
TEST #75G1
0
20
40
60
80
VERTICAL STRESS (PSI)

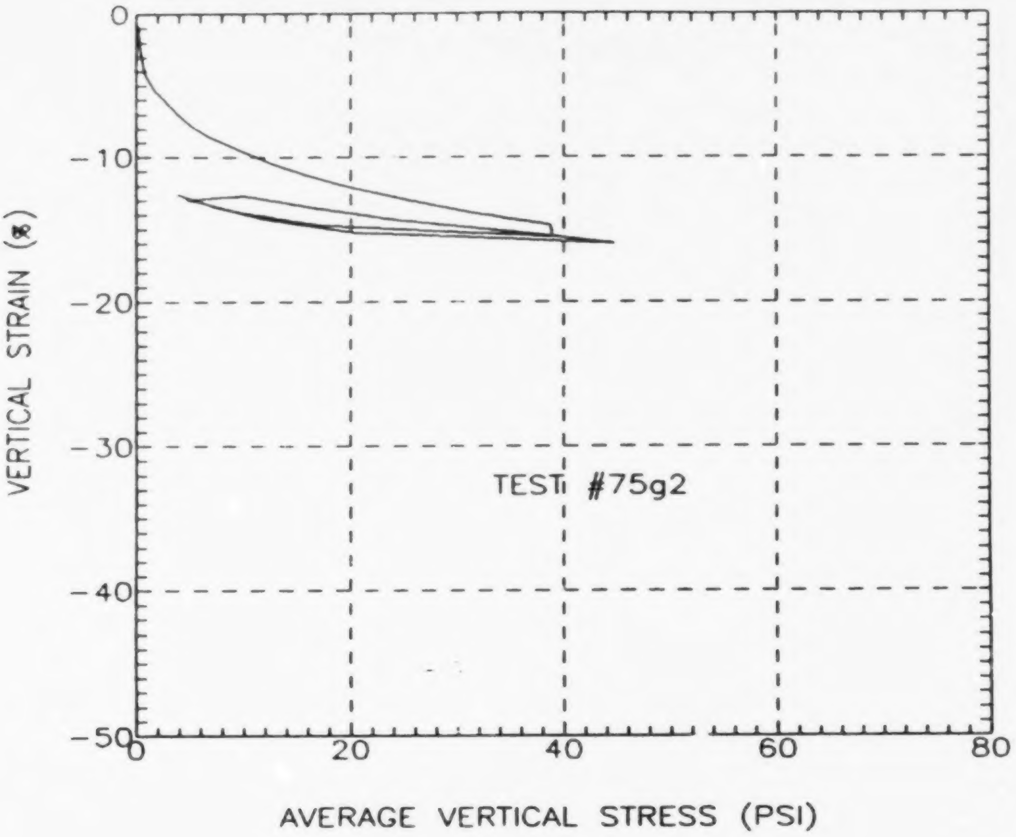

0
-10
-20
-30
-40
-50
0
20
40
60
80
VERTICAL STRAIN (%)
AVERAGE VERTICAL STRESS (PSI)
TEST #75g2

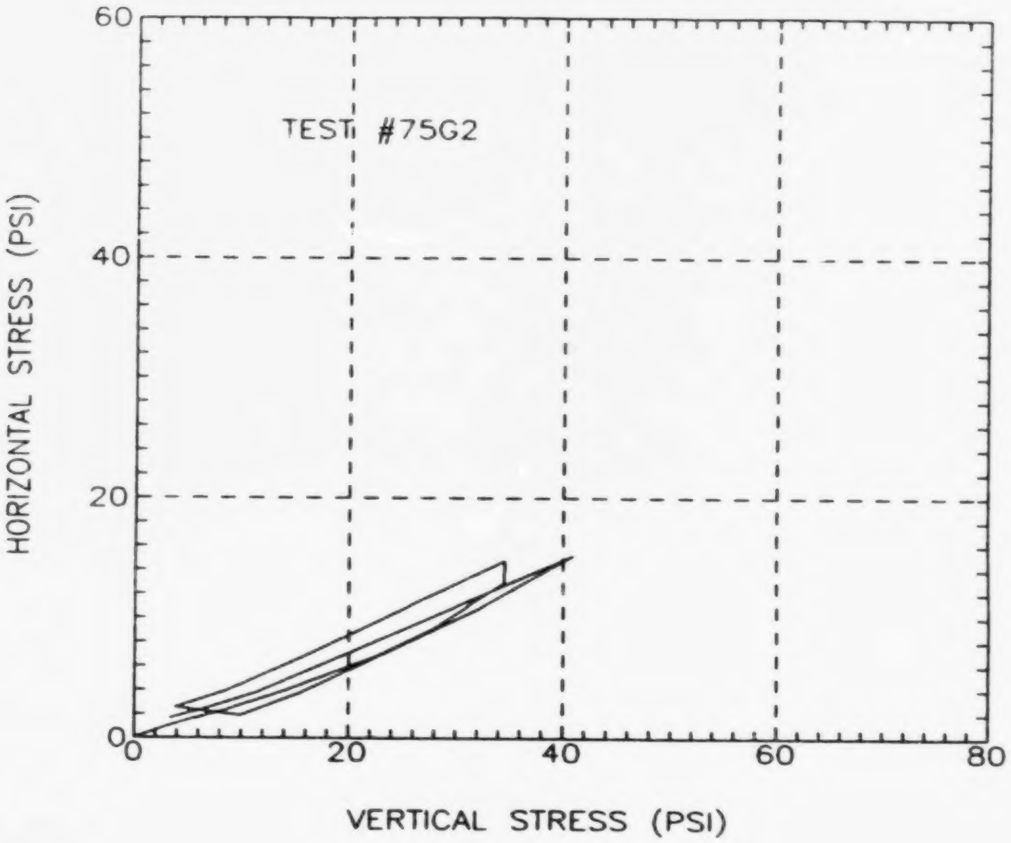
TEST #75G2
HORIZONTAL STRESS (PSI)
60
40
20
0
0
20
40
60
80
VERTICAL STRESS (PSI)

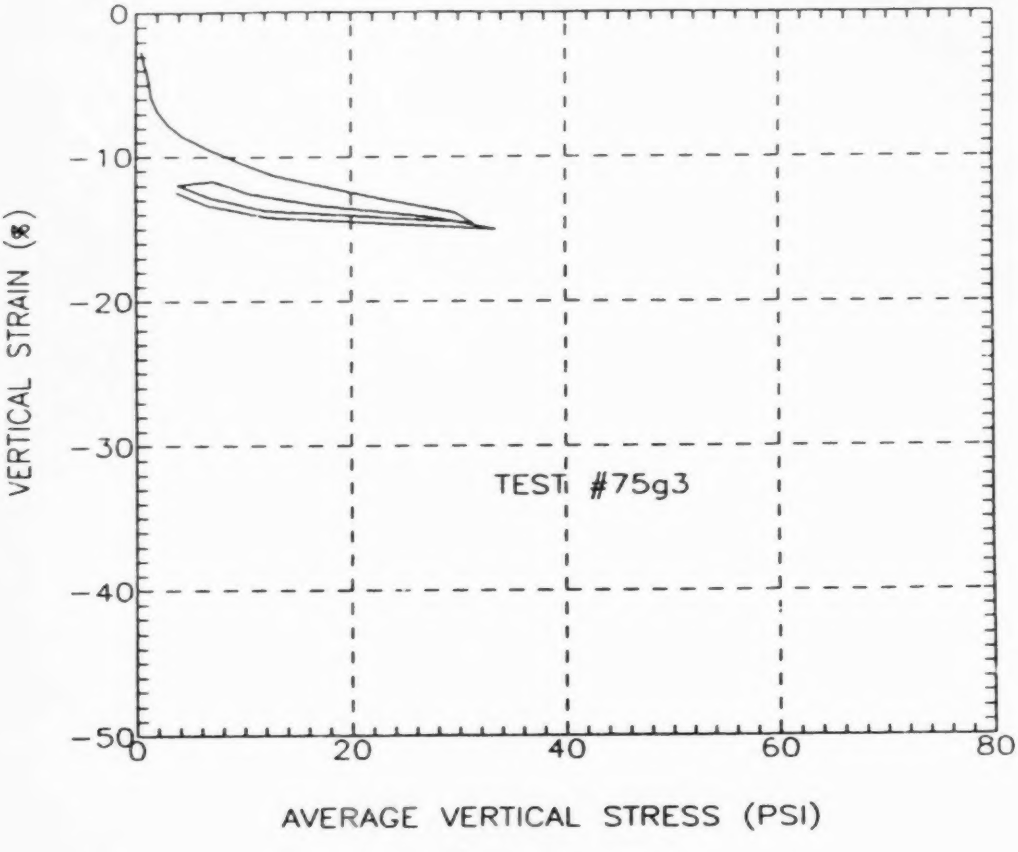
0
-10
-20
-30
-40
-50
0
20
40
60
80
VERTICAL STRAIN (%)
AVERAGE VERTICAL STRESS (PSI)
TEST #75g3

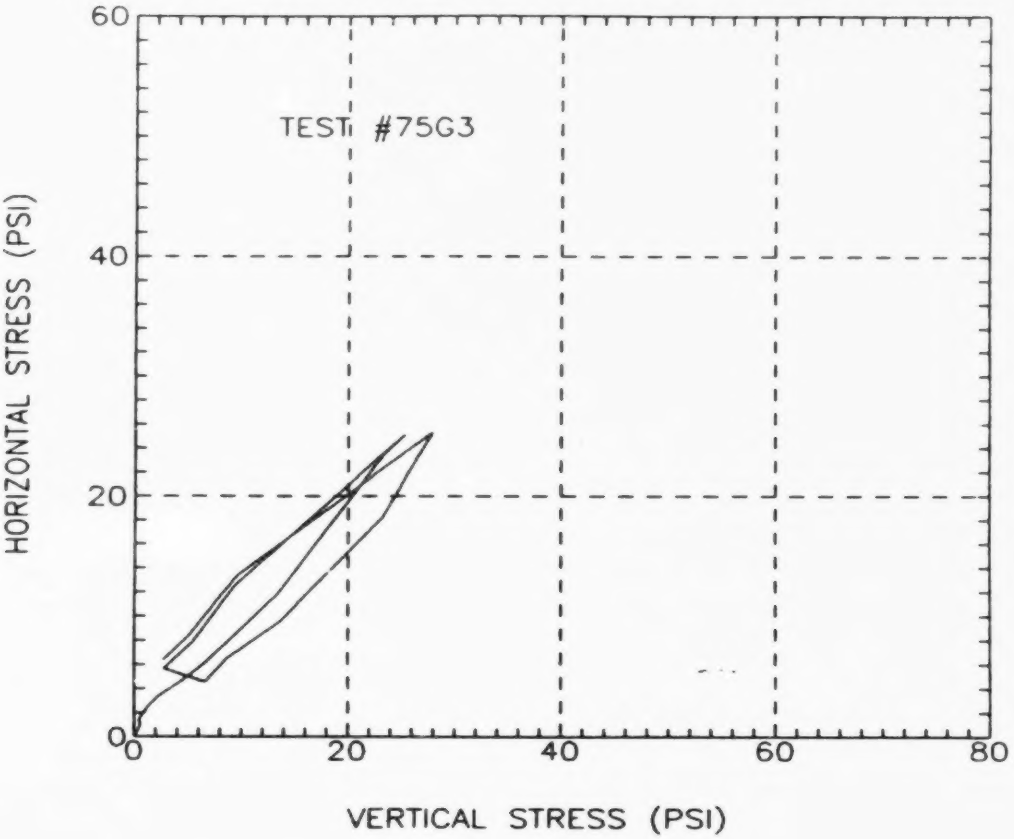
TEST #75G3
HORIZONTAL STRESS (PSI)
VERTICAL STRESS (PSI)
0
20
40
60
0
20
40
60
80

BLANK